DNA 4449F-2

ANALYSIS OF AEROSOLS AND FALLOUT FROM HIGH-EXPLOSIVE DUST CLOUDS

Volume II

Meteorology Research, Inc.
464 W. Woodbury Road
Altadena, California 91001

3 March 1977

Final Report for Period 3 May 1971—30 September 1973

CONTRACT Nos. DASA 01-71-C-0154
DNA 001-73-C-0040

THIS WORK SPONSORED BY THE DEFENSE NUCLEAR AGENCY
UNDER RDT&E RMSS CODE B342073464 N99QAXAA12819 H2590D.

Prepared for
Director
DEFENSE NUCLEAR AGENCY
Washington, D. C. 20305

Destroy this report when it is no longer needed. Do not return to sender.

UNCLASSIFIED

SECURITY CLASSIFICATION OF THIS PAGE *(When Data Entered)*

REPORT DOCUMENTATION PAGE

READ INSTRUCTIONS BEFORE COMPLETING FORM

1 REPORT NUMBER: DNA 4449F-2

2. GOVT ACCESSION NO.

3 RECIPIENT'S CATALOG NUMBER

4. TITLE *(and Subtitle)*: ANALYSIS OF AEROSOLS AND FALLOUT FROM HIGH-EXPLOSIVE DUST CLOUDS, Volume II

5 TYPE OF REPORT & PERIOD COVERED: Final Report for Period 3 May 71–30 Sep 73

6 PERFORMING ORG. REPORT NUMBER: MRI 76 FR-1419

7 AUTHOR(S): W. D. Green, M. J. Fegley

8 CONTRACT OR GRANT NUMBER(s): DASA 01-71-C-0154, DNA 001-73-C-0040

9. PERFORMING ORGANIZATION NAME AND ADDRESS: Meteorology Research, Inc., 464 W. Woodbury Road, Altadena, California 91001

10 PROGRAM ELEMENT, PROJECT, TASK AREA & WORK UNIT NUMBERS: NWED Subtask N99QAXAA128-19

11 CONTROLLING OFFICE NAME AND ADDRESS: Director, Defense Nuclear Agency, Washington, D.C. 20305

12 REPORT DATE: 3 March 1977

13 NUMBER OF PAGES: 232

14 MONITORING AGENCY NAME & ADDRESS *(if different from Controlling Office)*: DNA, SBIE

15 SECURITY CLASS *(of this report)*: UNCLASSIFIED

15a. DECLASSIFICATION DOWNGRADING SCHEDULE

16. DISTRIBUTION STATEMENT *(of this Report)*

Approved for public release; distribution unlimited.

17 DISTRIBUTION STATEMENT *(of the abstract entered in Block 20, if different from Report)*

18 SUPPLEMENTARY NOTES

This work sponsored by the Defense Nuclear Agency under RDT&E RMSS Code B342073464 N99QAXAA12819 H2590D.

19 KEY WORDS *(Continue on reverse side if necessary and identify by block number)*

High Explosive Dust Clouds
Airborne Dust Concentration
Size Distribution
Particle Densities
Instrument Development
Sweepup

20 ABSTRACT *(Continue on reverse side if necessary and identify by block number)*

Dust clouds from seven high-explosive detonations ranging from 20 to 500 tons in the Middle Gust-Mixed Company series were sampled using various aircraft-mounted instruments. A wet cyclone system proved to be the best device for sampling airborne dust. Dust concentrations as a function of time and location in the clouds were determined. One cloud was underflown as early as Z + 1:22, and another was entered at Z + 1:36. Fallout was measured on three tests, and various experiments were conducted to detect sweepup of dust from outside the crater zone. Gas samples were collected and analyzed ... inside the 500-ton Mixed Company III cloud. Selected airborne dust and fallout

DD FORM 1 JAN 73 1473 EDITION OF 1 NOV 65 IS OBSOLETE

UNCLASSIFIED

SECURITY CLASSIFICATION OF THIS PAGE *(When Data Entered)*

20. ABSTRACT (Continued)

samples were sized using an optical image processing computer. Density measurements were made to determine if particles expanded or melted in the fireball. Volume II contains ten appendices which include the following topics:

TABLE OF CONTENTS

VOLUME II

INTRODUCTION

Volume II of "Analysis of Aerosols and Fallout from High-Explosive Dust Clouds" contains ten appendices to Volume I. These appendices include descriptions of the airborne dust sampling instrumentation, the layout of the ground experiments, and a description of the laboratory techniques and analysis procedures used on the recovered dust samples.

Three of the appendices contain tables listing the size distributions and specific gravity of airborne dust and fallout samples. These tables and associated figures of

$$\text{Log } \eta_{T(j)} \frac{D_i}{\Delta D_i} \text{ vs Log } D_i$$

and particle density as a function of particle size comprise the main portion of Volume II and represent the primary data recovered during the Middle Gust Mixed Company Series.

In addition, Volume II contains the results of collection efficiency comparisons between the wet cyclone and the airborne filter sampler, a summary of environmental impact data collected in the Mixed Company III cloud, a description of the ground installations and operations during the Mixed Company III test, and the results of sieve analysis of the fallout collected after the Mixed Company III detonation.

APPENDIX I

AIRCRAFT INSTRUMENTATION

The requirement to sample large aerosol particles up to several millimeters in diameter presented a unique problem in instrumentation development. Standard aerosol sampling or detection equipment is designed to handle small samples, collected over long periods of time. This equipment normally samples an atmospheric aerosol which acts as a true suspension where particle motion is governed by Brownian motion, precipitation rates are measured in centimeters per hour and, for sampling purposes, the particles behave as an integral part of the air stream.

The dust generated by a high explosive detonation ranges from a true aerosol up to large ejecta blocks. The particles in the dust cloud lofted by thermal rise after the detonation typically have peak sizes in the 600-400 μm diameter range. These particles, being analogous to mist or light rain in a meteorological sense, precipitate fairly rapidly causing mass segregation in the cloud. Precipitation of these large particles within the sampling train of standard aerosol sensing devices would present problems of reentrainment and signal distortion which would be unacceptable in an experiment designed to collect integrated dust samples.

Particle collectors normally used for aerosol sampling, such as impactors or filters, were unacceptable due to the size of the particles and problems of nonretention.

A solution to the large-particle collection problem was found in an instrument developed on the program, referred to below as a wet cyclone, which used a commercial cyclone separator designed specifically to collect particles in the ≥15 μm diameter size range. This system, with modifications, was used throughout the program. Other devices were built and tested, including a high-volume dry cyclone and a filter tray sampler, but each proved unreliable due to sedimentation blowout or winnowing of the finer dust particles. Loss of the fines was a direct function of the length

of time required to collect the total sample, resulting in a variability in the effective collection efficiency.

Each of the instruments flown in one or more of the tests is described below.

AI.1 WET CYCLONE

The Wet Cyclone System was built around a Fisher-Klosterman XQ-3 cyclone separator with a rated collection efficiency of 94 percent for 25 μm diameter particles with a specific gravity of 1.0 gm/cc collected at 100 CFM and a pressure drop of 5.57 inches of water. Tests in the MRI fog tower indicated that the unit exceeded manufacturer's specification. Tests at MRI using the integrated wet cyclone system and a dust sample (TD) which simulated materials found in the detonation clouds demonstrated collection efficiencies of 93.0 percent to 96.5 percent (Appendix II).

The cyclone was mounted to the escape hatch of the C-45 with a large scoop passing forward through the door and standing about 12 inches from the outer skin of the aircraft. The sampling orifice measured 4 in. by 4 in. Dust entering the cyclone was spun out to the sides and washed into a collection jar by a continuous alcohol-water spray. Wet scrubbing reduced the blowby of the fine particles and assured that all material captured by the cyclone was washed into the jar.

Following each pass through the cloud, the jars were removed, capped and stored; the system flushed down with additional alcohol-water solution; and a new jar placed on the cyclone preparatory to reentering the cloud.

During flights, a high-volume air pump operating at approximately 100 CFM enabled the system to sample isokinetically for particles larger than 80 μm diameter with appropriate correction factors for particles below that limit. (See Appendix IV for calibration of the Cyclone System.)

AI.2 DRY CYCLONE

A Dry Cyclone System was designed on the pattern of the wet cyclone, omitting the spray system and substituting a larger sampling cone with an orifice of 30 square inches. Reduced collection efficiency was acknowledged, and the system was used primarily to improve the statistical sampling of large particles. The system was flown only on Middle Gust IV and Mixed Company III.

AI.3 DRY FILTER SAMPLER

A dry filter sampler was built and tested during Mine Throw I, Middle Gust II, and Middle Gust III. The filter holder was mounted vertically in the aircraft and tied to the same sampling cone used later for the dry cyclone. The filters were built into packages measuring 5 in. by 8 in. which resembled a film pack with removable cover. Once mounted in the holder, the cover was slipped out of the packet, exposing the filter. In operation, a gate valve was opened, and air containing dust was drawn through the filter by a high-volume air pump. Fine particles were retained in the filter while the larger particles remained free on the surface. After sampling, the cover was replaced, entrapping the particles and permitting the removal to the packet preparatory to inserting a new filter for the next test.

Prior to the tests, all filters were weighed and then reweighed after dust collection. Due to the large tare weight and variations due to relative humidity, this system was satisfactory only for large samples. All samples were subject to reentrainment of fines due to small leaks in the system.

AI.4 CONTINUOUS TAPE SAMPLER

A method of defining changes in the dust concentration and size distribution across the cloud during each penetration was attempted. Due to the large particle sizes encountered, continuous dry filter strip

tape samplers used in air pollution studies would not retain the dust quantitatively.

A special impactor employing a continuous strip of adhesive-backed clear plastic tape was built and tested. The tape was transported at 100 cm per minute past a 4 mm by 20 mm slit connected to an external probe. The probe, located in the same cluster with the cyclone and filter inlets, had an orifice measuring three square inches. Following impaction of the sample, a thin Mylar film was drawn over the adhesive surface, sandwiching the dust particles between the film and the tape.

The sampler functioned satisfactorily; however, spatial resolution of the dust was altered by some blowby of the fine particles. Particle density on the tape was acceptable; however, the low sampling rate precluded good statistical analysis of the samples as a function of time or spatial location in the cloud. This problem was further compounded by optical effects in the tape which precluded automatic analysis using the MRI Quantimet 720 Image Analyzer. The tapes have been retained for possible future analysis if warranted.

AI.5 FLUORESCENT PARTICLE (F. P.) DRUM SAMPLER

A standard Metronics F. P. drum sampler was employed in the aircraft to collect fluorescent particles released during the ground sweep-up experiments. The sampler operates on the same principle as the tape sampler but on a smaller scale, compatible with the 5 micron mean diameter of the F. P. particles. The inlet to this device was connected to the main sampling port on the C-45 which consisted of a 3 in. diameter tube running axially parallel to the aircraft and extending about a foot and a half ahead of the nose of the aircraft.

The sampler consisted of a revolving drum covered with black plastic tape which had been coated with a solution of rubber cement. Air samples containing dust were drawn through a narrow slit from the 3 in. tube during each pass and impacted on the tape as patches measuring

about one square centimeter. The inlet nozzle from the large tube was arranged to exclude the larger dust particles and preferentially sample material in the 1 to 10 μm range.

Fluorescent particles were sampled on the drum and were detected also in the bulk dust samples collected during certain passes through the dust clouds.

AI.6 TSI MICROBALANCE

During one test (Middle Gust II), a TSI microbalance was flown; however, results were negative. The device operates on the principle of detecting changes in the vibrational frequency of an oscillating quartz crystal as a function of aerosol buildup on the surface. The sampling area of the crystal was only 10 square millimeters and was saturated rapidly by the high dust concentrations encountered in the high-explosive clouds.

AI.7 INTEGRATING NEPHELOMETER

An MRI Integrating Nephelometer was flown on each flight, primarily to define the points of entry and exit and to profile the fine particle dust concentration within the cloud. The nephelometer is designed to measure visibility or the degradation of visibility due to the presence of optically scattering dust or aerosol particles in the diameter range of 0.1 to 1.0 μm. Since the particles of interest during the sampling and analysis were an order of magnitude larger, no attempt was made to analyze the nephelometer data other than to identify, in time, the points when the aircraft entered or left the cloud. Profiles across the cloud or stem were recorded and, in many cases, showed a high degree of variability.

AI.8 CONDENSATION NUCLEI COUNTER

An Environment-One Condensation Nuclei Monitor was flown on all tests after Middle Gust I. The monitor samples once every two seconds,

exposes the air to momentary high water vapor supersaturation by a process of rapid expansion, and is primarily sensitive to particles in the submicron range. Under high supersaturations (200-300 percent relative humidity) moisture condenses on the fine particles, causing growth into sizes which can be detected optically in the visible range. This device is used in air pollution studies to detect combustion products. During the Middle Gust-Mixed Company tests, the signals recorded from this instrument indicated a relative low concentration of submicron particles, implying low production or subsequent scavenging by other particles in the high concentration dust environment. Peak readings were noted at the edge of the cloud, partially supporting the later hypothesis.

AI.9 OTHER RECORDED PARAMETERS

Temperature, altitude, indicated airspeed, and turbulence were recorded continuously. Temperature increases in the cloud at the earliest point of entry (Middle Gust III Z + 1:32) did not exceed 1.5°C above ambient. Indicated airspeed was converted to true airspeed to calculate sampling rate. The turbulence measurement, using an MRI Universal Indicating Turbulence System (UITS) was used as an additional indicator of cloud entry and exit.

AI.10 GAS SAMPLING INSTRUMENTATION

During the Mixed Company III test, a second aircraft was utilized to monitor nitric oxide, ozone, carbon monoxide, and particulates in the cloud. In addition, bag samples were collected and analyzed for physiologically harmful products resulting from the detonation of TNT.

The aircraft was the MRI Cessna 205 which had been used extensively in California on various air pollution monitoring experiments. Continuous recording instruments included a REM NO-NO_x Monitor (Model 612), an Andros Carbon Monoxide Monitor (Model 7000), an Environment-One Condensation Nuclei Monitor (Model 100), and an MRI

Integrating Nephelometer (Model 2050). In addition to the gas and particulate data, altitude, turbulence, temperature, relative humidity, and airspeed were recorded on a Metrodata Data Logging System (Model 620). A special manifold was installed to collect gas samples in inflatable bags for later analysis.

Results of the gas sampling experiment were published as a special report entitled, "Environmental Impact Data - Mixed Company III Event. 500-Ton Tangent Sphere - 13 November 1972" (MRI 73 R-1060). This report is included as Appendix VIII.

APPENDIX II

COLLECTION EFFICIENCY TESTS- WET CYCLONE VS FILTER SAMPLER

FILTER SAMPLER

Weighed samples of BD and TD, ranging in weight from 3 to 200 mg., were introduced directly into the inlet (including the inlet valve) of the filter sampler and collected on a pre-weighed test filter. Tests were conducted on the bench with the vacuum pump on low speed. After each test the filter was reweighed to determine the quantity of sample collected, then emptied, cleaned with an air gun, and weighed again for the next test.

Changes in the weight of the filter due to changes in relative humidity were determined by the use of a blank filter. This blank filter was carried along with the test filter during testing and was weighed before and after each test. Changes in its weight were ascribed to changes in relative humidity, and corrections for corresponding changes in the weight of the test filter were made.

C. E. was calculated as Q out/Q in.

Results:

BD	Q in	C. E.	TD	Q in	C. E.
	3.4 mg	85%		4.0 mg	83%
	6.7	121%		5.3	81%
	9.5	125%		11.4	84%
	14.3	106%		14.4	90%
	19.9	107%		20.9	91%
	30.6	97%		28.7	98%
	57.8	96%		48.1	94%
	105.2	101%		105.8	93%
	151.5	105%		149.5	91%
	201.1	100%		205.5	92%
Overall C.E. = 104%			Overall C.E. = 90%		

CYCLONE SAMPLER

Tests were carried out on the bench with the vacuum pump operating on low speed.

Weighed samples of TD ranging from 0.5 to 1.0 gm. were introduced directly into the inlet of the cyclone sampler. After the introduction each sample, the cyclone sampler was flushed with water for ~ 10 sec while opening and closing the sample inlet, thus washing the sample into the collection jar. The jar was removed and the sampler was rinsed again with water before attaching a new jar and introducing the next sample.

The water-sample mixtures obtained from the cyclone sampler were suction-filtered using pre-weighed Whatman #5 filter papers. (Some loss of small sample particles occurred on the sides of the Büchner Funnel). The filter papers containing the samples were dried in a 90° C. oven for ≈ 15 min., then cooled and weighed. Collection efficiency was calculated as Q out/Q in. No corrections were made for loss of weight due to leeching of the filter paper; this weight loss is on the order of 0.01 gm and causes a decrease in the reported C.E. of 1% to 2%.

Results:	Q in	C.E.	
	0.5399 gm	96.5%	
	0.5417	94.3%	
	0.6625	95.7%	
	0.7280	95.3%	
	0.7647	95.0%	
	0.8503	93.0%	
	0.9628	96.1%	Overall C.E. = 95.0%
	0.9661	94.0%	

APPENDIX III

GROUND EXPERIMENTS AND INSTALLATIONS

AIII. 1 FLUORESCENT PARTICLES

Fluorescent particle releases were made at various distances from ground zero during all the tests except Mine Throw I and Mixed Company I. Fluorescent particle tracers have been a standard technique in the past to trace airflow from point as well as diffuse sources and were used in this application in an attempt to trace airflow and associated particle sweepup from the area just outside the crater.

Fluorescent particles (F. P.) are available in various sizes and colors but are all generically related to the fluorescent minerals in the Zn-Cd sulfide series. Mean particle sizes are around 2-5 μm diameter. The yellow, green, and red varieties of F. P. are unique and cannot be confused with natural materials which commonly fluoresce in the blue-white. Particles released into the air around ground zero were easily discernible in dust samples collected later by the aircraft.

Fluorescent particles were injected several feet into the air at varying distances from ground zero seconds before detonation and were swept into the stem as the cloud lifted off the ground. Aerosolization of the particles was achieved by discharging a small compressed air cylinder through a tube containing a charge of about 80 grams of F. P. Although some problems occurred due to imperfect discharge from the tubes, the experiment was generally successful.

AIII. 2 GLASS BEADS AND BUBBLES

Two types of traceable soil simulants were tested in the attempt to detect specific sweepup of dust into the cloud. Glass beads in the range of 44-88 μm diameter were spread on the surface of the apron with the expectation that they might be swept into the cloud and could be

detected microscopically in dust samples collected by the aircraft. The beads, which are similar to those used in reflective signs and roadway paint, are very visible when viewed microscopically under dark field illumination.

Glass bubbles which have similar reflective qualities but a lower density and thus higher probability of being lofted into the cloud, were also tested. In both cases, it was hoped that the beads or bubbles could be distinguished from other particles in the dust samples.

Examination of the actual samples did not reveal any particles that could be identified as originating from the tracer implantation on the apron. Post-shot examination of the "bead fields" indicated that the bulk of the material remained in-situ and was not lofted or moved far from the site. In some cases, snow or wet ground disrupted the experiment.

AIII.3 FALLOUT COLLECTIONS

A network of fallout collection trays was installed on the ground prior to Middle Gust III, Middle Gust IV, and Mixed Company III. Samples were collected, weighed, sized, and analyzed for particle specific gravity after each of these tests.

For Middle Gust III and IV, open pans elevated on two-foot pedestals to prevent local contamination were used. During Mixed Company III, special louvered trays were provided and maintained by Stanford Research Institute (SRI). SRI also did the initial weight and size distribution analysis of the Mixed Company samples followed at MRI by additional image analysis and gravimetric separation to determine the specific gravity of the particles.

AIII.4 TIME-LAPSE AND REAL-TIME PHOTOGRAPHY

Time-lapse and real-time photography was undertaken during all the tests except Mine Throw I and Mixed Company I. These photographs were used primarily to monitor the growth and movement of the dust cloud while the aircraft was sampling. In several cases, the C-45 could be seen penetrating and emerging from the cloud.

APPENDIX IV

LABORATORY ANALYSIS OF DATA

AIV.1 RAW DUST RETRIEVAL

The raw dust from each event arrived at MRI in either a "dry" state or in a water-alcohol suspension in laboratory jars.

For the dry dust retrieval, preweighed camel-hair brushes were used to brush the dust from the jars into preweighed petri dishes. Both the petri dishes and brushes were weighed when the procedure was complete and the total dust weight recorded.

The "wet" dust retrieval was considerably more complicated. The jars were first allowed to stand for a period of several days to maximize particle sedimentation. In the meantime, Millipore 47 mm filters were soaked in distilled water and heated at a temperature of 100°C for 20 minutes. They were then allowed to cool under room conditions for about 10-15 minutes.

The filter weight was recorded before and after each heating process. It was determined that after two such cycles the tare weight of the filter had stabilized to the accuracy required.

These specially prepared and preweighed filters were then attached to a siphon tube, and the siphon was used to draw the water-alcohol mixture from the top of the sample jars. The filter captured any dust particles still suspended in the solution. The used filters were then heated at 100°C and allowed to cool before final weighing. The dust remaining at the bottom of the jars was washed into small preweighed glass vials using a standard laboratory plastic wash bottle. These vials were loosely capped with aluminum foil and heated overnight at 100°C. After cooling for an hour, the vials were weighed. The filter and vial dust weights were then combined to yield the total weight of dust collected for that particular sample.

AIV.2 CALCULATION DETAILS, PASS LOG DATA

During the course of the seven high-energy tests described in this report, measurements of selected combinations of the following parameters were taken and recorded on strip charts produced by the Honeywell Visicorder:

- Altitude
- Temperature
- Indicated Airspeed (IAS)
- Turbulence

(MRI Portable Instrument Package (PIP))

- Nephelometer (linear scale)
- Nephelometer (logarithmic scale)
- Condensation Nuclei
- Drum Sampler Position
- Cyclone Flow Rate
- Drum Sampler Flow Rate
- Cyclone Valve Position
- Visual Entry/Exit Marker
- Tape Sampler Event Marker

A voice recording was also available.

A calculation of dust cloud width and dust concentration was performed for each pass of the aircraft. A summary of these data is referred to in this report as a "pass log."

The parameters necessary to perform this calculation or to provide spatial reference for the result were altitude, IAS, b_{scat}, cyclone valve position, visual entry/exit marker, and aircraft heading and location in the cloud taken from the voice recording.

The altitude mechanism of the PIP was calibrated to the serving airport altitude, and the altitude span was adjusted to match the total altitude variation expected during a given event. The altitude trace on the visicorder was a continuous and well defined trace, and altitudes were simply read directly from the trace to the nearest 50 feet.

The indicated airspeed trace was consistently a smeared band of varying width, and a systematic procedure for estimating airspeed from the charts was therefore devised. Because of the large number of readings required, it was felt that the process of estimating the mid-point of the band at each data point would require an excessive amount of time. Therefore, for each pass, an average half-width of the band was determined. The airspeed at the lower edge of the band was then measured during chart reduction, and the half-width correction was included in the computer processing. The airspeed measurements performed in this fashion were taken from the chart once every second while the aircraft was in the dust cloud. These values were then used to compute an average airspeed for each pass.

A combination of nephelometer output and recorded visual markers was used to determine the dust cloud entrance and exit times. The nephelometer output was most often used to determine entry. The entry time selected was that time at which the nephelometer trace showed a sudden increase in scattering coefficient. Exit determination was more difficult using the nephelometer because of the delay time of the instrument during reduction of the scattering coefficient. The visual exit marker was therefore most often used to determine exit time. Due to operational difficulties specific to individual events or passes, this procedure varied occasionally. The entry and exit criteria for each are therefore listed with the pass log in the tables in Section 3, Volume I.

The cyclone valve position marker or the visicorder chart was only used in those cases where the cyclone valve was inadvertently opened after entry into the cloud or closed before exit, as determined by the entry and exit criteria. Corrections to dust concentration were made using this information, and their magnitude is indicated in the pass by "remarks" section.

The cloud width in meters was determined from the simple equation:

$$\text{Width} = 0.447 \times \text{TAS} \times \Delta t$$

where

TAS = true airspeed, mph

Δt = time in cloud = $t_{entry} - t_{exit}$, secs.

As discussed in Section 3, only the wet cyclone dust retrieval data were used to calculate dust concentration. Flow rates in the cyclone(s) were nearly constant at 100 ACFM. The required flow rate for isokinetic sampling at typical aircraft speeds would have been over 400 ACFM. A calculation employing a conservative model of particle collection by the cyclone inlet indicated that even under these conditions, all particle sizes of interest in this study were collected with nearly 100 percent efficiency. Therefore, the volume of air "swept out" by the inlet cross section was used in calculating the dust concentration. Experiments with the cyclone, however, demonstrated that it had an overall collection efficiency (by weight) of 86.2 percent. This correction factor was therefore applied in the dust concentration equation:

$$C = \frac{M \cdot 10^5}{44.7 \cdot \eta \cdot \text{TAS} \cdot \Delta t_{corr} \cdot A}$$

or

$$C = \frac{89.6 \cdot M}{\text{TAS} \cdot \Delta t_{corr}}$$

where

C	= dust concentration, 10^{-8} gm/cc
M	= dust retrieval per pass, mg
TAS	= true airspeed, mph
Δt_{corr}	= time in cloud corrected (if necessary) for late/early cyclone valve opening/closing, secs
A	= area of inlet = 29.0 cm
η	= overall cyclone collection efficiency by mass

AIV.3 CYCLONE EVALUATIONS

AIV.3.1 Cyclone Characteristics

Although preliminary calculations and tests of the cyclone separator were performed before use in the field, a detailed study of the Fisher-Klosterman XQ-3 cyclones had not been performed. Certain discrepancies in cyclone data began to appear early in the program. The dry cyclone inlet area was nearly six times larger than the wet cyclone inlet area and, because of the inlet collection efficiency statements made previously, it was expected that the quantity of dust collected could be in roughly the same proportion. This proved not to be the case, with the ratio of wet-to-dry dust collected fluctuating randomly from pass to pass and event to event. In addition, some experimenters believed that the potential existed for large particles to be caught and retained in the inlet piping only to be collected at a later time, thus biasing size distribution in the large-particle range for late passes. A brief series of experiments was therefore performed on the cyclones to establish their characteristics and to determine which data were satisfactory for analytical use.

AIV.3.2 Cyclone Experiments

Cyclone separators commonly suffer from particle build-up on the walls due to electrostatic forces. When the build-up has reached a given level, the accumulated material will often fall away from the wall

in "lumps" only to allow another build-up. This random process of wall loading and unloading is enhanced when cyclone vibrations occurs (as in an aircraft). In addition, the collection efficiency spectrum for cyclones is rather broad when compared to other particle separating devices, and particle blow-through is to be expected. The randomness of the ratio of wet-to-dry dust collection could have thus been a result of a combination of random unloading of either or both cyclones and the associated particle blow-through, and particle hang up in the cyclone inlet. The problem was further complicated by the fact the one cyclone wall was wet which would therefore alter its operating characteristics. Tests of cyclone efficiencies at flight flow rates (100 ACFM) were therefore required. Wind tunnel tests, though potentially most definitive of cyclone and inlet efficiencies, were considered prohibitive in cost. To generate the required dynamic pressure at the inlet to achieve these flow rates without changing the size of cyclone blower motors, and to allow examination of flow patterns in the immediate vicinity of the cyclone inlets, the experiments were carried out in the back of a small truck moving down an uncongested freeway.

AIV.3.2.1 Description of Truck Experiments

Two types of dust were first selected and analyzed to determine their size distribution using Quantimet 720 procedures discussed in a subsequent section. For conciseness, the two types are referred to by the initials "TD" and "BD". One dust was found to have a size distribution quite similar to many of the dust observed in the actual flights (TD), while the other was selected for its large particle content for use in "particle hang-up" experiments (BD).

The cyclones, inlets, and aircraft-mounting door were attached to a small pickup truck complete with portable power and water alcohol

sources. The power was used to drive the two hurricane blowers attached to the cyclone outlets, and a compressed air chamber with valve and regulator were used to force the water-alcohol mixture from its holding tank into the wet cyclone.

The cyclone inlets were aligned with the horizontal to create a 0° angle of attack orientation. Black tufting material was carefully taped to the inlets at various locations to assure the experimenter that unwanted flow patterns did not exist due to the proximity of the truck cab. The truck was driven at varying speeds chosen to be 30, 50, and 70 miles per hour. The cyclone flow rates therefore varied between about 88 and 106 ACFM. Preweighed amounts of both TD and BD were injected directly into the cyclone inlet in a fashion that would prevent large "lumps" of dust to fall on the walls. The weight ranges were chosen to represent typical amounts retrieved in actual field experiments. 10, 75, 200, and 500 milligrams, and occasionally as much as 2 grams, were injected into the dry cyclone. The samples were always injected in increasing amounts. Numerous retrieval jars were carried with the truck, and a plastic sheath was placed around the jar-mount on the sampler to allow the operator to remove and cap jars while the truck was in motion.

The usual procedure of the operator was to have the suction blowers operating at all times. When the truck speed was at the prescribed value, the inlet valve of the sampler of interest was opened. The operator then opened the vial containing the preweighed dust sample in the upper portion of the inlet making sure that no dust could be lost. The sample was then carefully injected and the vial recapped and stored, and the cyclone flow rate recorded from the suction blower. The inlet valve was then closed. In the case of the wet cyclone, the water inlet valve was then opened and the cyclone inlet valve was cycled open and closed several times. This allowed the water-alcohol solution trickling down the cyclone walls to develop swirl and thus wash more area more effectively. The inlets

were next examined for particle hang-up. Then, a "background" sample was taken on each cyclone to detect any dust that may have been retained in the cyclone and dislodged when the valves were opened and clear air was allowed to blow through. Upon return to the lab, all vials were weighed, and the retrieved dust was processed as discussed in Paragraph AIV. 1.

AIV. 3. 2. 2 Experimental Results

The most immediate result of these experiments was the determination that virtually no particles are detained in the wet cyclone inlet. A few BD particles were observed in the dry cyclone inlet on one occasion but were never discovered there in any previous or subsequent tests. Since, in the end, wet cyclone dust data were used solely in sizing analysis and concentration calculations, this one anomalous situation was discounted.

An overall cyclone collection efficiency was defined as retrieved dust mass divided by input dust mass, and plots of this efficiency as a function of sample size for both TD and BD were prepared. The wet cyclone was much more stable in its operation with an average overall efficiency of 86. 2 percent with a 1-0 error band of 2. 8 percent. The results were convincing enough to discount all dry cyclone data, and only wet cyclone data were used for the purposes of analysis in this report.

AIV. 3. 3 Theoretical Considerations

For the purposes of analyzing size distribution data, it was necessary to estimate the collection efficiency of the cyclone itself and its inlet as a function of particle size. These theoretical studies, which are described in the following pages, completed the post-test evaluation of the wet cyclone.

AIV. 3. 3. 1 Inlet Efficiency Calculations

As stated before, the flow through the cyclones was 100 ACFM while that required for isokinetic sampling can be calculated to be over 400 ACFM. This condition of anisokinetic sampling does not allow straightforward calculation of inlet collection efficiency. A conservative model more conducive to calculation was therefore chosen. Using this model, it is assumed that no flow goes through the inlet and that the inlet can therefore be treated as a "ribbon" in a free stream. Langmuir and Blodgett (1945)* developed a mathematical model predicting spherical particle collection efficiency on such a ribbon, although their model is only two-dimensional.

That model is described in terms of the particle Reynolds number given by:

$$R_e = \frac{2a\rho_a \vartheta}{u}$$

and a parameter K, given by

$$K = \frac{2\rho_s a 2 \vartheta}{9 u b}$$

where

a	=	particle radius
ρ_a	=	density of air
ρ_s	=	density of particle
ϑ	=	free stream velocity (aircraft speed)
u	=	viscosity of air
b	=	half-span of ribbon

* - Langmuir, I., and K. B. Blodgett, 1945: Mathematical Investigation of water droplet trajectories. General Electric Research Laboratory Report No. RL-225, Schenectady, New York, 47 pp.

For small values of the parameter K, the collection efficiency is given by:

$$E = 1.35 \left(\log 8 K_o\right)^2$$

where $$\left(K_o - 1/8\right) = \left(\frac{\tau}{\lambda_s}\right) \left(K - 1/8\right)$$

and where $$\frac{\tau}{\tau_s} = \frac{1}{R_e} \int_o^{R_e} \frac{dR_e}{\left(\frac{C_d R_e}{24}\right)}$$

where

C_d = particle drag coefficient

For large values of the parameter K, the efficiency is given by:

$$E = \frac{K}{K + H_e}$$

where

$$H_e = 0.48 + 0.046 \, R_e^{0.63}$$

Because the model is two-dimensional, it was further assumed that reasonably representative efficiencies could be obtained if the calculations were performed twice using each half-span of the idealized model. The efficiency curves were generated in this fashion, and it was observed that the number count would be low by the following amounts,

26 μm	-	9%
48 μm	-	3%
80 μm	-	1%

where the sizes were picked to correspond with mean diameters of size distribution bins, as discussed in Appendix IV.4.2.

AIV.3.3.2 Cyclone Efficiency Calculations

The manufacturers of the cyclones used on the sampling aircraft have published a collection efficiency curve for the dry-wall cyclone. This efficiency is defined in terms of a critical particle diameter, Dc. Dc is the diameter of the smallest particle to be collected with 100 percent efficiency. At the flow rate encountered in both the aircraft and the ground experiments (100 ACFM), and assuming a particle density of 2.5 gm/cm^3, the value of Dc is 108.3 microns. In addition, the manufacturer provides an empirical relation which relates the overall collection efficiency (by mass) to Dc.

$$E = 99.9 - 0.75\,Pc$$

where Pc is the percentage by mass of particles less than Dc in diameter.

Since the TD dust size distribution resembled quite closely much of the observed dust, this size information was used, in conjunction with the measured overall efficiency computed in the previous section, to indicate the wet-walled cyclone efficiency as a function of size. It was determined that 40.5 percent of the TD dust particles were less than 108 microns in size. Using the above relation, this indicated a dry-wall overall collection efficiency of 70 percent. By using the observed efficiency of 86.2 ± 8.4 percent (3σ value) in the same relation, it was possible to determine by trial and error that the critical size for the wet walls was:

$$Dc = 35 \pm \frac{33}{20} \text{ microns.}$$

An interesting side result is that wetting the walls of the cyclone evidently cut the critical size by 2/3 and increased the overall collection efficiency by 16 percent.

In order to be conservative in subsequent analyses regarding the number concentration of fine particles, it was decided to use the maximum

value of Dc as the critical diameter in the wet-walled cyclone. As a result, the apparent particle number counts were low by the following amounts due to cyclone efficiency:

26 μm	-	3%
48 μm	-	1%
80 μm	-	0%

Combining the results of subsections 3.3.1 and 3.3.2 of this appendix, the total particle number counts would be low by the following amounts due to inlet/cyclone efficiencies:

26 μm	$1 - \frac{1}{.91} \frac{1}{.97}$	=	13.3%
48 μm	$1 - \frac{1}{.97} \frac{1}{.99}$	=	4.1%
80 μm	$1 \cdot \frac{1}{.99}$	=	1.0%

The calculations of subsequent sections include these correction factors.

AIV.4 DENSITY AND SIZE DISTRIBUTION MEASUREMENTS

Dust from most of the aircraft passes for the seven events were analyzed for particle size distribution using MRI's Quantimet 720 Image Analyzing Computer. In addition, several samples were analyzed for density distribution using a densitometric flask. Using these two tools in concert for these special cases it was possible to generate not only particle number counts in a given size range, but to specify what fraction of the particles were of a given density range. The procedures and analysis leading to these results are described in the following subsections.

AIV. 4. 1 Density Separations

To perform density separation on selected dust samples, a preweighed quantity of the dust was deposited in a separatory flask full of Bromoform ($CHBr_3$), having a density of 2.85 gm/cm^3. Particles more dense than this would settle to the bottom of the flask. If a sufficient quantity of dust settled to the bottom it was carefully removed from the bottom of the flask. If not, acetone (density = 0.798 gm/cc) was added and carefully mixed until the required amount of dust was available. The dust and Bromoform/acetone mixture was then drawn off into a preweighed petri dish and stored. The fluid density was also recorded. The procedure was repeated at least two more times (occasionally three) until most of the dust had sunk and been drawn off. Mild agitation was performed periodically to assure that surface tension effects did not suspend particles that were of higher density than the fluid. On a few occasions a small amount of dust was retrieved from the top of the flask.

The petri dishes were then placed in moderate heat ($\approx 50\,^{\circ}C$) and ventilated to evaporate off the acetone and Bromoform. The dishes were reweighed after being allowed to stand at room temperature for several hours, and the sum of the masses retrieved in this fashion was compared to the original dust weight as a check of particle loss. Generally the loss fraction was less than 1 percent.

The question arises during this type of laboratory separation as to just how much time is required for particle settling in a fluid suspension. The procedure used during the density separations was to insert the dust and examine the suspension after five minutes. If large movements of particles were detected, more time was allowed until movement could not be detected. Generally speaking, the five-minute period proved sufficient. To verify this procedure, however, some simple calculations were performed. Assuming spherical particles and Stokes drag, the equation of motion for the dust particles is given by:

$$\frac{\pi}{6} D^3 \rho_p \frac{d^2y}{dt^2} = \frac{\pi}{6} D^3 (\rho_p - \rho_f) g - 3\pi \mu D \frac{dy}{dt}$$

where y = particle displacement, positive downward

D = particle diameter

ρ_p = particle density

ρ_f = fluid density $< \rho_p$

g = acceleration of gravity

μ = fluid viscosity

The solution to the above differential equation, with $y(o) = o$ and $o(o) = o$ assumed, is:

$$y(t) = (1-f) \frac{g}{\gamma^2} (e^{-\gamma t} - 1) + \frac{g}{\gamma} (1-f)t$$

where $f = \frac{\rho f}{\rho_p}$

and $\gamma = \frac{18\mu}{\rho_p D^2}$

Assuming a 30-micron particle of density 2.0 gm/cm^3, and using a value of viscosity of 1.89×10^{-2} gm/cm sec, the following brief table indicates the distance traveled by the particle in five minutes as a function of f.

f	y(cm)
0.8	3.11
0.9	1.56
0.95	0.78
0.99	0.16

The conclusions to be drawn from this brief calculation are straightforward. In order for a significant error by mass to be made due to slow particle settling, a large number of fine particles would be involved. Since a displacement of a large number of particles of 0.78 cm would easily be observable by the naked eye, one can be assured that the five-minute procedure discussed previously produces negligible error.

AIV.4.2 Size Analysis

In preparation for size distribution analysis, the dust that was either sized directly or separated into density gradations was placed in a standard laboratory gel. All the dust from a given sample was put in the gel at once to circumvent the problem of size distribution biasing during the act of removing a portion of a sample from its original container.

The particles were washed into the gel when it was quite warm and fluid. As it cooled, the mixture was agitated, producing a very homogeneous dispersement of the particles. When the temperature of the mixture was such that the particles were held in suspension but the gel had not "set," aliquots of the dust-gel mixture were drawn using a large diameter pipette and placed on microscope slides. Cover glasses placed over the sample were then used to disperse the gel droplet over the slide and force out air bubbles. The slides were allowed to stand until the gel had hardened into a permanent mount for the dust particles. The slides were then processed on the Quantimet 720 as discussed below.

The advantages of this method were numerous: (1) biasing due to excessive handling could be avoided; (2) simple laboratory equipment allowed excellent control of the suspension; (3) truly representative dust samples could be presented to the Quantimet for analysis; and (4) the final product allowed either permanent storage or, with treatment by water vapor and heat, total restoration of the original sample.

The method was tested prior to actual application to the Middle Gust-Mixed Company samples. These tests consisted of drawing several aliquot from a single vial of TD treated with gel and comparing the resulting size distributions. The number count in the smallest size range was found to agree to within 10-15 percent for all the aliquots, and this was deemed acceptable for the analyses in this report. In addition, for the cases where density separation was performed, a size distribution of a portion of an original sample was determined and compared to that constructed from the three or four density gradations generation from another portion of the same original sample. This test also verified the laboratory procedure to the accuracy required.

The actual processing of the slide samples for size distribution was done using MRI's Quantimet 720 Image Analyzing Computer. Basically, the Quantimet determines the length of the maximum horizontal chord of each particle in the television image presented to it by a microscope. An automatic multiplexing unit is available, called the Size Distributor (a tradename of Image Analysing Computers, Inc., Monsey, N. Y.), which yields the number count of particles larger than a predetermined size set for each of eight channels. These critical sizes are chosen by the machine operator. By subtracting the number count generated in two consecutive channels, one obtains the total particle count between the two associated critical sizes. These incremental size ranges are referred to as "bins."

The particle size range of interest for the high-energy tests was determined early in the program to be between 20 and 1500 microns. Because this is a rather broad range, two microscope magnifications were required for the analysis - 25 and 40 power. The eight bin size ranges were selected as follows:

	40X	25X
Bin 1	20-32 microns	128-192 microns
Bin 2	32-64	192-256
Bin 3	64-96	256-384
Bin 4	96-128	384-512
Bin 5	128-192	512-768
Bin 6	192-256	768-1024
Bin 7	256-384	1024-1536
Bin 8	> 384	> 1536

Because larger particles were more scarce, a larger area of the microscope slides had to be analyzed at 25 power to obtain a statistically representative sample. This implied that a special normalization of the 25 power size distribution data to the 40 power data had to be performed. Three bins are seen to overlap in the above table. Since the total particle count was always highest in the Bin 5-Bin 1 combination (as opposed to Bin 6-Bin 2, etc.), the ratio of Bin 1, 25 power, to Bin 5, 40 power, was used as the normalizing factor. Note that this process yields 11 complete bins of count data.

AIV.4.3 Size Distribution Calculation Details

The following analysis of size distribution results has been generalized to the case of multiple density stages: the samples for which no density separation was done are simply one-dimensional cases of the following results.

In order to determine particle density distributions, it is necessary to normalize the raw Quantimet count to the mass of particles collected after each density separation. To do this, a mean density for each separation must be estimated. The particles collected after settling in the separatory funnel actually have densities defined between two boundaries that shall be denoted:

$\rho_u^*(\ell)$ = upper density boundary of density separation ℓ

$\rho_\ell(\ell)$ = lower density boundary of density separation ℓ

For the purposes of this analysis, the average density of particles in a given separation will be taken as the mean of these two boundaries, i.e.,

$$\bar{\rho}(\ell) = \frac{\rho_u(\ell) + \rho_\ell(\ell)}{2}$$

If N(i, ℓ) is the raw Quantimet number count (after 40X-25X normalization) for bin i, density separation ℓ, the total particle number count in bin i retrieved during that separation is:

$$\tilde{N}(i, \ell) = \frac{m(\ell)}{\frac{\pi}{6}\bar{\rho}(\ell)\Sigma_s N(s, \ell) D(s)^3} \cdot N(i, \ell)$$

where m (ℓ) is the mass of dust retrieved during the separation, and D(i) is the mean diameter of bin i as determined from the simple relation:

$$D(i) = \frac{D(i)_u + D(i)_\ell}{2}$$

Here, $D(i)_u$ and $D(i)_\ell$ are the boundaries of bin i. Thus, D(i) is 26 microns, etc. Note that spherical particles have been assumed. The total number of particles thus retrieved in bin i for all separations is:

$$N_\tau(i) = \Sigma_\ell \tilde{N}(i, \ell)$$

The fraction of particles in bin i of mean density ℓ is given by:

$$f(i, \ell) = \frac{\tilde{N}(i, \ell)}{N_\tau(i)} = \frac{\tilde{N}(i, \ell)}{\Sigma_\ell \tilde{N}(i, \ell)}$$

Another way of stating the above result is that f(i, ℓ) represents the fraction of particles in the size range of:

* - Fortran-like subscripts will be used for convenience.

$$D(i)_{\ell} < D < D(i)_{u}$$

which are in the density range:

$$\rho_{\ell}(\ell) < \rho < \rho_{u}(\ell) \quad .$$

The mean density for the bin i is now a natural extension being given by:

$$\rho(i) = \Sigma_{\ell} f(i, \ell)\, \bar{\rho}(\ell)$$

The output of the Quantimet 720 was in the form of punched paper tape. This paper tape was processed by MRI's PDP-8 computer using the above relations, and the tabular output by pass is presented in the data portion of this report.

It was further decided to normalize the size distributions to the mass concentration determined from the pass log calculation. In this fashion, not only the slope of the distribution curve would be available, but also an estimate of the absolute number of particles per cubic centimeter in the cloud would be directly visible on size distribution plots. This number concentration for bin i is given by:

$$\eta_{\tau}(i) = \frac{M}{\frac{\pi}{6} \Sigma_{s} \rho(s) N_{\tau}(s) D(s)^{3}} \cdot N_{\tau}(i)$$

where M is the pass concentration and $\rho(s)$ is the mean density of bin s.

Finally, the size distribution was generated in terms of the general function:

$$\log \left(\frac{dN(i)}{d \log D} \right) \quad \text{vs} \quad \log D$$

This "continuous" relationship has been approximated for the purposes of this report by:

$$\log \left(\eta_{T_{(i)}} \frac{D_{(i)}}{\Delta D(i)} \right) \text{ vs } \log D(i)$$

where $D_{(i)}$ is the mean size of bin i and $\Delta D_{(i)}$ is the "width" or range of bin i. One should note that a size distribution of the form:

$$\frac{dN}{d \log D} = CD^{-\beta}$$

on log-log paper will be the straight line,

$$\log \left(\frac{dN}{d \log D} \right) = \log C - \beta \log D$$

where β is the absolute value of the slope. The equivalent result stated in the common Junge type distribution format is:

$$\frac{dN}{dD} = CD^{-(\beta + 1)}$$

As a conclusion to this section, it should be pointed out that, in the case where no density separations were performed, a mean density for each bin was arbitrarily selected to be 2.0 gm/cm^3. This approximates the mean densities observed for those samples where separation was performed. This assumption allows one to estimate the number of concentrations of particles in those cloud passes for which the separations were not performed.

In addition, the fallout samples were normalized to ground measurements of fallout mass per unit area. 2.0 gm/cm^3 were also used where density separations were not performed.

Finally, because of a programming error, the tabular printout size distributions for cases where no density separations were performed ($\tilde{N}(i, 1)$, $N_T(i)$) were calculated using a mean density of 0.01 gm/cm^3. Since these results were later normalized to pass/fallout concentrations using a density of 2.0 gm/cm^3, the error was not corrected on the printouts.

AIV.5 ERROR ANALYSIS

In order to define the limits of accuracy of the calculations described in Paragraph 4.3 of this appendix, a detailed error analysis was undertaken. This analysis can be broken into two distinct portions: that relating to the pass log calculations, and that of the density and size distribution calculations.

AIV.5.1 Pass Log Data

The sources of error in the dust concentration calculations are in the measurement of airspeed, time in the dust cloud, total dust weight, and in the experimental error associated with the cyclone efficiency determination discussed previously in this appendix.

The error in airspeed is of two origins. The first is due to the smeared trace on the Visicorder as discussed previously. During the course of a pass, the width of this trace varied sporadically. Therefore, the half-width correction factor discussed previously was in error. For each pass, the maximum and minimum half-width were determined and compared to the half-width correction factor. The largest difference between maximum/minimum half-width and the nominal value thus represented the maximum possible error in airspeed since the difference was not averaged over the time span of the pass.

The second airspeed error was due to the instrument characteristics. Since the airspeed indicated by the portable instrument package is directly proportional to the dynamic pressure of the pitot system,

$$\rho_{alt} \; V_{act}^2 = \rho_{s.l.} \; V_{ind}^2$$

where ρ_{alt} = air density at altitude

$\rho_{s.l.}$ = air density at sea level

V_{ind} = indicated airspeed

and V_{act} = actual or true airspeed.

The TAS for the pass log calculations was determined from the IAS by:

$$TAS = \sqrt{\frac{\rho_{s.l.}}{\rho_{alt}}} \cdot IAS$$

For this calculation, a standard atmosphere (and hence, standard density lapse rate) was assumed. For the purposes of this calculation, a nominal latitude of 40° North in the month of July was assumed. The standard deviation of the density at 10,000 feet is 0.233×10^{-4} slugs/feet^3 which corresponds to 1.3 percent.

One method of estimating the contributions to the total error by each of the above sources is by the use of first order differentials:

$$d\,TAS \cong -\frac{1}{2} \frac{(\rho_{s.l.})^{1/2}}{(\rho_{act})^{3/2}} \cdot IAS\, d\,\rho_{alt} + \sqrt{\frac{\rho_{s.l.}}{\rho_{alt}}} \cdot d\,IAS$$

Put into relative error form

$$\frac{d\,TAS}{TAS} \cong -\frac{1}{2} \frac{d\,\rho_{alt}}{\rho_{alt}} + \frac{d\,IAS}{IAS}$$

For non-infinitesimal errors, this becomes

$$\frac{\Delta\,TAS}{TAS} = -\frac{1}{2} \frac{\Delta\,\rho_{alt}}{\rho_{alt}} + \frac{\Delta\,IAS}{IAS}$$

Both errors are "$\pm$" quantities and unrelated since the second error represents a chart measuring error so that maximum error can be given as:

$$\frac{\Delta TAS}{TAS_{max}} = \frac{1}{2}\left|\frac{\Delta \rho_{alt}}{\rho_{alt}}\right| + \left|\frac{\Delta IAS}{IAS}\right|$$

To be consistent, the quantity $\Delta \rho_{alt}$ must be equated to $3\sigma\rho$, where $\sigma\rho$ is the standard deviation of the density. Thus, the general formula for airspeed error used in pass log calculations is:

$$\frac{\Delta TAS}{TAS} = \frac{3}{2}(.013) + \left|\frac{\Delta IAS}{IAS}\right|$$

The measurement of time on the Visicorder charts was determined to be accurate to within 0.1 second in most cases. Unfortunately, judgement was required as to when the aircraft was actually crossing the boundaries of the cloud. The judgement involved in using visual exit criteria is obvious; the reduction of nephelometer traces for entry time is more subtle because of the slight lag in instrument response. To avoid unnecessary complexity* in analyzing the pass data, it was decided to treat the criteria as being absolute. Thus, the total time error is simply the sum of the time measurement errors at entry and exit. Occasionally, however, when questionable traces or visual responses were recorded, the error was increased.

To determine the error in dust measurement, a series of laboratory experiments was run whereby a sample of dust was preweighed, injected

---

* - The magnitude of dust cloud concentration is of more interest than the exact value of the third significant digit.

into a water-alcohol mixture, and reconstructed using the retrieval techniques discussed in Paragraph AIV.1. It was determined that the resolution of the procedure was 6.8 percent on average (always a loss) with a minimum absolute resolution of 0.5 mg. This did not include the weighing error of the electronic balances used which was conservatively estimated to be 0.5 mg. Hence, the error in measured mass was taken always to be:

$$M = \begin{cases} +0.5 \text{ mg} + \max(6.8\%,\ 0.5 \text{ mg}) \\ -0.5 \text{ mg} \end{cases}$$

The experiment error in cyclone overall collection efficiency was stated to be 2.8 percent (1σ). Because maximum error has been used consistently in the above analysis, the 3σ error in the cyclone efficiency was used (8.4 percent) in pass log error calculations.

Using the same finite-differential approximation method discussed previously, the relative error in cloud width and pass concentration are given by:

$$\left(\frac{\Delta W}{W}\right)_{max} \cong \left|\frac{\Delta TAS}{TAS}\right| + \left|\frac{\Delta(\Delta t)}{\Delta t}\right|$$

and

$$\left(\frac{\Delta C}{C}\right)_{max} = \left|\frac{\Delta M}{M}\right| + \left|\frac{\Delta TAS}{TAS}\right| + \left|\frac{\Delta \left|\Delta t_{corr}\right|}{\Delta t_{corr}}\right| + \left|\frac{\Delta \eta}{\eta}\right|$$

where

$$\left|\frac{\Delta \eta}{\eta}\right| = \frac{0.084}{0.862} = 0.097$$

Note that because of distinctions in some of the terms in "+" errors and "-" errors, $(\Delta C/C)_{max}$ cannot be given as a simple "+" error. Therefore, the error calculation was performed once for the "+" side and

once for the "-" side, and both results have been recorded in the pass log tables. Generally speaking, the errors accumulated as above were bounded by +30 percent and -20 percent. This magnitude of error is not at all unusual in aerosol work.

AIV.5.2 Density and Size Distribution Data

The analysis of size distribution errors is much more complex than that of the pass log data. To begin with, the differential approximation method is virtually impossible to apply because mathematical inconsistencies develop when one attempts to isolate the "+" terms when calculating the maximum relative error.*

Instead, a method of estimating the size distribution errors using the theory of error propagation as summarized by Beers (1957)** was selected. Beers indicates that, if the dependent variable z is calculated using the independent variables x and y by the relation:

$$z = z(x, y)$$

where x and y are statistical quantities (ones for which several distinct measurements are available), then the standard deviation in z is given by:

$$S_z = \sqrt{\left(\frac{\partial z}{\partial x}\right)^2 S_x^2 + \left(\frac{\partial z}{\partial y}\right)^2 S_y^2 + 2\rho_{xy}\left(\frac{\partial z}{\partial x}\right)\left(\frac{\partial z}{\partial y}\right) S_x S_y}$$

* - This occurs loosely speaking, because number counts have been normalized by quotients that contain summations: summations which always have as one term the number count to be normalized. Thus, errors considered negative (positive) for one bin calculation would be by necessity positive (negative) for another bin calculation.

** - Beers, Y., 1957: Introduction to the Theory of Error. Massachusetts, Addison-Wesley Pub. Co., 65 pp.

where S_x, S_y = deviation in x, y

and

$$\rho_{zy} = \frac{1}{(K-1) S_x S_y} \left[\sum_{n=1}^{K} (x_n y_n) - K \bar{x} \bar{y} \right]$$

where ρ_{xy} = correlation coefficient between x and y

K = number of data points for x and y

$\bar{x}$, $\bar{y}$ = observed mean of x and y

when x and y are truly independent (uncorrelated).

$$\rho_{xy} = 0$$

so that the deviation in z is given by

$$S_z^2 = \left(\frac{\partial z}{\partial x}\right)^2 S_x^2 + \left(\frac{\partial z}{\partial y}\right)^2 S_y^2$$

In order to apply this method to the size distributions, one must assume that the error measured or estimated for a given parameter is equal to the standard deviation of several such measurements or estimates of the same parameter. Because most errors estimated in this section are maximum possible errors, the results of this analysis will therefore be conservative.

To apply the model, the basic size distribution normalization curves are required and are repeated here for convenience. See Paragraph AIV.4.3 for symbol definitions.

$$\eta_\tau(i) = \frac{M}{\frac{\pi}{6} \sum_s \rho(s) N_\tau(s) D(s)^3} \cdot N_\tau(i)$$

where

$$N_\tau(i) = \sum_\ell \tilde{N}(i, \ell)$$

and $\tilde{N}(i, \ell)$ is given by

$$\tilde{N}(i, \ell) = \frac{m(\ell)}{\frac{\pi}{6} \bar{\rho}(\ell) \sum_s N(s, \ell) D(s)^3} \bullet N(i, \ell)$$

The final form of the size distributions was given as

$$\log \eta_\tau(i) \frac{D(i)}{\Delta D(i)} \Bigg) \quad \text{vs. } \log D(i)$$

Thus, the final form of the $1 - \sigma$ error bands is

$$\log \left\{ \left(\eta_\tau(i) \pm S_{\eta_\tau}(i) \right) \frac{D(i)}{\Delta D(i)} \right\} \quad \text{vs. } \log D(i)$$

Applying the propagations model

$$S^2_\eta(i) = \sum_s \left\{ \left(\frac{\partial \eta_\tau(i)}{\partial N_\tau(s)} \right)^2 S^2_{N\tau}(s) + \left(\frac{\partial \eta_\tau(i)}{\partial \rho(s)} \right)^2 S^2_\rho(s) \right\} + \left(\frac{\partial \eta_\tau(i)}{\partial M} \right)^2 S^2_M$$

If MF(i) is defined as

$$MF(i) = \frac{N_\tau(i) \ \rho(i) \ D(i)^3}{\sum_s N_\tau(s) \ \rho(s) \ D(s)^3}$$

than the above derivatives are given by

$$\frac{\partial \eta_\tau(i)}{\partial N_\tau(s)} = \begin{cases} \left(1 - MF(i)\right) \bullet \dfrac{\eta_\tau(i)}{N_\tau(i)} & \text{for } s = i \\ -MF(s) \bullet \dfrac{\eta_\tau(s)}{N_\tau(s)} & \text{for } s \neq i \end{cases}$$

$$\frac{\partial \eta_\tau(i)}{\partial \rho(s)} = -\frac{\eta_\tau(i)}{\rho(s)} \quad MF(s) , \qquad \text{all } s, i$$

$$\frac{\partial \eta_\tau(i)}{\partial M} = \frac{\eta_\tau(i)}{M} \qquad \text{all } i$$

The values of $S_{N\tau(i)}$ and $s\rho_{(i)}$ are calculated by applying the deviation equation to the other normalizations, yielding

$$S^2_{N_\tau(i)} = \sum_{\ell} S^2_{\tilde{N}(i,\ell)}$$

and

$$S^2_{(i)} = \left(\frac{\partial \rho(i)}{\partial N_\tau(i)}\right) S^2_{N_\tau(i)} + \sum_{\ell}\left\{\left(\frac{\partial \rho(i)}{\partial \tilde{N}(i,\ell)}\right)^2 S^2_{\tilde{N}(i,\ell)} + \left(\frac{\partial \rho(i)}{\partial \bar{\rho}(\ell)}\right)^2 S_{\bar{\rho}(\ell)}\right\}$$

where the derivatives are given by

$$\frac{\partial \rho(i)}{\partial N_\tau(i)} = \frac{\rho(i)}{N_\tau(i)} , \qquad \text{all } i$$

$$\frac{\partial \rho(i)}{\partial \tilde{N}(i,\ell)} = \frac{\bar{\rho}(\ell)}{N_\tau(i)} , \qquad \text{all } i, \ell$$

$$\frac{\partial \rho(i)}{\partial \bar{\rho}(\ell)} = \frac{\tilde{N}(i,\ell)}{N_\tau(i)} , \qquad \text{all } i, \ell$$

Required for the above calculation is $S^2_{\tilde{N}(i,\ell)}$, which is given by

$$S^2_{\tilde{N}(i,\ell)} = \left(\frac{\partial \tilde{N}(i,\ell)}{\partial m(\ell)}\right)^2 S^2_{m(\ell)} + \sum_{j}\left\{\left(\frac{\partial \tilde{N}(i,\ell)}{\partial N(j,\ell)}\right)^2 S^2_{N(j,\ell)}\right\} + \left(\frac{\partial \tilde{N}(i,\ell)}{\partial \bar{\rho}(\ell)}\right)^2 S^2_{\bar{\rho}(\ell)}$$

If $VF(i,\ell)$ is defined as

$$VF(i,\ell) = \frac{N(i,\ell)\,D(i)^3}{\sum_s N(s,\ell)\,D(s)^3}$$

then the derivatives for the latter deviation equation are

$$\frac{\partial \tilde{N}(i,\ell)}{\partial N(j,\ell)} = \begin{cases} (1 - VF(i,\ell)) \cdot \dfrac{\tilde{N}(i,\ell)}{N(i,\ell)}, & \text{for } j = 1 \\ -VF(j,\ell) \cdot \dfrac{\tilde{N}(i,\ell)}{N(j,\ell)}, & \text{for } j \neq 1 \end{cases}$$

$$\frac{\partial \tilde{N}(i,\ell)}{\partial m(\ell)} = \frac{\tilde{N}(i,\ell)}{m(\ell)}$$

and

$$\frac{\partial \tilde{N}(i,\ell)}{\partial \bar{\rho}(\ell)} = -\frac{\tilde{N}(i,\ell)}{\bar{\rho}(\ell)}$$

This completed model of syi distribution errors was programmed and applied to all available data with the results being plotted in the form of nominal values and 1σ error bands.

The measurement errors to be input into these calculations are S_M, $S_{m(\ell)}$, $S_{\bar{\rho}(\ell)}$, and $S_{N(i\,\ell)}$. Each is discussed briefly in the following paragraphs.

The value of S_M, the pass concentration error, is determined from the pass log data. However, the error recorded in the pass concentration column was calculated using the 3σ error from the cyclone overall collection efficiency experiments. The error in concentration was therefore adjusted downward by 2σ to be consistent with the use of S_m which is a 1σ quantity.

$S_{m(\ell)}$ is the error in the measurement of the separated mass for density band ℓ. As discussed previously, this error is taken to be 6.8 percent of the sample or 0.5 mg, whichever is greater.

$S_{\bar{\rho}(\ell)}$ is the error in mean density of separation ℓ. Since $\bar{\rho}_{(\ell)}$ was given as

$$\rho_{(\ell)} = \frac{\rho_u(\ell) - \rho_\ell(\ell)}{2}$$

a conservative estimate of $S_{\bar{\rho}(\ell)}$ is given by

$$S_{\bar{\rho}_{(\ell)}} = \frac{\rho_u(\ell) - \rho_\ell(\ell)}{2}$$

In those cases where the first separation was of particles that sank in the pure Bromoform, $\rho_u(\ell)$ was arbitrarily taken to be 3.0, and $\bar{\rho}_{(1)}$ was taken to be 2.85 (= ρ Bromaform). The error was then given by

$$S_{\bar{\rho}(1)} = \rho_u(1) - \bar{\rho}(1) = 0.15 \text{ gm/cc.}$$

A similar procedure was followed for the cases where the last separation was removal of floating particles.

$S_{N(i,\ell)}$ is the error in determining the size distribution using the Quantimet 720. This error occurs whenever the total number of particles sized and counted is other than ∞. The relative error in number count in a given bin is given by the theory of Poisson as

$$\epsilon_N = \frac{1}{\sqrt{N}}$$

Applying this to the situation at hand, where S is an absolute error,

$$S_{N(i,\ell)} = \epsilon_{N(i,\ell)}$$

$$= \sqrt{N(i,\ell)}$$

It is to be noted, however, that the Poisson formula specifies the actual number count of a given bin. In this analysis, it must be recalled that bin overlap was used to generate $N(i, \ell)$. Therefore, even though bin 5, 25X and bin 1, 40X, cover the same size range, the count from 25X analysis for bins 5-11 must be used in the number count error equation listed above.

Finally, it should be noted that this analysis has not included errors in calculating D(i). The Quantimet 720 sizes particles according to their maximum horizontal (scan direction) chord. Its specifications indicate that it can do this with negligible error. However, the maximum horizontal chord of a particle may or may not be the appropriate diameter to use in specifying the particle, depending on the degree of irregularity and orientation to the scan direction. It becomes difficult to estimate sizing error (related to number count) over a range of sizes and such an effort was not included. Neglecting this, one could also question the validity of using the midpoint of the bin size range as the mean size ($D(\ell)$). of the particles in bin 1. To examine this problem, a simple set of calculations was performed to determine the error in such as assumption.

If D_u, D_ℓ = the upper and lower diameters of a bin, and ΔN is the number count contained in the bin, then

$$\Delta N = \int_{D_\ell}^{D_u} \frac{\partial N}{\partial D} \, \partial D$$

Also, if $\tilde{D}$ represents the true mean particle size, it is given by

$$\tilde{D}^3 = \frac{1}{\Delta N} \int_{D_L}^{D_u} D^3 \frac{\partial N}{\partial D} \partial D$$

As discussed previously, the Junge form of a typical dust size is given by

$$\frac{\partial N}{\partial D} = CD^{-(\beta + 1)} = CD^{\alpha}$$

where $-\beta$ is slope observed on log-log plots of size distribution dat
Using this in the above integral, one gets

$$\tilde{D} = \begin{cases} \sqrt[3]{\frac{\alpha + 1}{\alpha + 4} \cdot \frac{D_u^{4+\alpha} - D_L^{4+\alpha}}{D_u^{1+\alpha} - D_L^{1+\alpha}}} & , \quad \alpha \neq -4 \\ \sqrt[3]{3} \cdot \frac{\ln \frac{D_u}{D_L}}{D_L^{-3} - D_u^{-3}} & , \quad \alpha = -4 \end{cases}$$

These calculations were performed for several of the bins used on the Quantimet 720 and for several of the slopes observed on the size distribution plots. The results are summarized in Table AIV-1. This table indicates that the largest errors were made for the most part in small size ranges where the slopes were large in absolute value. However, even at a relatively high slope of -0.3, the largest error was less than 0.6 percent.

Despite the fact that the magnitude of these errors is comparable to those in other sections, the fact that the larger ones occur at the low end of the spectrum where few slope measurements are made precluded

Table AIV-1. Mean size errors for various Junge distributions and bin size ranges.

$\tilde{D}$	% Difference

Bin Dimensions (Microns) D_L	D_U	$\bar{D}$	Log-Log Slope α	-1.5 -2.5		-2.0 -3.0		-2.5 -3.5		-3.0 -4.0	
20	32	26		25.3	2.8	25.1	3.6	24.8	4.8	24.6	5.7
96	128	112		110.9	1.0	110.5	1.4	110.1	1.7	109.5	2.3
192	256	224		221.7	1.0	220.9	1.4	220.2	1.7	219.1	2.2
384	512	448		443.4	1.0	441.9	1.4	440.4	1.7	438.2	2.2
1024	1536	1280		1254.0	2.1	1245.6	2.8	1237.2	3.5	1227.0	4.3

$$* \% \text{ Difference} = \frac{|\tilde{D} - \bar{D}|}{\bar{D}} \bullet 100\%$$

the necessity for inclusion of these errors. In addition, because the calculation of these errors for use in correcting the slope requires the knowledge of the final result, the process is iterative by nature an and is deemed excessively complex for the problem at hand.

APPENDIX V

SIZE DISTRIBUTION DATA-AIRBORNE DUST SAMPLES

SIZE DISTRIBUTION

Middle Gust I Pass 1

Size (Microns)	dN/dLOG D (per cc)	Error +	Error -
26	1.27 E-2	1.81 E-2	7.27 E-3
48	5.94 E-3	8.50 E-3	3.38 E-3
80	4.77 E-3	6.80 E-3	2.74 E-3
112	5.44 E-3	7.79 E-3	3.10 E-3
160	3.68 E-3	5.25 E-3	2.12 E-3
224	2.09 E-3	3.01 E-3	1.17 E-3
320	4.44 E-4	6.68 E-4	2.21 E-4
448	3.28 E-4	4.94 E-4	1.62 E-4
640	1.73 E-4	2.42 E-4	1.03 E-4
896	3.82 E-6	7.75 E-6	********
1280	2.73 E-6	4.45 E-6	1.00 E-6

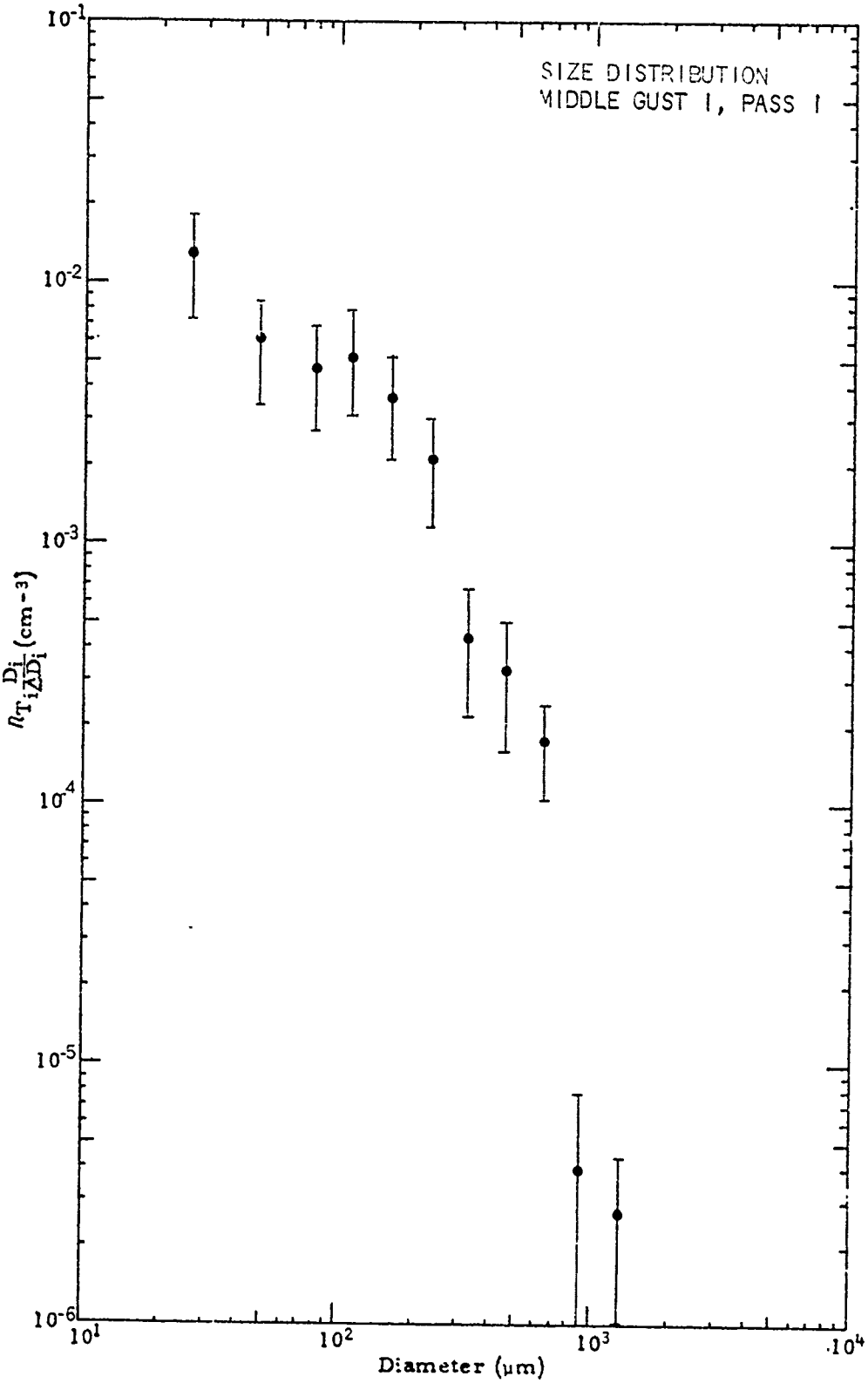
SIZE DISTRIBUTION
MIDDLE GUST 1, PASS 1
10^{-1}
10^{-2}
10^{-3}
10^{-4}
10^{-5}
10^{-6}
$n_T \frac{D_i}{\sum D_i}$ (cm^{-3})
10^1
10^2
10^3
10^4
Diameter (μm)

SIZE DISTRIBUTION

Middle Gust I Pass 2

Size (Microns)	dN/dLOG D (per cc)	Error +	Error -
26	9.12 E-3	1.37 E-2	4.58 E-3
48	6.30 E-3	9.41 E-3	3.18 E-3
80	5.12 E-3	7.64 E-3	2.60 E-3
112	3.01 E-3	4.51 E-3	1.52 E-3
160	1.78 E-3	2.66 E-3	9.05 E-4
224	8.93 E-4	1.36 E-3	4.27 E-4
320	3.20 E-4	4.90 E-4	1.50 E-4
448	9.22 E-5	1.65 E-4	1.94 E-5
640	4.49 E-5	7.69 E-5	1.29 E-5
896	1.68 E-5	2.47 E-5	8.87 E-6
1280	0.0	0.0	0.0

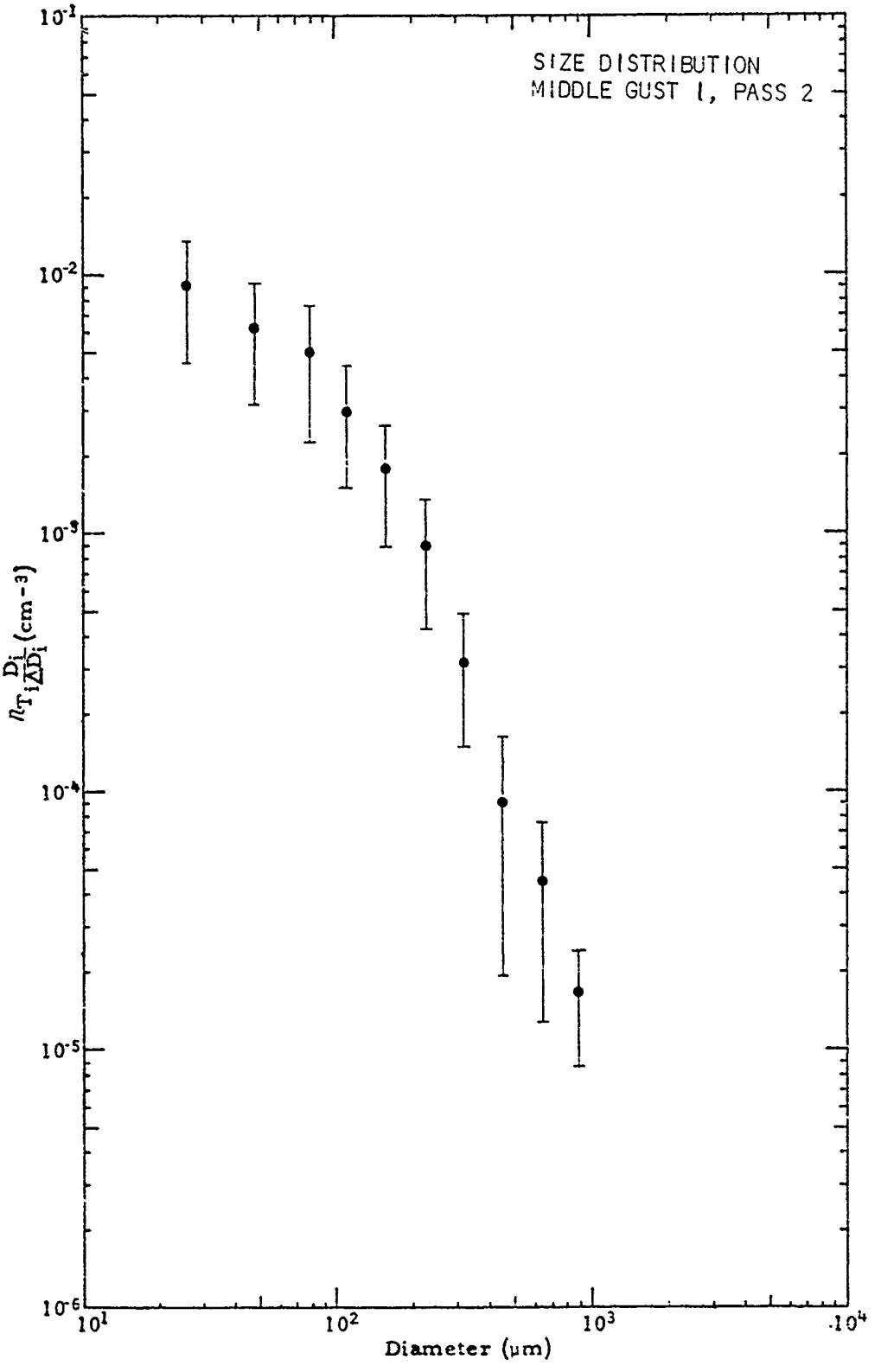
SIZE DISTRIBUTION
MIDDLE GUST 1, PASS 2
10^{-1}
10^{-2}
10^{-3}
10^{-4}
10^{-5}
10^{-6}
$n_T \frac{D_i}{\Delta D_i}$ (cm^{-3})
10^1
10^2
10^3
10^4
Diameter (μm)

SIZE DISTRIBUTION

Middle Gust I Pass 3

Size (Microns)	dN/dLOG D (per cc)	Error +	Error -
26	1.56 E-2	2.81 E-2	3.08 E-3
48	6.16 E-3	1.08 E-2	1.50 E-3
80	9.48 E-4	1.71 E-3	1.83 E-4
112	1.77 E-4	3.39 E-4	1.56 E-5
160	1.27 E-4	2.67 E-4	********
224	5.11 E-5	1.71 E-4	********
320	7.24 E-5	1.27 E-4	1.79 E-5
448	0.0	0.0	0.0
640	0.0	0.0	0.0
896	8.51 E-4	1.38 E-3	3.21 E-6
1280	0.0	0.0	0.0

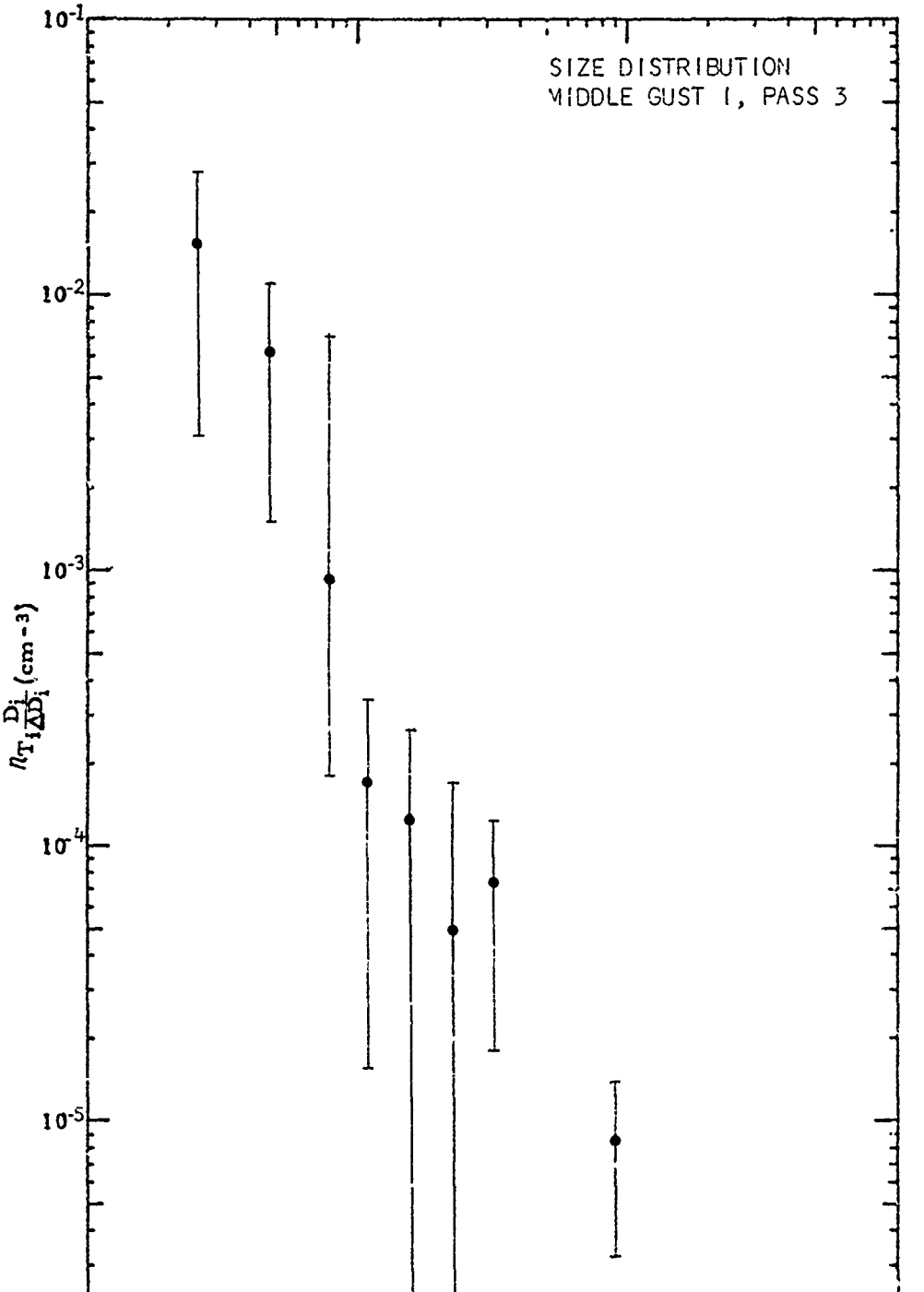
SIZE DISTRIBUTION
MIDDLE GUST I, PASS 3
10^{-1}
10^{-2}
10^{-3}
10^{-4}
10^{-5}
10^{-6}
$n_{T_i} \frac{D_i}{\Delta D_i}$ (cm^{-3})
10^1
10^2
10^3
10^4
Diameter (μm)

SIZE DISTRIBUTION

Middle Gust I Pass 5

Size (Microns)	dN/dLOG D (per cc)	Error +	Error -
26	1.07 E-2	1.55 E-2	5.93 E-3
48	7.17 E-3	1.03 E-2	4.05 E-3
80	2.31 E-3	3.33 E-3	1.29 E-3
112	1.64 E-3	2.37 E-3	9.08 E-4
160	7.07 E-4	1.03 E-3	3.88 E-4
224	2.64 E-4	4.20 E-4	1.08 E-4
320	8.63 E-5	1.39 E-4	3.37 E-5
448	1.13 E-5	1.63 E-5	6.34 E-6
640	0.0	0.0	0.0
896	0.0	0.0	0.0
1280	0.0	0.0	0.0

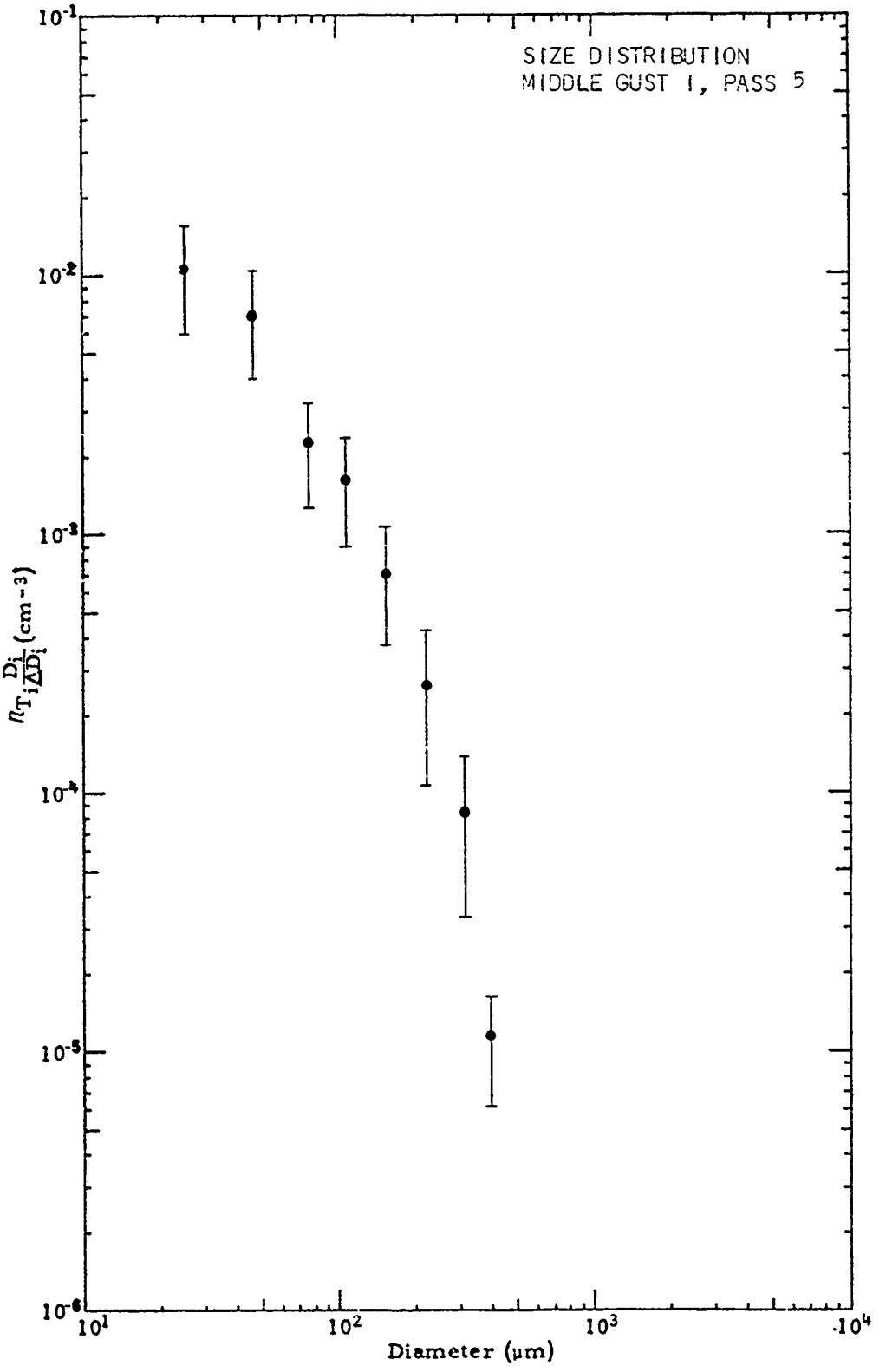
SIZE DISTRIBUTION
MIDDLE GUST 1, PASS 5
10^{-1}
10^{-2}
10^{-3}
10^{-4}
10^{-5}
10^{-6}
$n_{T_i} \frac{D_i}{\sum D_i}$ (cm^{-3})
10^1
10^2
10^3
10^4
Diameter (μm)

SIZE DISTRIBUTION

Middle Gust I Pass 6

Size (Microns)	dN/dLOG D (per cc)	Error +	Error -
26	8.95 E-3	1.18 E-2	4.86 E-3
48	4.81 E-3	6.74 E-3	2.89 E-3
80	1.70 E-3	2.39 E-3	1.01 E-3
112	9.62 E-4	1.36 E-3	5.67 E-4
160	2.60 E-4	3.84 E-4	1.36 E-4
224	9.56 E-5	1.73 E-4	1.82 E-5
320	8.99 E-6	2.04 E-5	********
448	6.29 E-6	8.88 E-6	3.71 E-6
640	0.0	0.0	0.0
896	0.0	0.0	0.0
1280	0.0	0.0	0.0

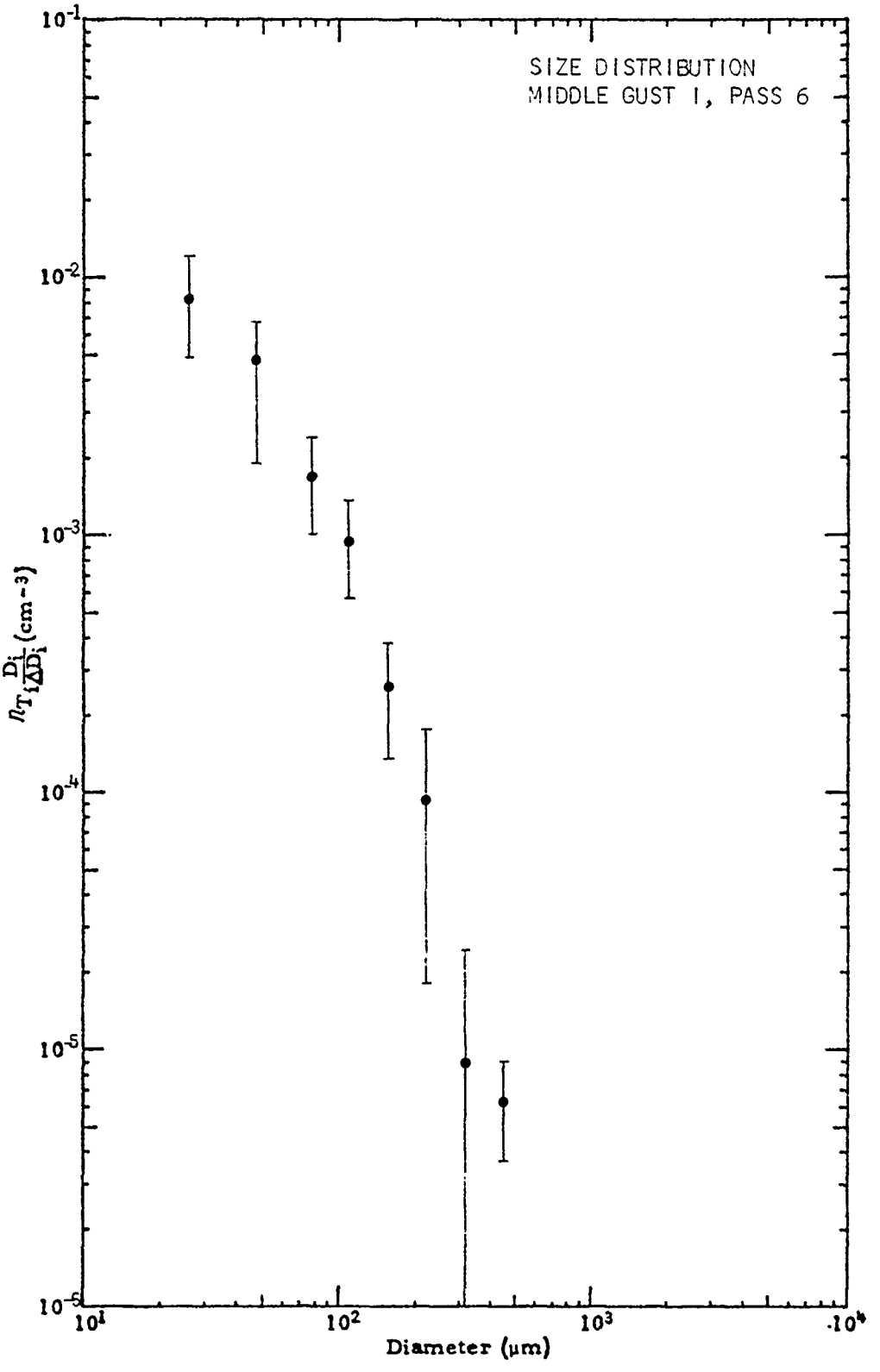
SIZE DISTRIBUTION
MIDDLE GUST I, PASS 6
10^{-1}
10^{-2}
10^{-3}
10^{-4}
10^{-5}
10^{-6}
$n_{T_i}\frac{D_i}{\Delta D_i}$ (cm^{-3})
10^1
10^2
10^3
10^4
Diameter (μm)

SIZE DISTRIBUTION

Mine Throw I Pass 4

Size (Microns)	dN/dLOG D (per cc)	Error +	Error -
26	1.93 E-1	2.48 E-1	1.39 E-1
48	1.52 E-1	1.94 E-1	1.10 E-1
80	1.03 E-1	1.31 E-1	7.43 E-2
112	5.75 E-2	7.34 E-2	4.16 E-2
160	2.38 E-2	3.04 E-2	1.73 E-2
224	7.97 E-3	1.07 E-2	5.28 E-3
320	1.71 E-3	2.50 E-3	9.23 E-4
448	2.28 E-4	3.60 E-4	9.65 E-5
640	1.27 E-4	1.93 E-4	6.07 E-5
896	0.0	0.0	0.0
1280	0.0	0.0	0.0

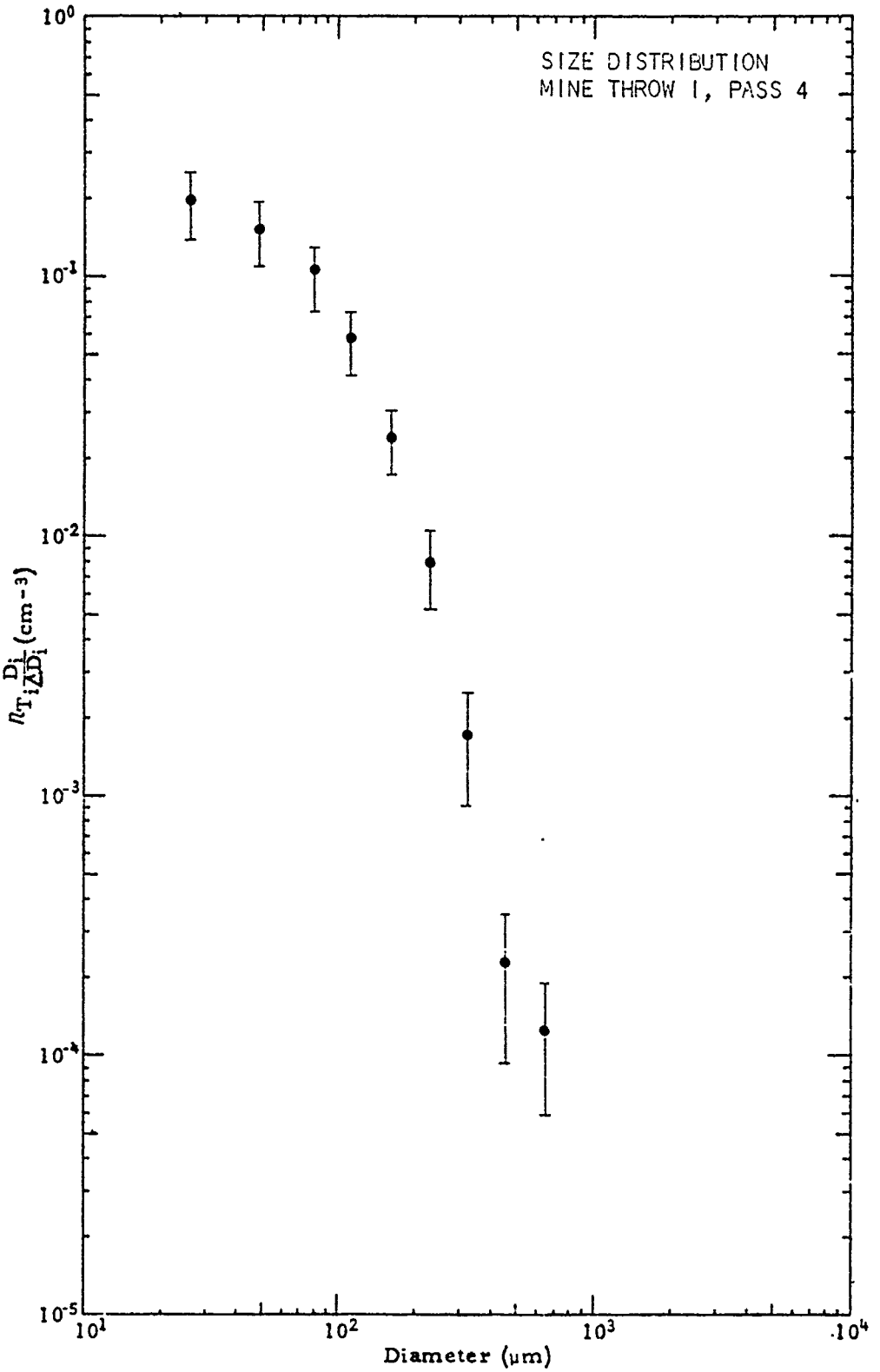
SIZE DISTRIBUTION
MINE THROW 1, PASS 4
10^0
10^{-1}
10^{-2}
10^{-3}
10^{-4}
10^{-5}
$n_{T_i} \frac{D_i}{\sum D_i}$ (cm^{-3})
10^1
10^2
10^3
10^4
Diameter (μm)

SIZE DISTRIBUTION

Mine Throw I Pass 7

Size (Microns)	dN/dLOG D (per cc)	Error +	Error -
26	2.15 E-1	2.84 E-1	1.46 E-1
48	9.52 E-2	1.25 E-1	6.54 E-2
80	2.91 E-2	3.83 E-2	1.99 E-2
112	1.32 E-2	1.75 E-2	8.90 E-3
160	5.46 E-3	7.26 E-3	3.67 E-3
224	1.63 E-3	2.37 E-3	8.89 E-4
320	4.08 E-4	7.06 E-4	1.10 E-4
448	0.0	0.0	0.0
640	0.0	0.0	0.0
896	0.0	0.0	0.0
1280	0.0	0.0	0.0

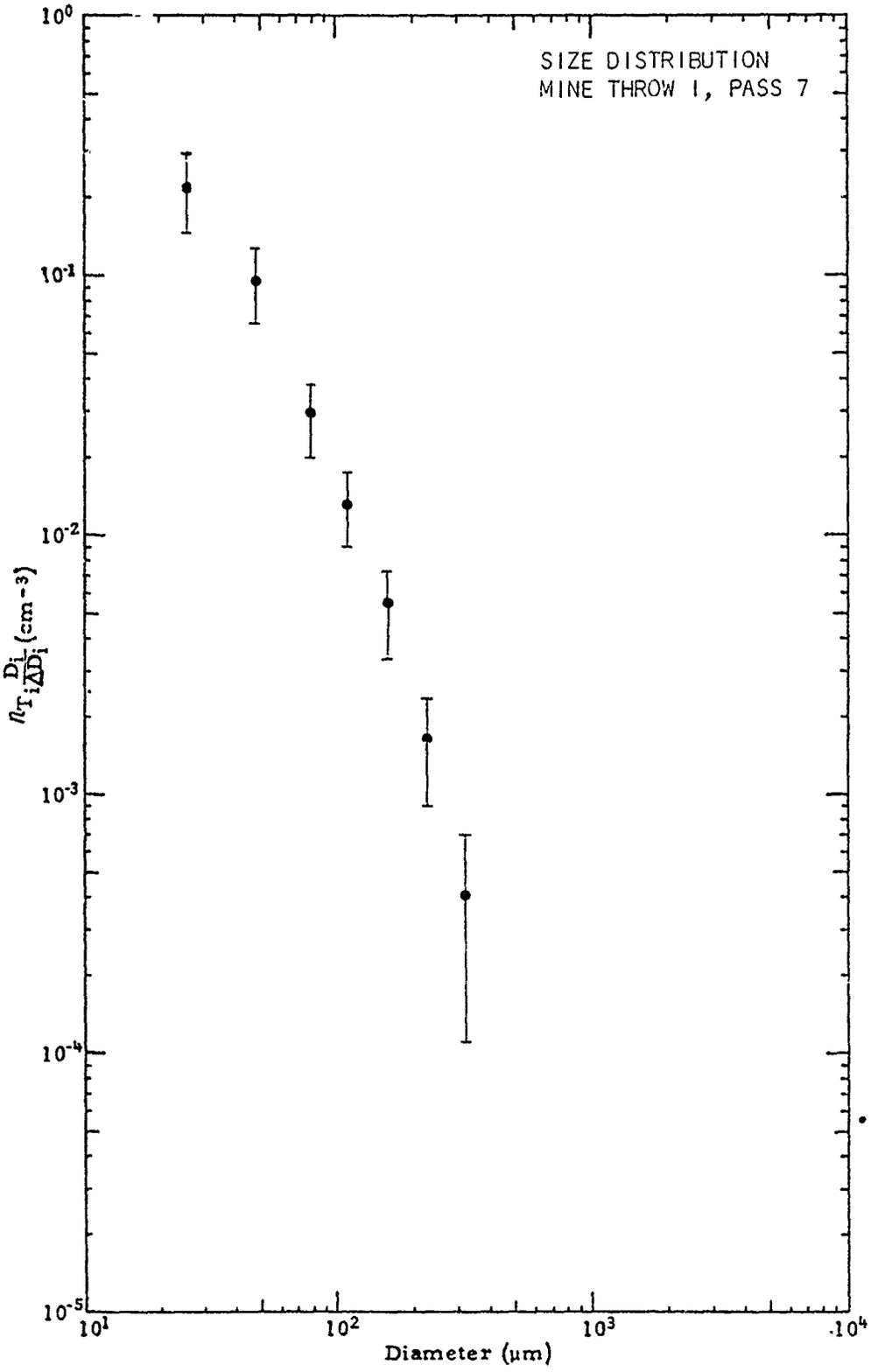
SIZE DISTRIBUTION
MINE THROW 1, PASS 7
10^0
10^{-1}
10^{-2}
10^{-3}
10^{-4}
10^{-5}
$n_T \frac{D_i}{\Delta D_i}$ (cm^{-3})
10^1
10^2
10^3
10^4
Diameter (μm)

SIZE DISTRIBUTION

Middle Gust III Pass 1

Size (Microns)	dN/dLOG D (per cc)	Error +	Error -
26	2.12 E-1	2.90 E-1	1.33 E-1
48	1.24 E-1	1.68 E-1	7.93 E-2
80	6.06 E-2	8.24 E-2	3.88 E-2
112	3.52 E-2	4.79 E-2	2.26 E-2
160	2.06 E-2	2.80 E-2	1.31 E-2
224	1.12 E-2	1.54 E-2	6.98 E-3
320	5.45 E-3	7.48 E-3	3.42 E-3
448	2.37 E-3	3.34 E-3	1.40 E-3
640	1.19 E-3	1.63 E-3	7.57 E-4
896	6.42 E-5	9.90 E-5	2.94 E-5
1280	0.0	0.0	0.0

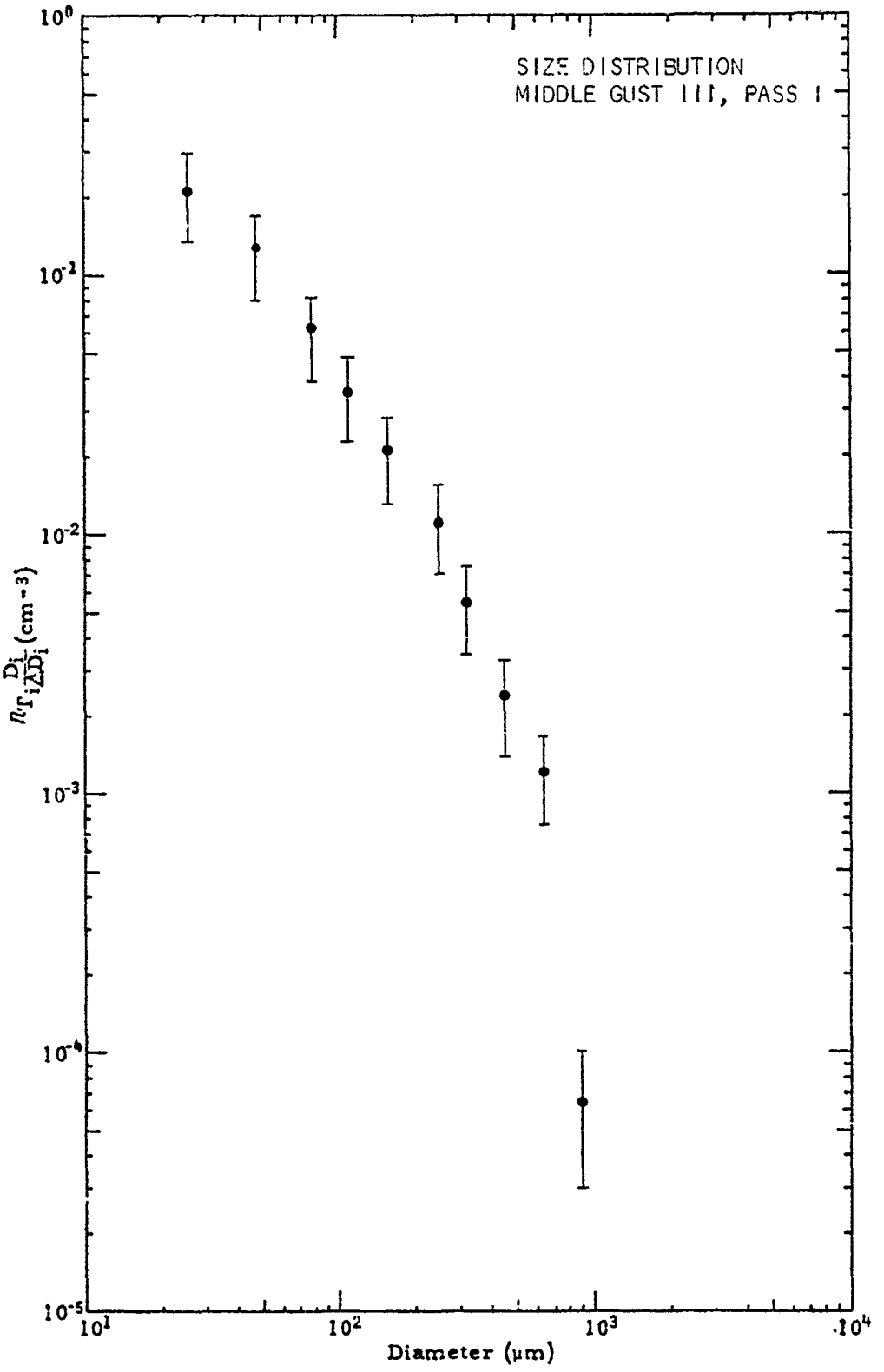
SIZE DISTRIBUTION
MIDDLE GUST III, PASS 1
10^0
10^{-1}
10^{-2}
10^{-3}
10^{-4}
10^{-5}
$n_{r_i \frac{D_i}{\Delta D_i}}$ (cm^{-3})
10^1
10^2
10^3
10^4
Diameter (μm)

SIZE DISTRIBUTION

Middle Gust III Pass 2

Size (Microns)	dN/dLOG D (per cc)	Error +	Error -
26	3.56 E-2	4.99 E-2	2.14 E-2
48	2.81 E-2	3.93 E-2	1.68 E-2
80	2.09 E-2	2.94 E-2	1.25 E-2
112	1.60 E-2	2.25 E-2	9.57 E-3
160	9.62 E-3	1.35 E-2	5.76 E-3
224	4.39 E-3	6.94 E-3	2.84 E-3
320	2.36 E-3	3.34 E-3	1.39 E-3
448	1.12 E-3	1.62 E-3	6.14 E-4
640	3.92 E-4	5.69 E-4	2.15 E-4
896	7.39 E-5	1.54 E-4	********
1230	3.08 E-5	5.02 E-5	1.14 E-5

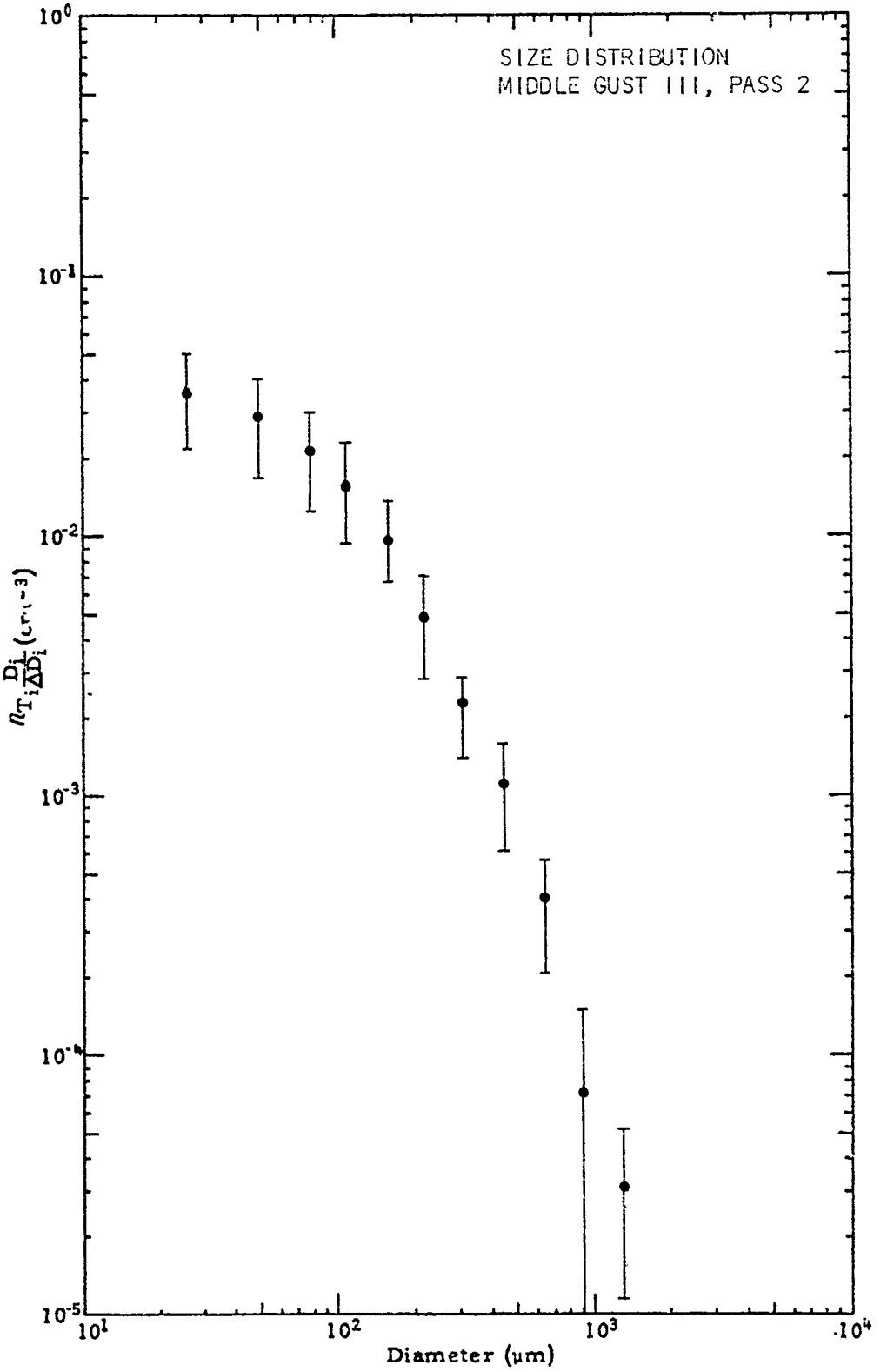
SIZE DISTRIBUTION
MIDDLE GUST III, PASS 2
10^0
10^{-1}
10^{-2}
10^{-3}
10^{-4}
10^{-5}
$n_T \frac{D_i}{\Delta D_i}$ (cm^{-3})
10^1
10^2
10^3
10^4
Diameter (μm)

SIZE DISTRIBUTION

Middle Gust III Pass 3

Size (Microns)	dN/dLOG D (per cc)	Error +	Error -
26	3.33 E-2	4.41 E-2	2.24 E-2
48	1.38 E-2	1.84 E-2	9.20 E-3
80	8.93 E-3	1.18 E-2	6.02 E-3
112	5.80 E-3	7.72 E-3	3.89 E-3
160	3.38 E-3	4.50 E-3	2.25 E-3
224	2.45 E-3	3.27 E-3	1.64 E-3
320	1.38 E-3	1.82 E-3	9.40 E-4
448	5.52 E-4	7.49 E-4	3.55 E-4
640	8.46 E-5	1.29 E-4	4.05 E-5
896	1.73 E-5	3.23 E-5	2.38 E-6
1280	1.03 E-5	1.44 E-5	6.29 E-6

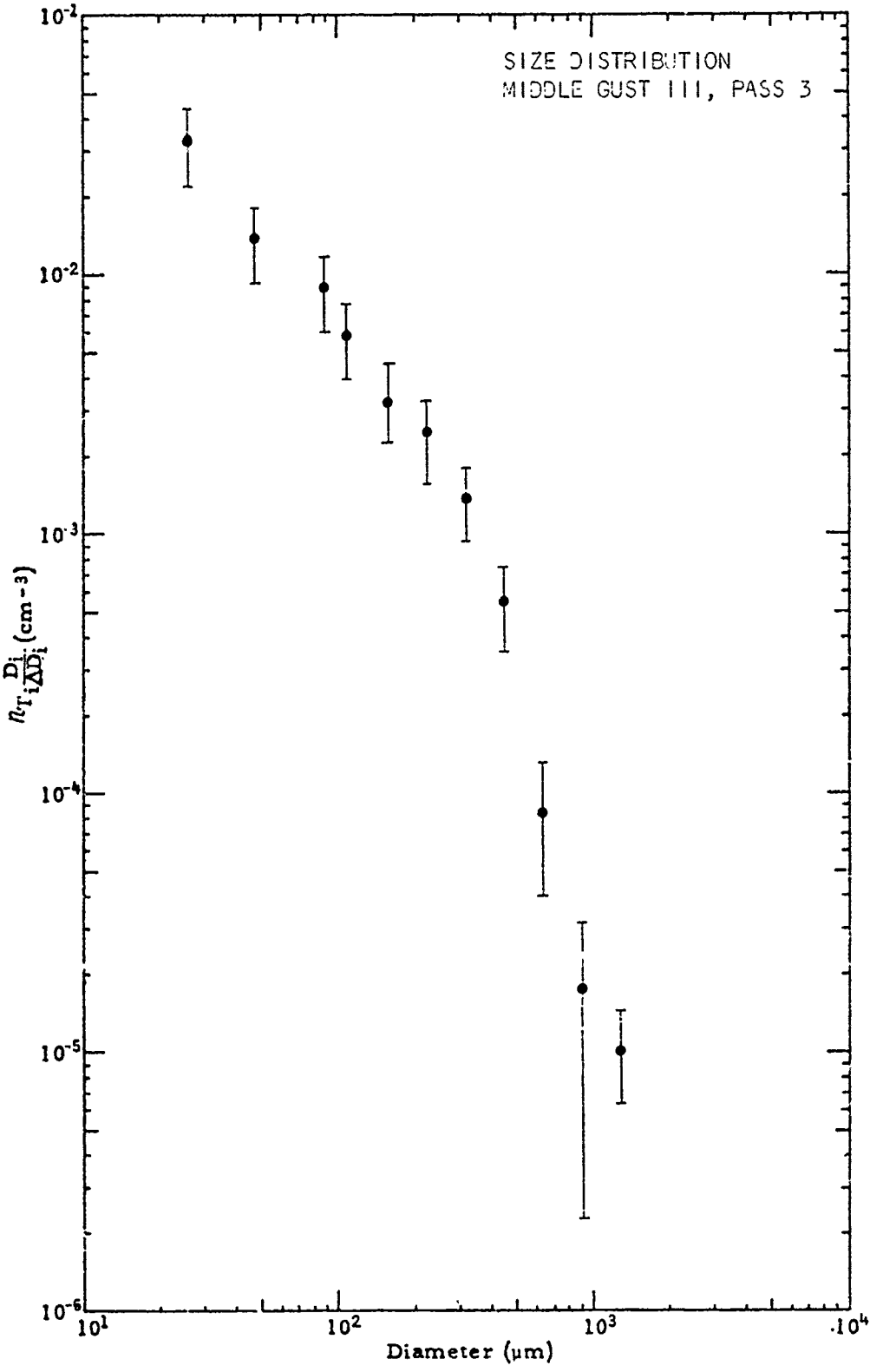
SIZE DISTRIBUTION
MIDDLE GUST III, PASS 3
10^{-1}
10^{-2}
10^{-3}
10^{-4}
10^{-5}
10^{-6}
$n_T \frac{D_i}{\sum D_i}$ (cm^{-3})
10^1
10^2
10^3
10^4
Diameter (μm)

SIZE DISTRIBUTION

Middle Gust III Pass 5

Size (Microns)	dN/dLOG D (per cc)	Error +	Error -
26	6.09 E-2	9.21 E-2	2.97 E-2
48	3.59 E-2	5.53 E-2	1.65 E-2
80	2.24 E-2	3.40 E-2	1.08 E-2
112	1.44 E-2	2.17 E-2	7.01 E-3
160	5.09 E-3	7.79 E-3	2.39 E-3
224	2.82 E-3	4.31 E-3	1.32 E-3
320	1.76 E-3	2.64 E-3	8.88 E-4
448	7.78 E-4	1.24 E-3	3.18 E-4
640	2.83 E-4	4.62 E-4	1.04 E-4
896	2.33 E-5	3.60 E-5	1.07 E-5
1280	0.0	0.0	0.0

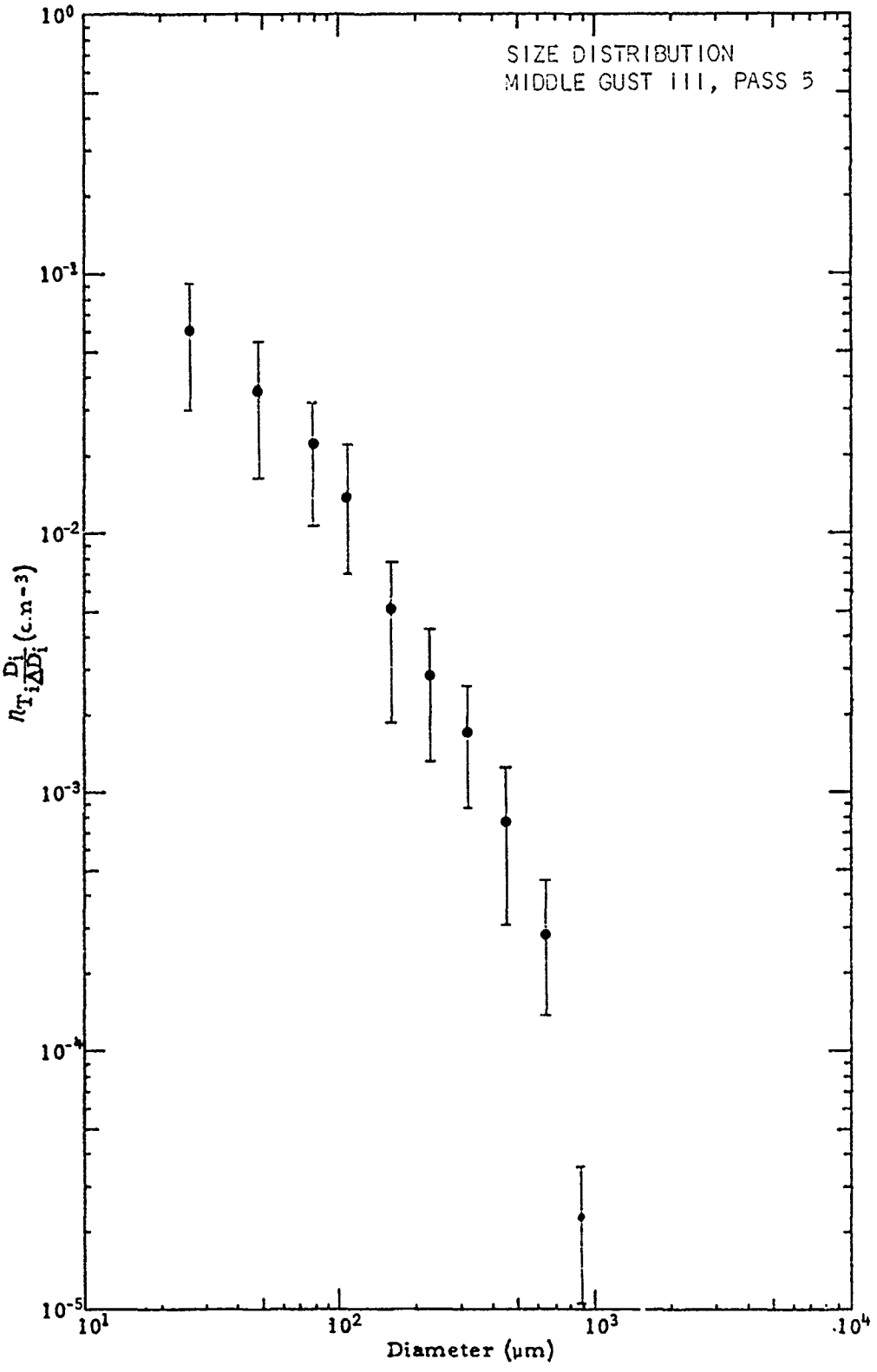
SIZE DISTRIBUTION
MIDDLE GUST III, PASS 5
10^0
10^{-1}
10^{-2}
10^{-3}
10^{-4}
10^{-5}
$n_{T_i} \frac{D_i}{\Delta D_i}$ (c.m^{-3})
10^1
10^2
10^3
10^4
Diameter (μm)

SIZE DISTRIBUTION

Middle Gust III Pass 6

Size (Microns)	dN/dLOG D (per cc)	Error +	Error -
26	1.58 E-2	2.29 E-2	8.72 E-3
48	7.33 E-3	1.06 E-2	4.05 E-3
80	3.35 E-3	4.86 E-3	1.83 E-3
112	2.48 E-3	3.61 E-3	1.35 E-3
160	1.23 E-3	1.80 E-3	6.56 E-4
224	9.46 E-4	1.39 E-3	5.07 E-4
320	2.89 E-4	4.30 E-4	1.49 E-4
448	9.78 E-5	1.87 E-4	8.80 E-6
640	1.50 E-5	2.15 E-5	8.40 E-6
896	2.09 E-5	2.98 E-5	1.21 E-5
1280	0.0	0.0	0.0

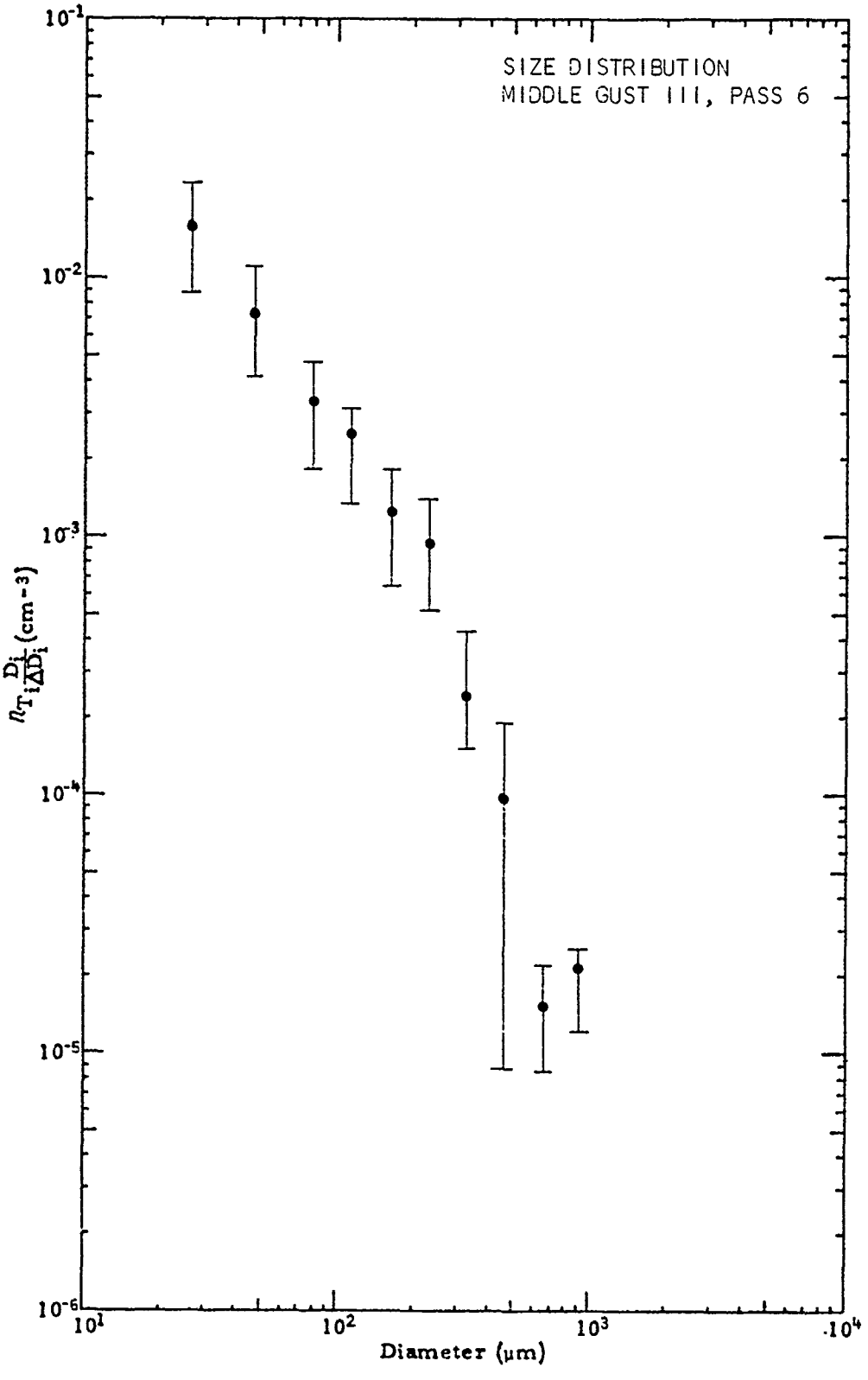
SIZE DISTRIBUTION
MIDDLE GUST III, PASS 6
10^{-1}
10^{-2}
10^{-3}
10^{-4}
10^{-5}
10^{-6}
$n_{T_i} \frac{D_i}{\Delta D_i}$ (cm^{-3})
10^1
10^2
10^3
10^4
Diameter (μm)

SIZE DISTRIBUTION

Middle Gust III Pass 7

Size (Microns)	dN/dLOG D (per cc)	Error +	Error -
26	2.10 E-2	3.37 E-2	8.30 E-3
48	8.72 E-3	1.40 E-2	3.48 E-3
80	3.72 E-3	5.96 E-3	1.47 E-3
112	2.29 E-3	3.69 E-3	8.96 E-4
160	1.36 E-3	2.18 E-3	5.36 E-4
224	7.94 E-4	1.29 E-3	2.95 E-4
320	3.3$\frac{1}{2}$ E-4	5.43 E-4	1.34 E-4
448	1.12 E-4	1.97 E-4	2.70 E-5
640	3.29 E-5	6.79 E-5	********
896	0.0	0.0	0.0
1230	0.0	0.0	0.0

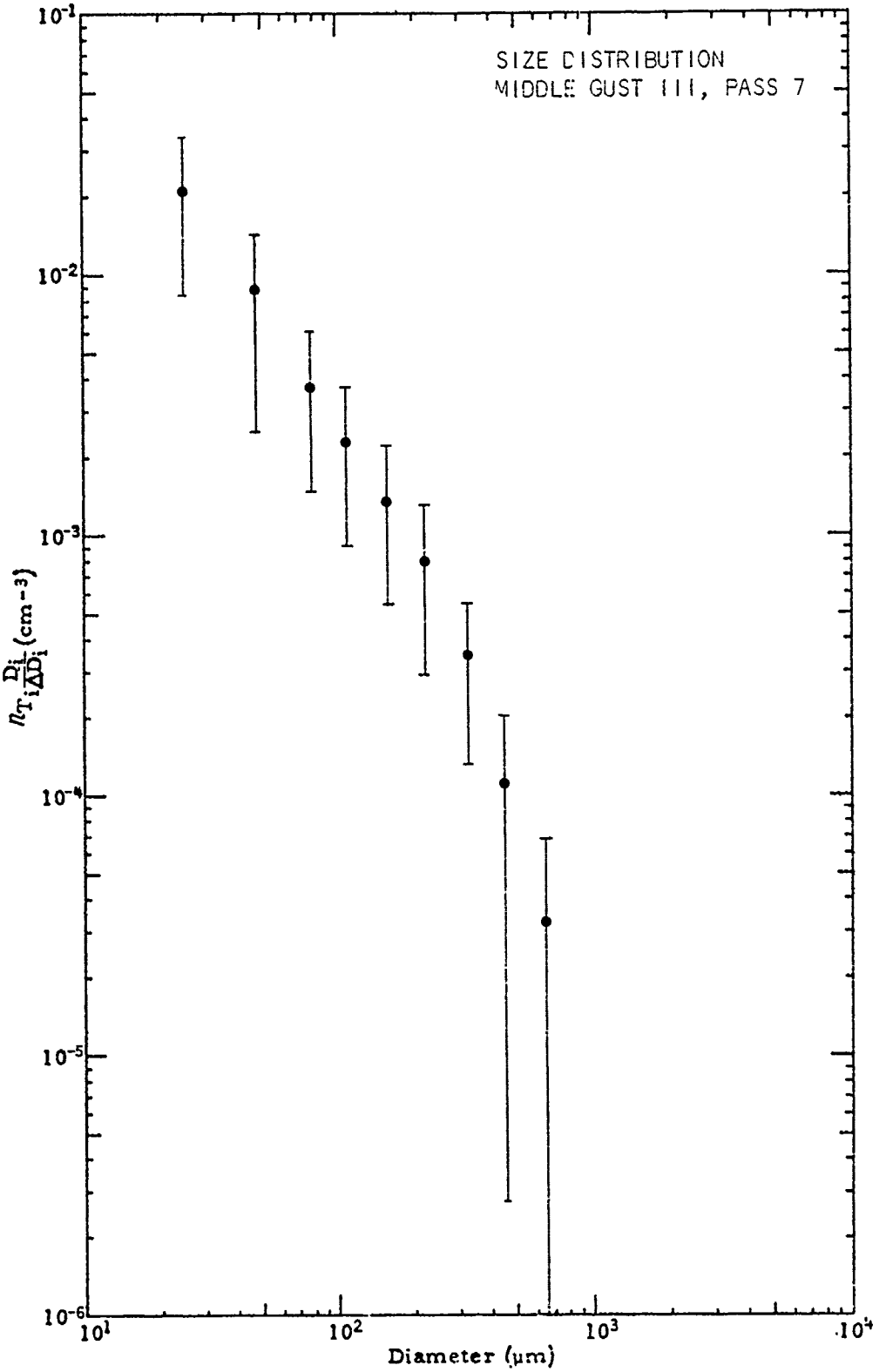
SIZE DISTRIBUTION
MIDDLE GUST III, PASS 7
10^{-1}
10^{-2}
10^{-3}
10^{-4}
10^{-5}
10^{-6}
$n_{T_i} \frac{D_i}{\Delta D_i}$ (cm^{-3})
10^1
10^2
10^3
10^4
Diameter (μm)

SIZE DISTRIBUTION

Middle Gust III Pass 8

Size (Microns)	dN/dLOG D (per cc)	Error +	Error -
26	3.81 E-3	6.74 E-3	8.75 E-4
48	1.96 E-3	3.46 E-3	4.55 E-4
80	1.82 E-3	3.22 E-3	4.33 E-4
112	9.97 E-4	1.76 E-3	2.33 E-4
160	5.37 E-4	9.50 E-4	1.25 E-4
224	2.68 E-4	4.83 E-4	5.23 E-5
320	1.49 E-4	2.60 E-4	3.75 E-5
448	3.28 E-5	7.44 E-5	********
640	1.32 E-5	3.30 E-5	********
896	4.27 E-6	7.46 E-6	1.09 E-6
1280	0.0	0.0	0.0

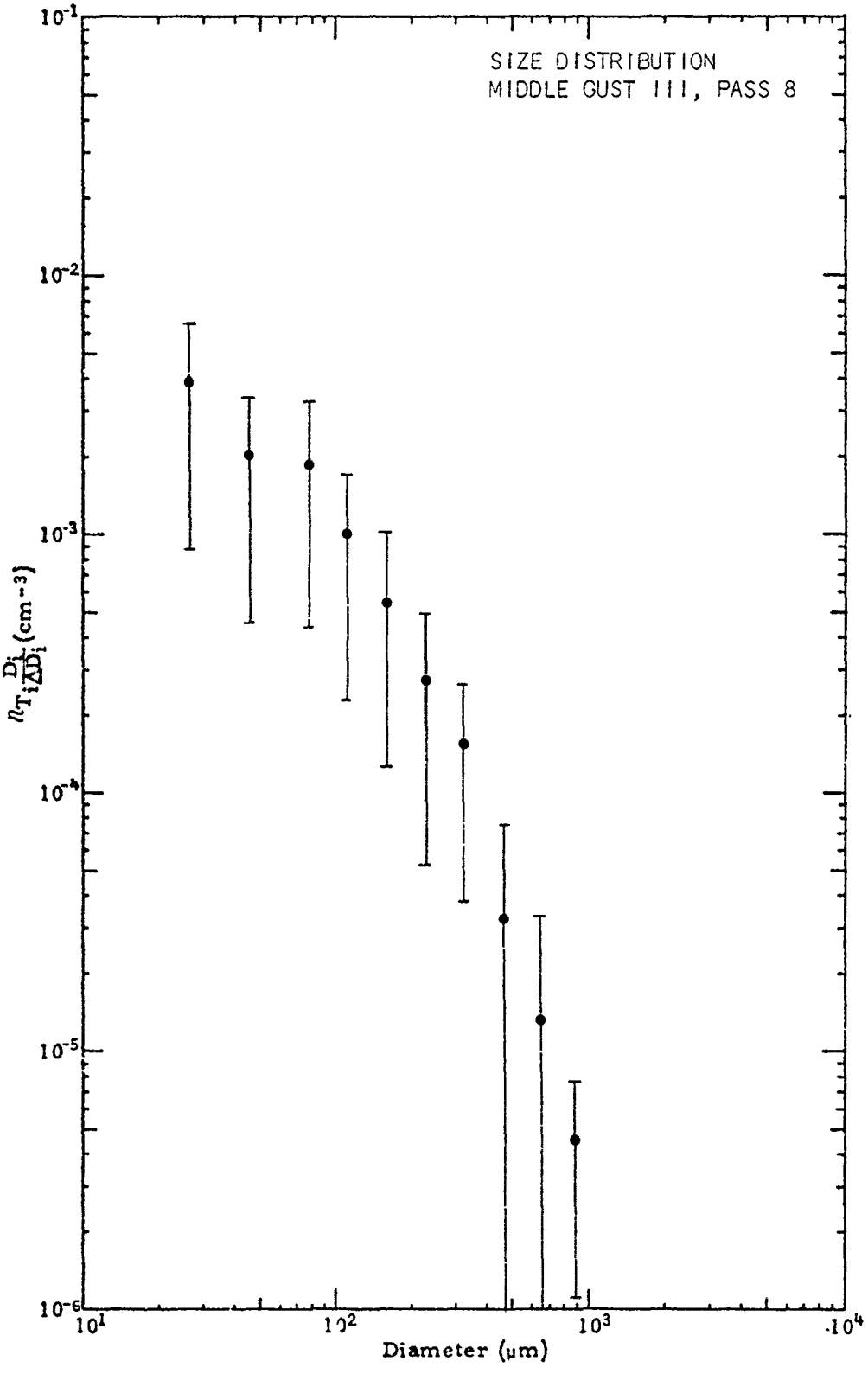
SIZE DISTRIBUTION
MIDDLE GUST III, PASS 8
10^{-1}
10^{-2}
10^{-3}
10^{-4}
10^{-5}
10^{-6}
$n_{T_i} \frac{D_i}{\Delta D_i}$ (cm^{-3})
10^1
10^2
10^3
10^4
Diameter (μm)

SIZE DISTRIBUTION

Middle Gust III Pass 9

Size (Microns)	dN/dLOG D (per cc)	Error +	Error -
26	1 97 E-3	2.77 E-3	1.18 E-3
48	9.45 E-4	1.33 E-3	5.59 E-4
80	7.46 E-4	1.07 E-3	4.25 E-4
112	1.04 E-3	1.48 E-3	5.96 E-4
160	1.14 E-3	1.58 E-3	7.00 E-4
224	6.17 E-4	8.75 E-4	3.59 E-4
320	3.81 E-4	5.04 E-4	2.57 E-4
448	2.81 E-5	5.34 E-5	2.67 E-6
640	0.0	0.0	0.0
896	0.0	0.0	0.0
1280	0.0	0.0	0.0

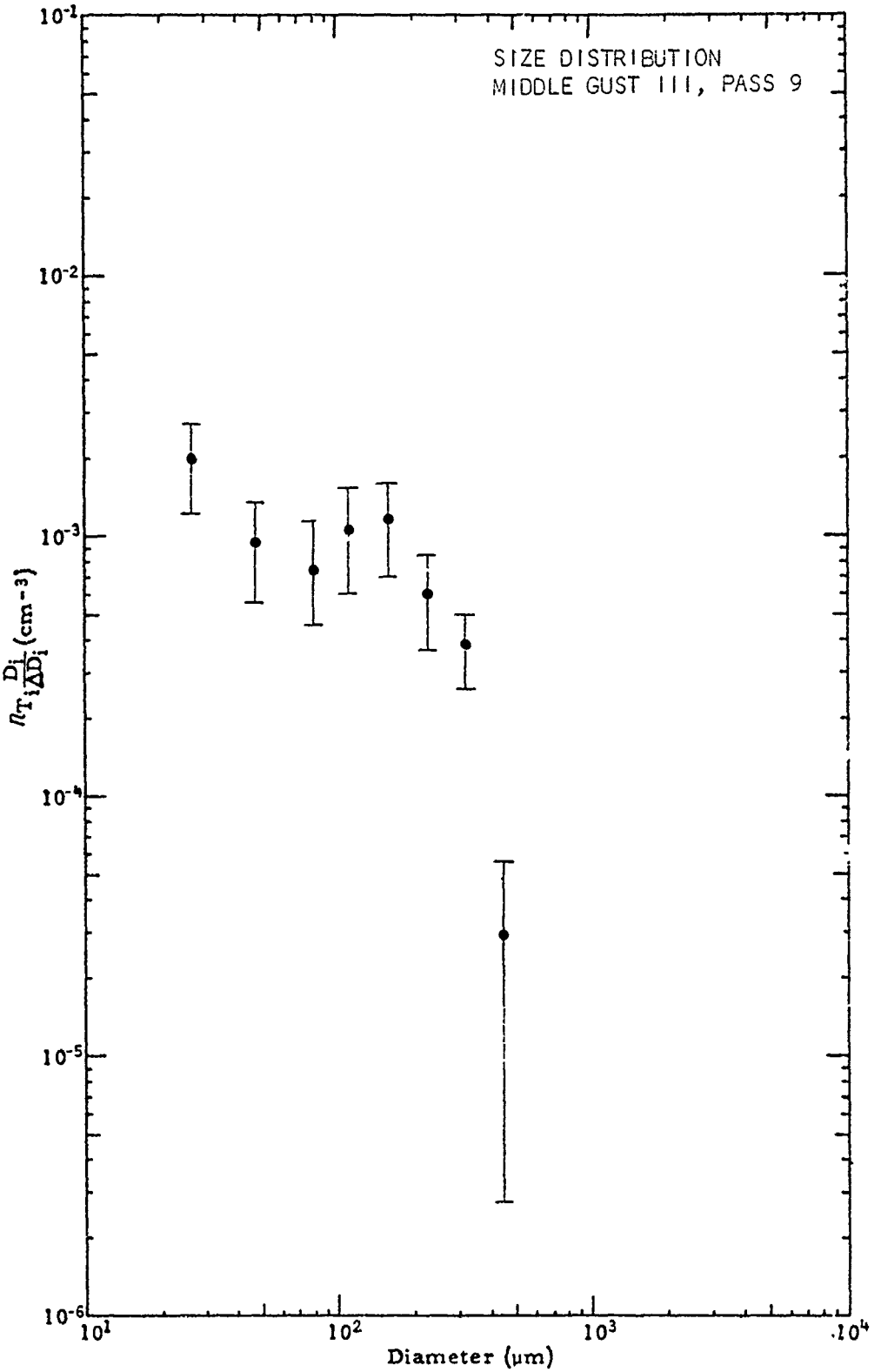
SIZE DISTRIBUTION
MIDDLE GUST III, PASS 9
10^{-1}
10^{-2}
10^{-3}
10^{-4}
10^{-5}
10^{-6}
$n_{T_i} \frac{D_i}{\Delta D_i}$ (cm^{-3})
10^1
10^2
10^3
10^4
Diameter (μm)

SIZE DISTRIBUTION

Middle Gust III Pass 10

Size (Microns)	dN/dLOG D (per cc)	Error +	Error -
26	1.64 E-2	2.34 E-2	9.50 E-3
48	1.12 E-2	1.59 E-2	6.58 E-3
80	5.49 E-3	7.76 E-3	3.23 E-3
112	3.03 E-3	4.29 E-3	1.78 E-3
160	1.51 E-3	2.14 E-3	8.83 E-4
224	5.54 E-4	8.37 E-4	2.71 E-4
320	1.42 E-4	2.39 E-4	4.44 E-5
448	5.23 E-6	7.43 E-6	3.02 E-6
640	0.0	0.0	0.0
896	0.0	0.0	0.0
1280	0.0	0.0	0.0

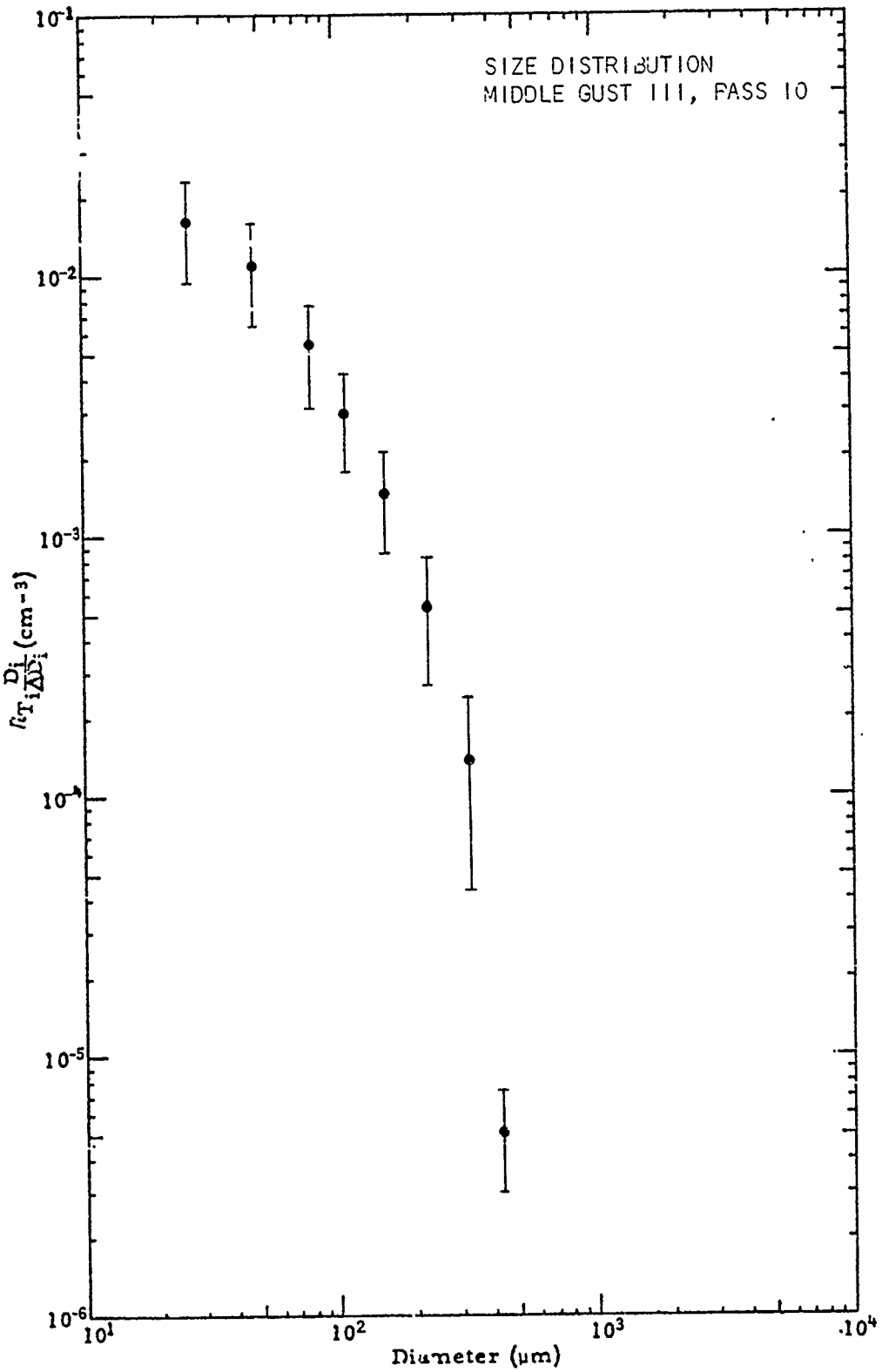
SIZE DISTRIBUTION
MIDDLE GUST III, PASS 10
10^{-1}
10^{-2}
10^{-3}
10^{-4}
10^{-5}
10^{-6}
$f_{T_i} \frac{D_i}{\Delta D_i}$ (cm^{-3})
10^1
10^2
10^3
10^4
Diameter (μm)

SIZE DISTRIBUTION

Mixed Company I Pass 1

Size (Microns)	dN/dLOG D (per cc)	Error +	Error -
26	2.46 E-1	3.47 E-1	1.44 E-1
48	1.96 E-1	2.76 E-1	1.15 E-1
80	1.19 E-1	1.68 E-1	7.05 E-2
112	8.30 E-2	1.17 E-1	4.92 E-2
160	4.24 E-2	5.96 E-2	2.51 E-2
224	2.36 E-2	3.34 E-2	1.38 E-2
320	1.02 E-2	1.43 E-2	6.12 E-3
448	1.94 E-3	3.24 E-3	6.48 E-4
640	7.12 E-3	1.24 E-3	1.83 E-4
896	0.0	0.0	0.0
1280	7.31 E-6	1.16 E-5	2.98 E-6

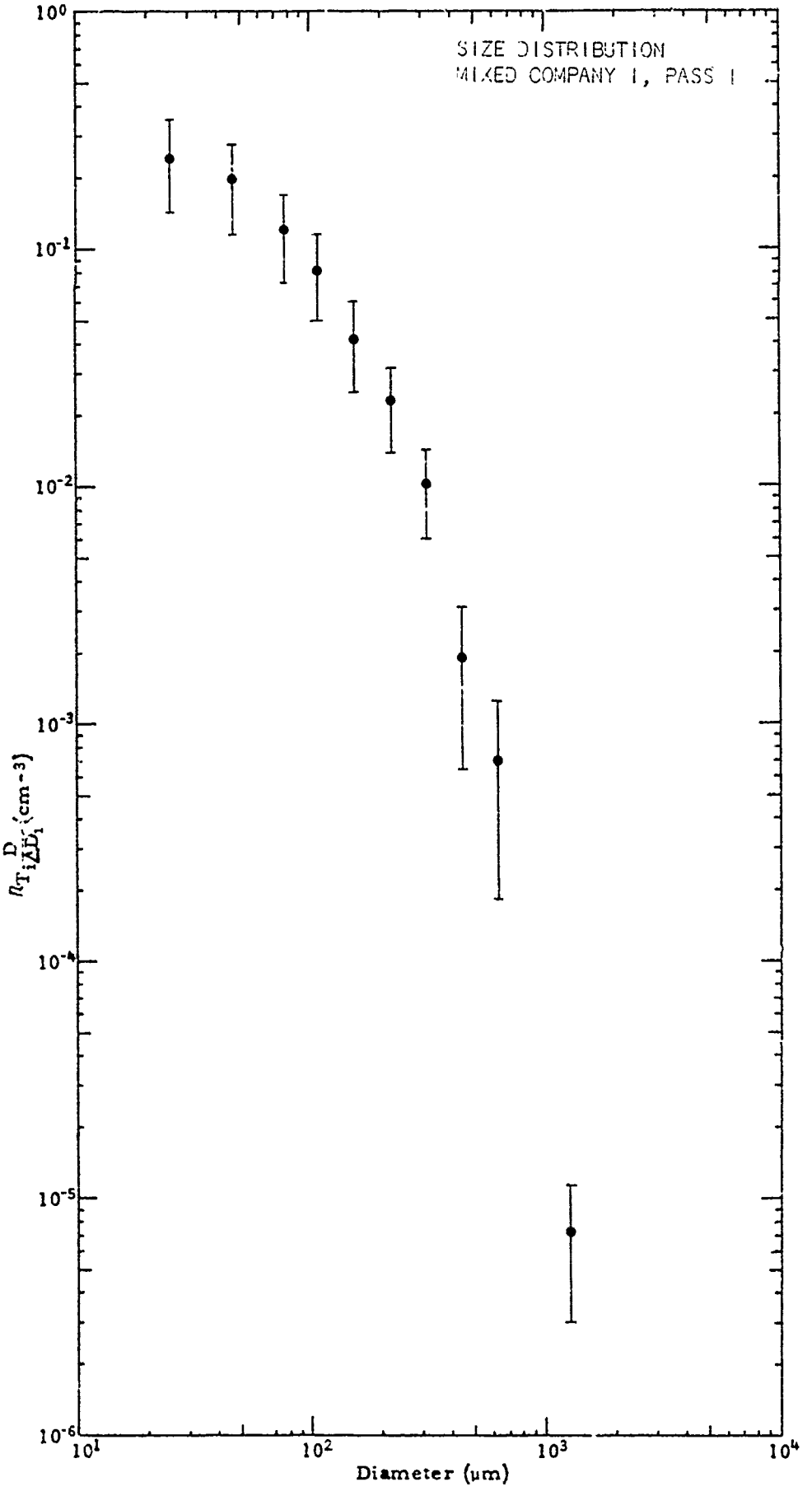
SIZE DISTRIBUTION
MIXED COMPANY 1, PASS 1
10^0
10^{-1}
10^{-2}
10^{-3}
10^{-4}
10^{-5}
10^{-6}
$n_{T_i}^{D}\Delta D_i$ (cm^{-3})
10^1
10^2
10^3
10^4
Diameter (μm)

SIZE DISTRIBUTION

Mixed Company I Pass 2

Size (Microns)	dN/dLOG D (per cc)	Error +	Error -
26	1.51 E-1	1.98 E-1	1.04 E-1
48	9.66 E-2	1.25 E-1	6.77 E-2
80	5.15 E-2	6.66 E-2	3.64 E-2
112	3.89 E-2	5.02 E-2	2.77 E-2
160	2.05 E-2	2.63 E-2	1.46 E-2
224	1.01 E-2	1.31 E-2	7.10 E-3
320	3.52 E-3	4.56 E-3	2.47 E-3
448	1.03 E-3	1.44 E-3	6.13 E-4
640	7.29 E-5	1.06 E-4	3.97 E-5
896	0.0	0.0	0.0
1280	0.0	0.0	0.0

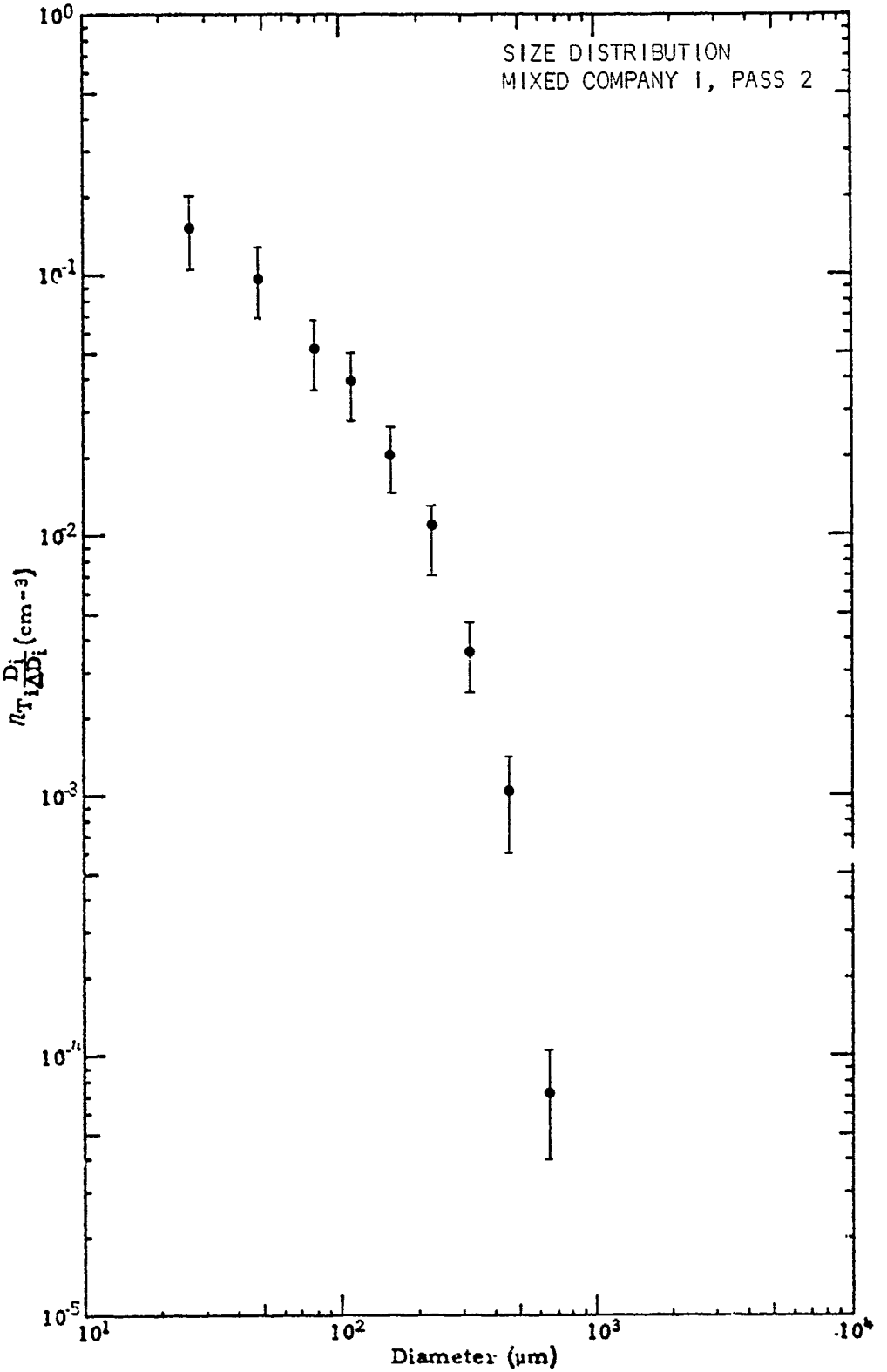
SIZE DISTRIBUTION
MIXED COMPANY 1, PASS 2
10^0
10^{-1}
10^{-2}
10^{-3}
10^{-4}
10^{-5}
$n_{T_i} \frac{D_i}{\Delta D_i}$ (cm^{-3})
10^1
10^2
10^3
10^4
Diameter (μm)

SIZE DISTRIBUTION

Mixed Company I Pass 11

Size (Microns)	dN/dLOG D (per cc)	Error +	Error -
26	9.50 E-2	1.51 E-1	3.91 E-2
48	5.36 E-2	8.45 E-2	2.28 E-2
80	2.33 E-2	3.67 E-2	9.96 E-3
112	1.30 E-2	2.04 E-2	5.53 E-3
160	4.66 E-3	7.44 E-3	1.89 E-3
224	1.73 E-3	3.01 E-3	4.43 E-4
320	5.05 E-4	9.56 E-4	5.50 E-5
448	1.75 E-4	4.35 E-4	********
640	1.04 E-5	1.65 E-5	4.31 E-6
896	0.0	0.0	0.0
1280	0.0	0.0	0.0

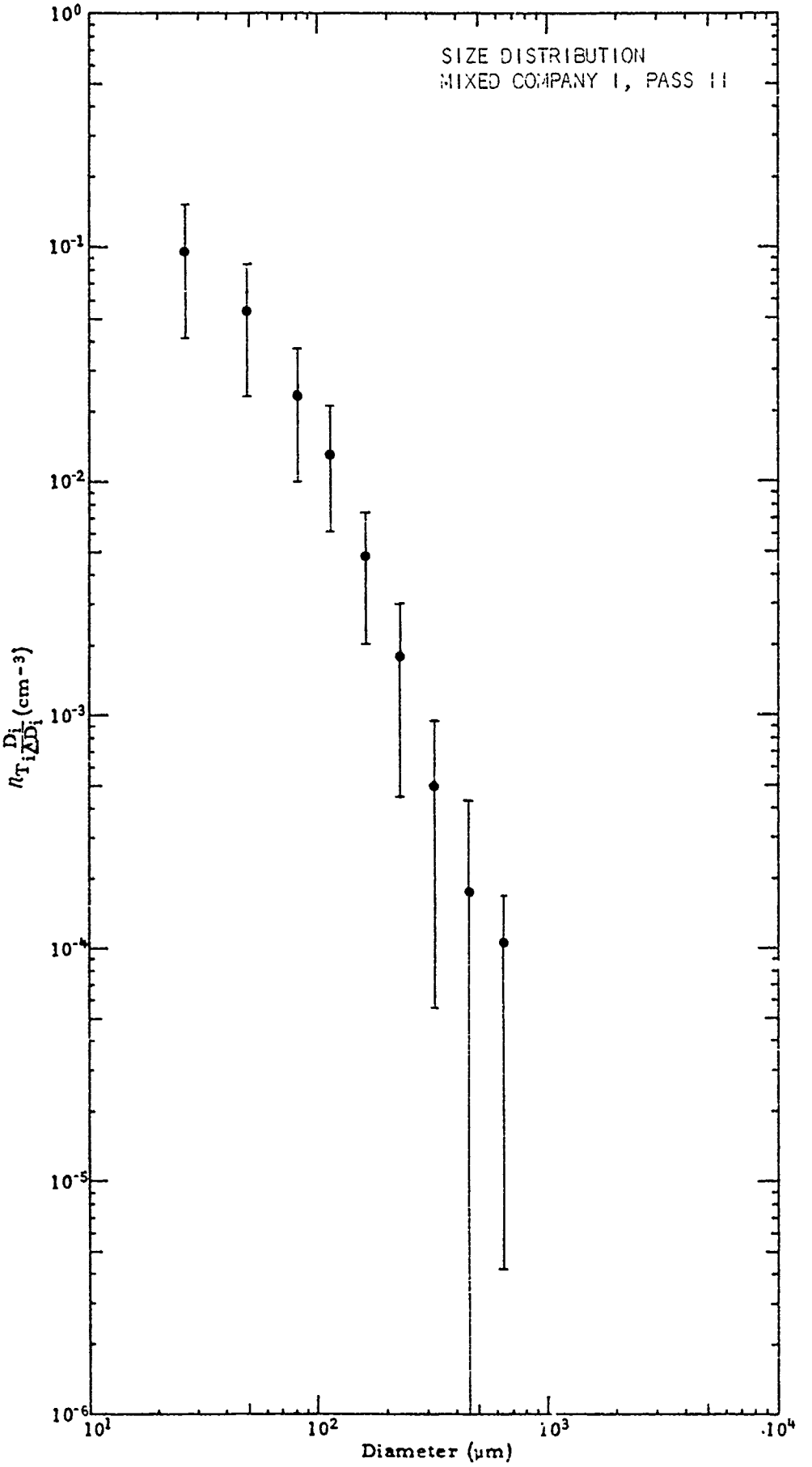
SIZE DISTRIBUTION
MIXED COMPANY 1, PASS 11
10^0
10^{-1}
10^{-2}
10^{-3}
10^{-4}
10^{-5}
10^{-6}
$n_T \frac{D_i}{\sum D_i}$ (cm^{-3})
10^1
10^2
10^3
10^4
Diameter (μm)

SIZE DISTRIBUTION

Middle Gust IV Pass 2

Size (Microns)	dN/dLOG D (per cc)	Error +	Error -
26	1.50 E-1	2.35 E-1	6.51 E-2
48	6.00 E-2	9.33 E-2	2.67 E-2
80	1.87 E-2	2.91 E-2	8.31 E-3
112	8.64 E-3	1.35 E-2	3.81 E-3
160	4.55 E-3	7.16 E-3	1.93 E-3
224	2.24 E-3	3.66 E-3	8.10 E-4
320	1.44 E-3	2.25 E-3	6.37 E-4
448	4.23 E-4	7.84 E-4	6.12 E-5
640	1.27 E-4	2.40 E-4	1.32 E-5
896	2.57 E-6	5.74 E-6	********
1280	1.56 E-5	2.40 E-5	7.16 E-6

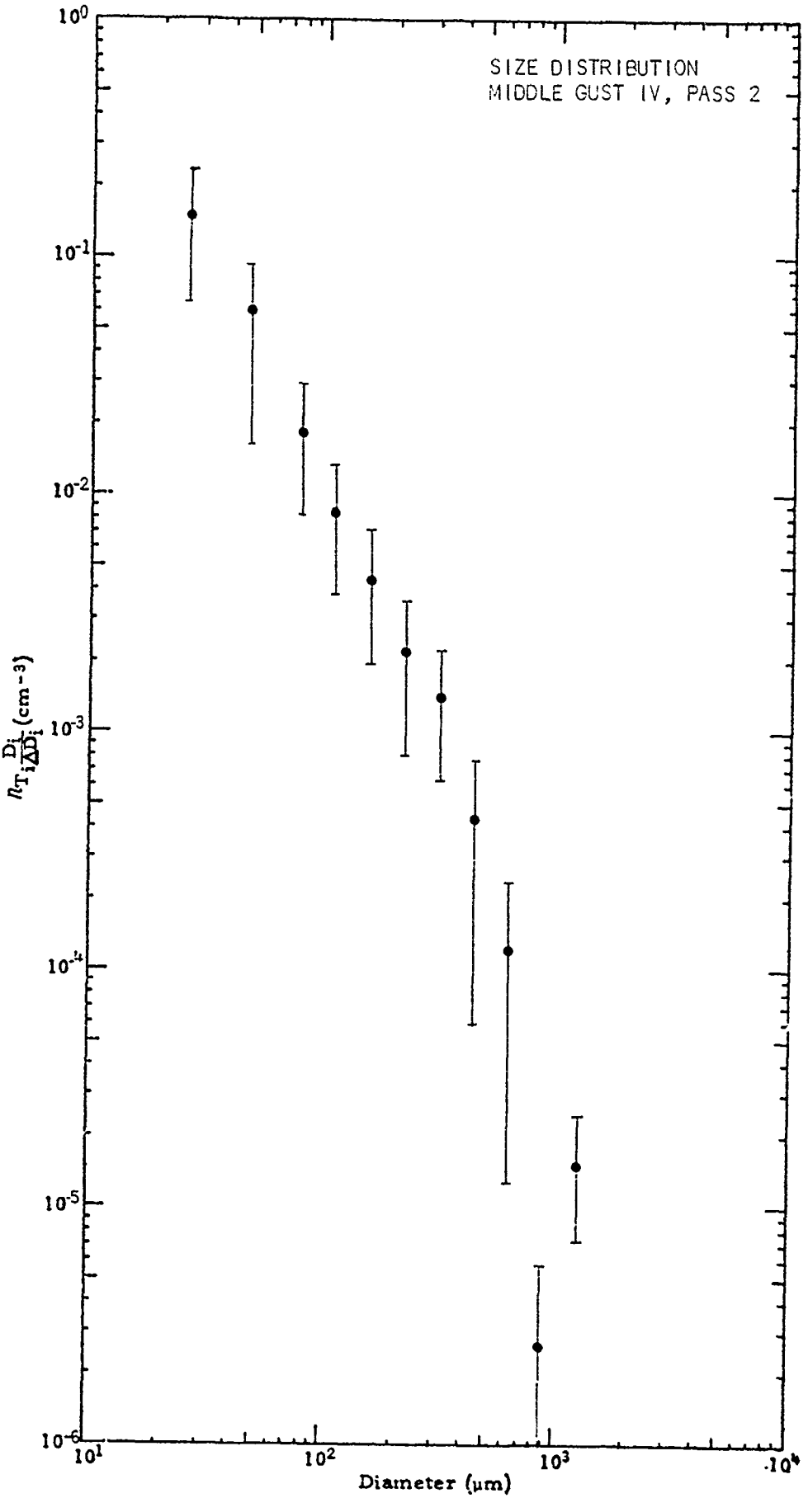
SIZE DISTRIBUTION
MIDDLE GUST IV, PASS 2
10^0
10^{-1}
10^{-2}
10^{-3}
10^{-4}
10^{-5}
10^{-6}
$n_{T_i} \frac{D_i}{\Delta D_i}$ (cm^{-3})
10^1
10^2
10^3
10^4
Diameter (μm)

SIZE DISTRIBUTION

Middle Gust IV Pass 4

Size (Microns)	dN/dLOG D (per cc)	Error +	Error -
26	4.15 E-3	6.31 E-3	1.99 E-3
48	1.57 E-3	2.36 E-3	7.69 E-4
80	5.28 E-4	8.00 E-4	2.55 E-4
112	2.89 E-4	4.43 E-4	1.35 E-4
160	1.68 E-4	2.58 E-4	7.78 E-5
224	9.63 E-5	1.15 E-4	4.12 E-5
320	3.28 E-5	5.26 E-5	1.30 E-5
448	2.09 E-5	3.58 E-5	6.13 E-6
640	7.35 E-6	1.20 E-5	2.75 E-6
896	4.41 E-6	6.87 E-6	1.95 E-6
1280	0.0	0.0	0.0

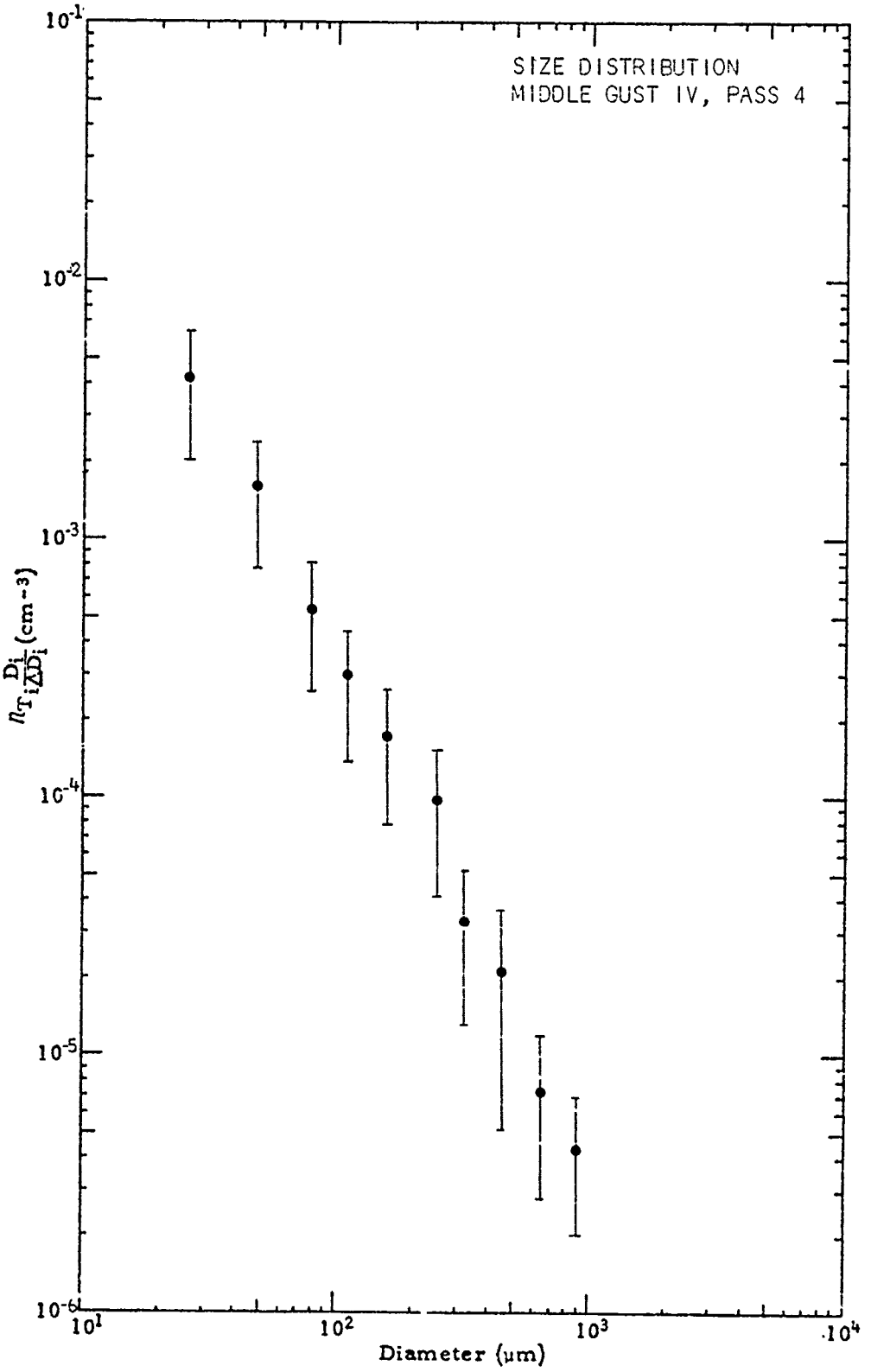
SIZE DISTRIBUTION
MIDDLE GUST IV, PASS 4
10^{-1}
10^{-2}
10^{-3}
10^{-4}
10^{-5}
10^{-6}
$n_T \frac{D_i}{\sum D_i}$ (cm^{-3})
10^1
10^2
10^3
10^4
Diameter (μm)

SIZE DISTRIBUTION

Mixed Company III Pass 2

Size (Microns)	dN/dLOG D (per cc)	Error +	Error -
26	1.79 E-2	2.63 E-2	9.55 E-3
48	7.07 E-3	1.03 E-2	3.81 E-3
80	3.19 E-3	4.70 E-3	1.69 E-3
112	2.26 E-3	3.34 E-3	1.18 E-3
160	2.01 E-3	2.95 E-3	1.07 E-3
224	1.16 E-3	1.71 #-3	6.15 E-4
320	5.13 E-4	7.48 E-4	2.73 E-4
448	2.28 E-4	3.45 E-4	1.10 E-4
640	8.13 E-5	1.22 E-4	4.07 E-5
896	0.0	0.0	0.0
1280	8.55 E-6	1.39 E-5	3.17 E-6

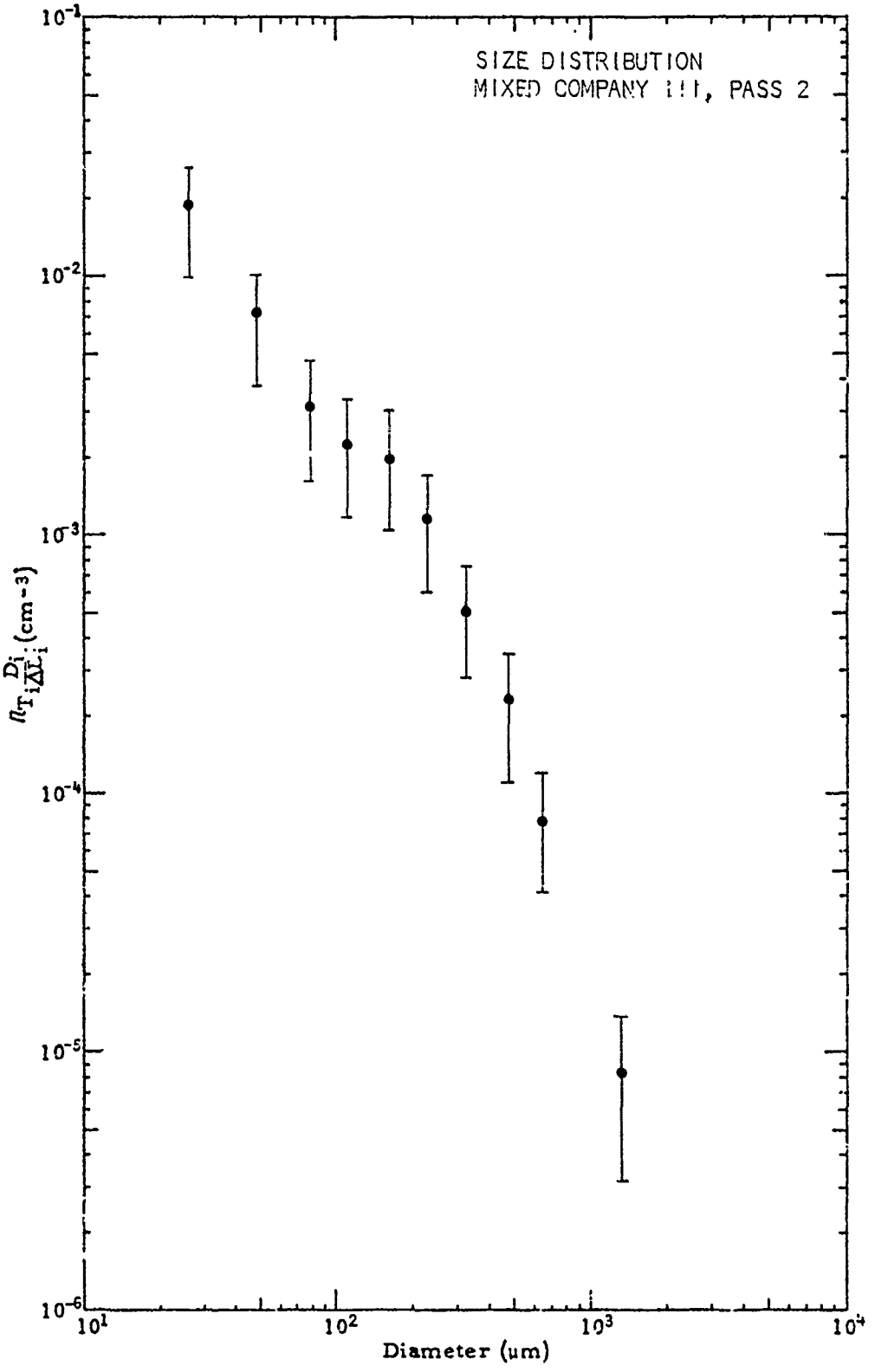
SIZE DISTRIBUTION
MIXED COMPANY III, PASS 2
10^{-1}
10^{-2}
10^{-3}
10^{-4}
10^{-5}
10^{-6}
$n_T \frac{D_i}{i\Delta D_i}$ (cm^{-3})
10^1
10^2
10^3
10^4
Diameter (um)

SIZE DISTRIBUTION

Mixed Company III Pass 3

Size (Microns)	dN/dLOG D (per cc)	Error +	Error -
26	1.55 E-2	1.99 E-2	1.10 E-2
48	9.77 E-3	1.27 E-2	6.88 E-3
80	7.43 E-3	9.56 E-3	5.30 E-3
112	5.98 E-3	7.63 E-3	4.34 E-3
160	2.94 E-3	3.73 E-3	2.15 E-3
224	1.29 E-3	1.66 E-3	9.21 E-4
320	5.30 E-4	6.77 E-4	3.83 E-4
448	1.16 E-4	1.82 E-4	5.02 E-5
640	5.53 E-6	7.73 E-6	3.32 E-6
896	0.0	0.0	0.0
1280	0.0	0.0	0.0

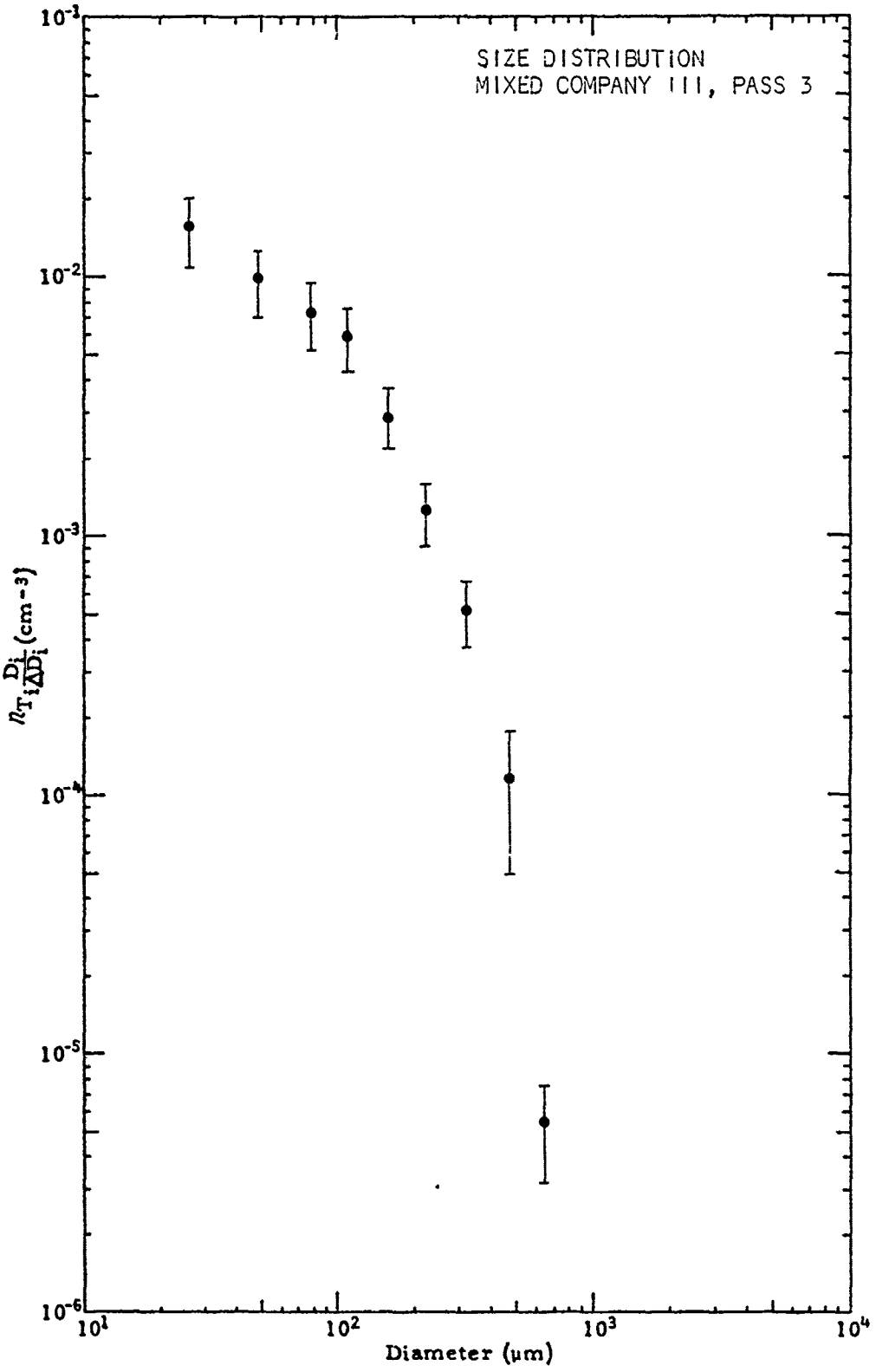
SIZE DISTRIBUTION
MIXED COMPANY III, PASS 3
10^{-1}
10^{-2}
10^{-3}
10^{-4}
10^{-5}
10^{-6}
$n_{T_i} \frac{D_i}{\Delta D_i}$ (cm^{-3})
10^1
10^2
10^3
10^4
Diameter (μm)

SIZE DISTRIBUTION

Mixed Company III Pass 4

Size (Microns)	dN/dLOG D (per cc)	Error +	Error -
26	2.47 E-1	4.65 E-1	2.92 E-2
48	1.10 E-1	2.04 E-1	1.58 E-2
80	5.02 E-2	9.27 E-2	7.61 E-3
112	2.58 E-2	4.76 E-2	3.85 E-3
160	6.44 E-3	1.29 E-2	********
224	2.01 E-3	5.19 E-3	********
320	3.48 E-4	1.66 E-3	********
448	2.98 E-5	5.63 E-5	3.38 E-6
640	2.13 E-5	4.01 E-5	2.54 E-6
896	0.0	0.0	0.0
1280	0.0	0.0	0.0

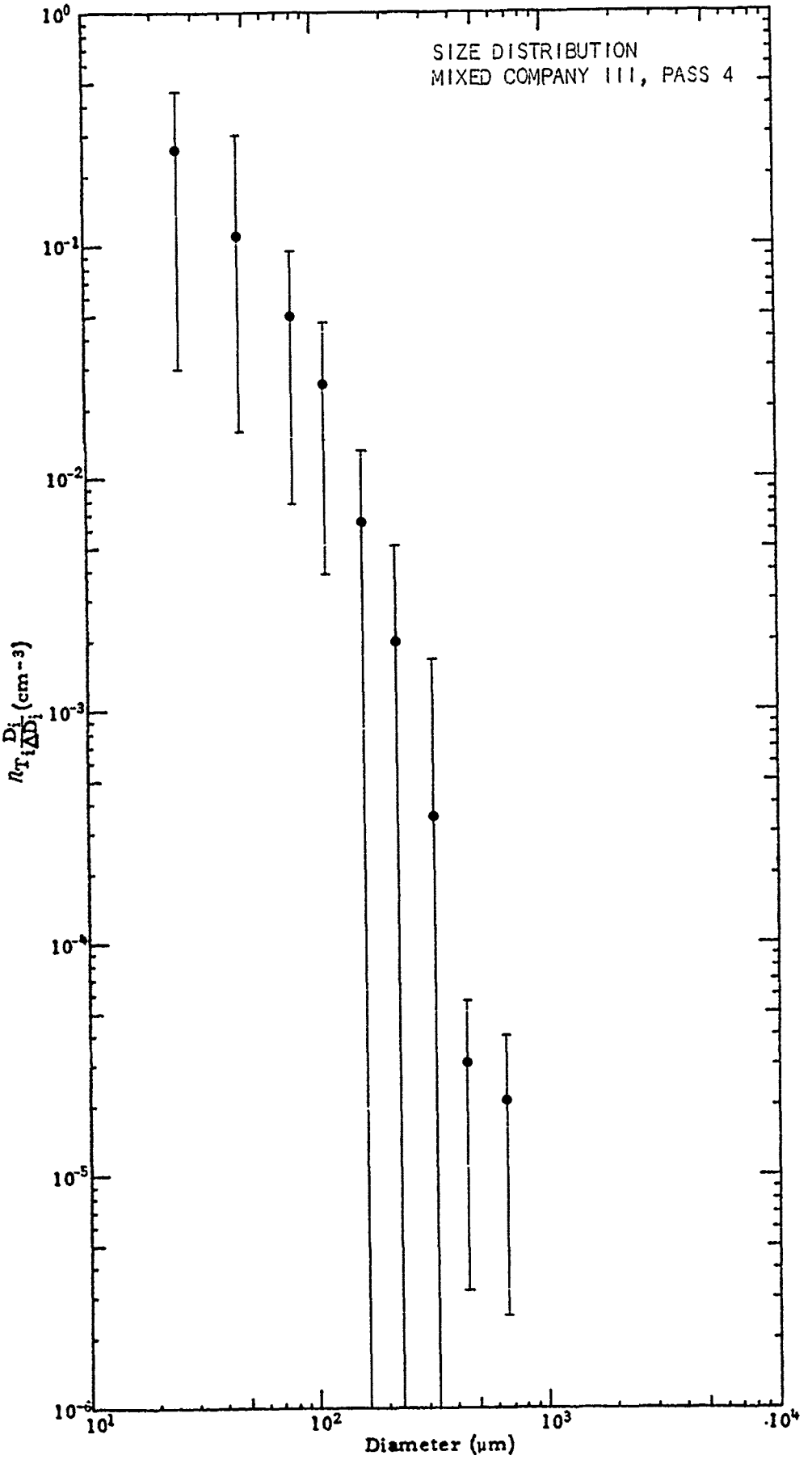
SIZE DISTRIBUTION
MIXED COMPANY III, PASS 4
10^0
10^{-1}
10^{-2}
10^{-3}
10^{-4}
10^{-5}
10^{-6}
$n_{T_i} \frac{D_i}{\Delta D_i}$ (cm^{-3})
10^1
10^2
10^3
10^4
Diameter (μm)

SIZE DISTRIBUTION

Mixed Company III Pass 5

Size (Microns)	dN/dLOG D (per cc)	Error +	Error -
26	3.18 E-2	4.30 E-2	2.07 E-2
48	2.29 E-2	3.08 E-2	1.51 E-2
80	1.49 E-2	1.99 E-2	9.96 E-3
112	8.49 E-3	1.13 E-2	5.67 E-3
160	3.87 E-3	5.17 E-3	2.57 E-3
224	1.83 E-3	2.50 E-3	1.17 E-3
320	8.15 E-4	1.10 E-3	5.34 E-4
448	1.88 E-4	2.99 E-4	7.73 E-5
640	3.97 E-5	7.33 E-5	6.08 E-6
896	0.0	0.0	0.0
1280	0.0	0.0	0.0

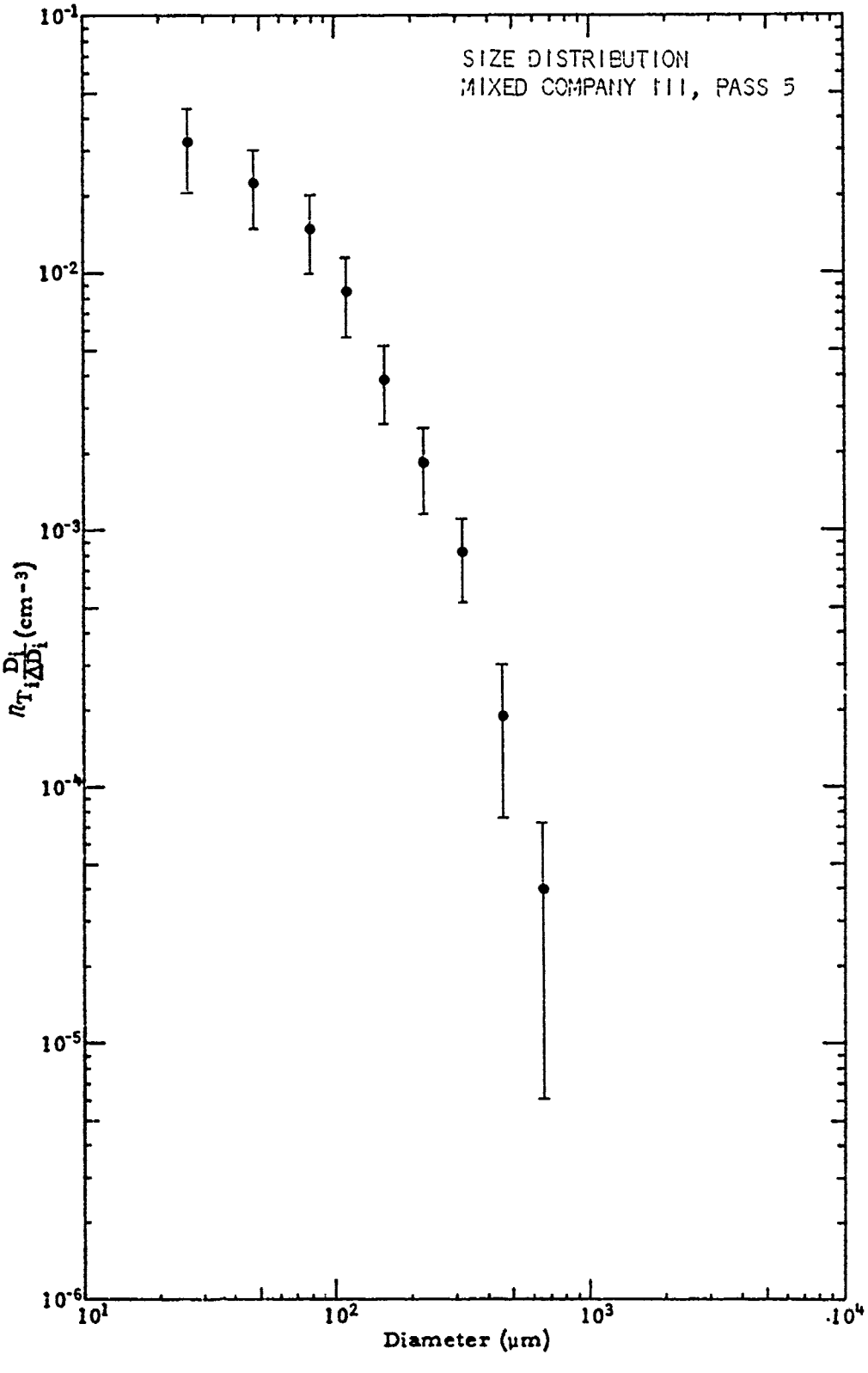
SIZE DISTRIBUTION
MIXED COMPANY III, PASS 5
10^{-1}
10^{-2}
10^{-3}
10^{-4}
10^{-5}
10^{-6}
$n_T \frac{D_i}{\sum D_i}$ (cm^{-3})
10^1
10^2
10^3
10^4
Diameter (μm)

SIZE DISTRIBUTION

Mixed Company III Pass 8

Size (Microns)	dN/dLOG D (per cc)	Error +	Error -
26	4.15 E-3	7.39 E-3	9.00 E-4
48	3.22 E-3	5.71 E-3	7.34 E-4
80	2.14 E-3	3.78 E-3	5.05 E-4
112	1.13 E-3	2.00 E-3	2.62 E-4
160	4.31 E-4	7.68 E-4	9.38 E-5
224	2.01 E-4	3.75 E-4	2.81 E-5
320	3.44 E-5	7.59 E-5	********
448	3.21 E-5	7.92 E-5	********
640	5.73 E-6	1.00 E-5	1.42 E-6
896	0.0	0.0	0.0
1280	0.0	0.0	0.0

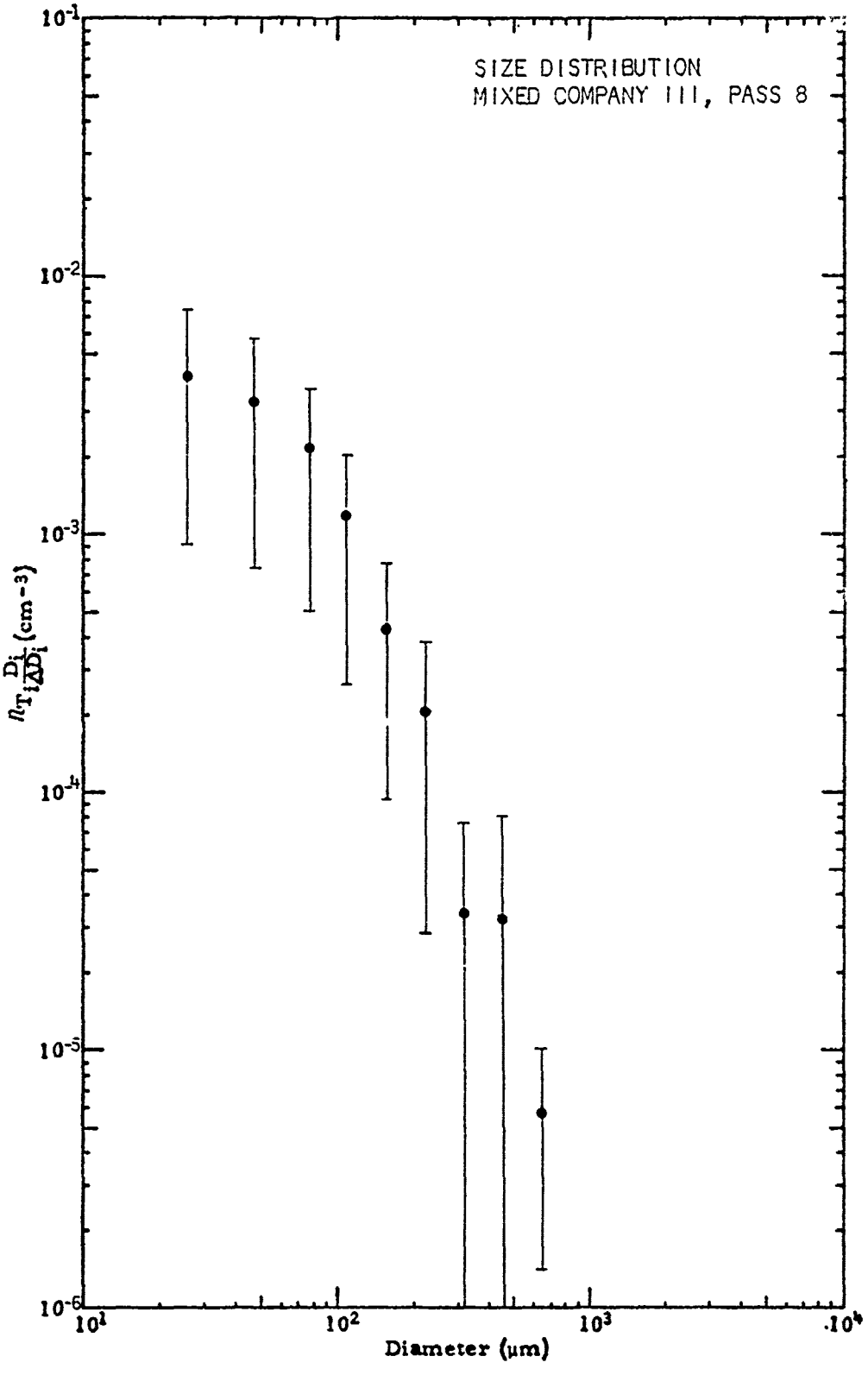
SIZE DISTRIBUTION
MIXED COMPANY III, PASS 8
10^{-1}
10^{-2}
10^{-3}
10^{-4}
10^{-5}
10^{-6}
$n_{T_i} \frac{D_i}{\Delta D_i}$ (cm^{-3})
10^1
10^2
10^3
10^4
Diameter (μm)

SIZE DISTRIBUTION

Mixed Company III Pass 9

Size (Microns)	dN/dLOG D (per cc)	Error +	Error -
26	1.04 E-2	1.50 E-2	5.73 E-3
58	6.16 E-3	8.89 E-3	3.43 E-3
80	4.22 E-3	6.09 E-3	2.36 E-3
112	2.44 E-3	3.53 E-3	1.35 E-3
160	1.49 E-3	2.15 E-3	8.24 E-4
224	9.15 E-4	1.33 E-3	4.97 E-4
320	2.89 E-4	4.21 E-4	1.57 E-4
448	5.99 E-5	1.26 E-4	********
640	0.0	0.0	0.0
896	0.0	0.0	0.0
1280	0.0	0.0	0.0

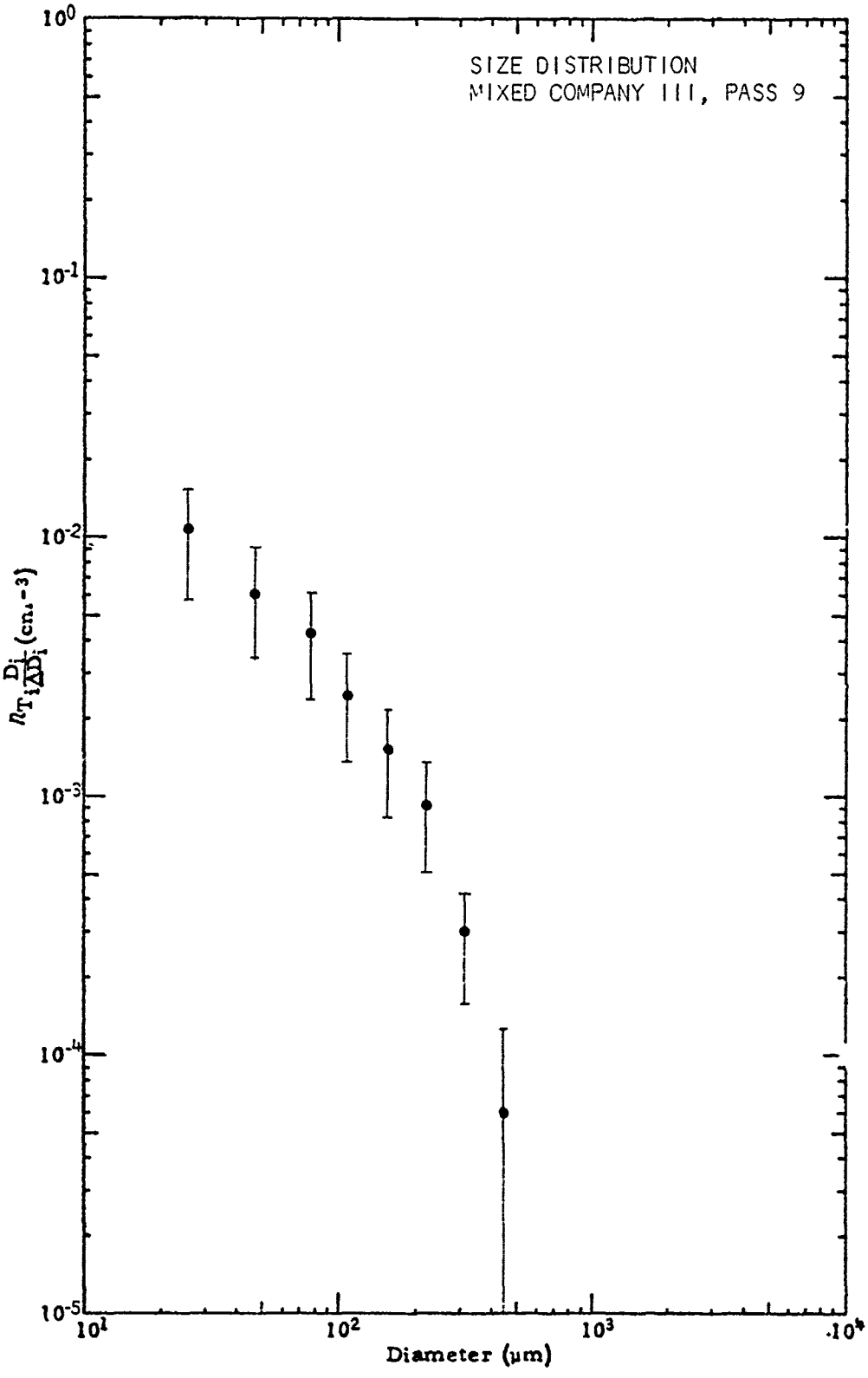
SIZE DISTRIBUTION
MIXED COMPANY III, PASS 9
10^0
10^{-1}
10^{-2}
10^{-3}
10^{-4}
10^{-5}
$n_{T_i} \frac{D_i}{\Delta D_i}$ (cm.$^{-3}$)
10^1
10^2
10^3
10^4
Diameter (μm)

SIZE DISTRIBUTION

Mixed Company III Pass 11

Size (Microns)	dN/dLOG D (per cc)	Error +	Error -
26	1.50 E-2	2.16 E-2	8.44 E-3
48	6.86 E-3	9.81 E-3	3.91 E-3
80	3.67 E-3	5.24 E-3	2.11 E-3
112	2.51 E-3	3.57 E-3	1.45 E-3
160	8.96 E-4	1.28 E-3	5.18 E-4
224	1.34 E-4	2.33 E-4	3.45 E-5
320	4.03 E-5	8.98 E-5	********
448	1.41 E-5	3.15 E-5	********
640	0.0	0.0	0.0
896	0.0	0.0	0.0
1280	0.0	0.0	0.0

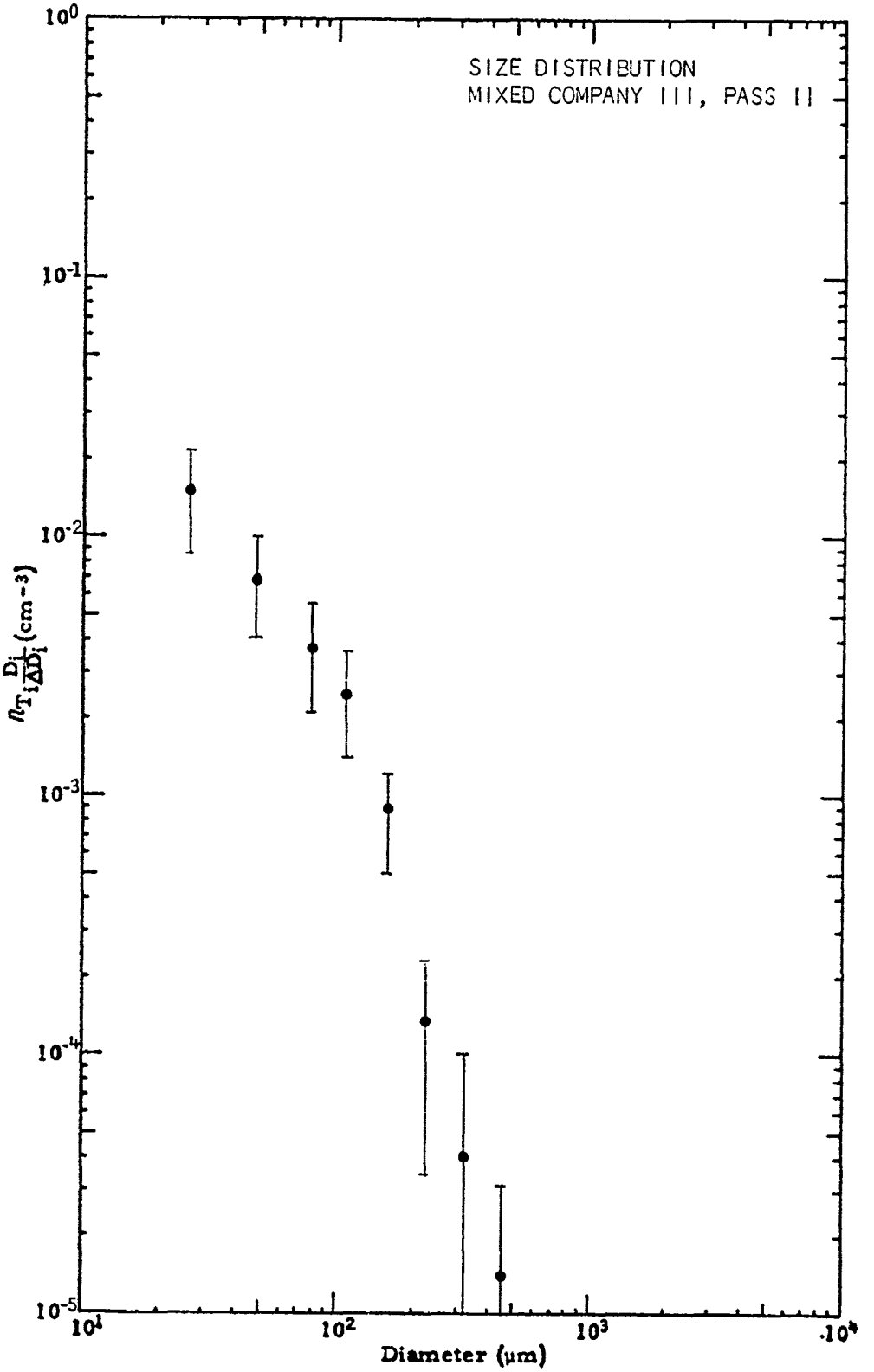
SIZE DISTRIBUTION
MIXED COMPANY III, PASS II
10^0
10^{-1}
10^{-2}
10^{-3}
10^{-4}
10^{-5}
$n_T \frac{D_i}{\Delta D_i}$ (cm^{-3})
10^1
10^2
10^3
10^4
Diameter (μm)

SIZE DISTRIBUTION

Mixed Company III Pass 14

Size (Microns)	dN/dLOG D (per cc)	Error +	Error -
26	3.03 E-2	4.13 E-2	1.94 E-2
48	1.13 E-2	1.52 E-2	7.47 E-3
80	2.27 E-3	3.07 E-3	1.46 E-3
112	9.65 E-4	1.32 E-3	6.06 E-4
160	2.56 E-4	3.78 E-4	1.34 E-4
224	6.35 E-5	1.23 E-4	4.45 E-6
320	2.51 E-5	4.78 E-5	2.35 E-6
448	0.0	0.0	0.0
640	0.0	0.0	0.0
896	0.0	0.0	0.0
1280	0.0	0.0	0.0

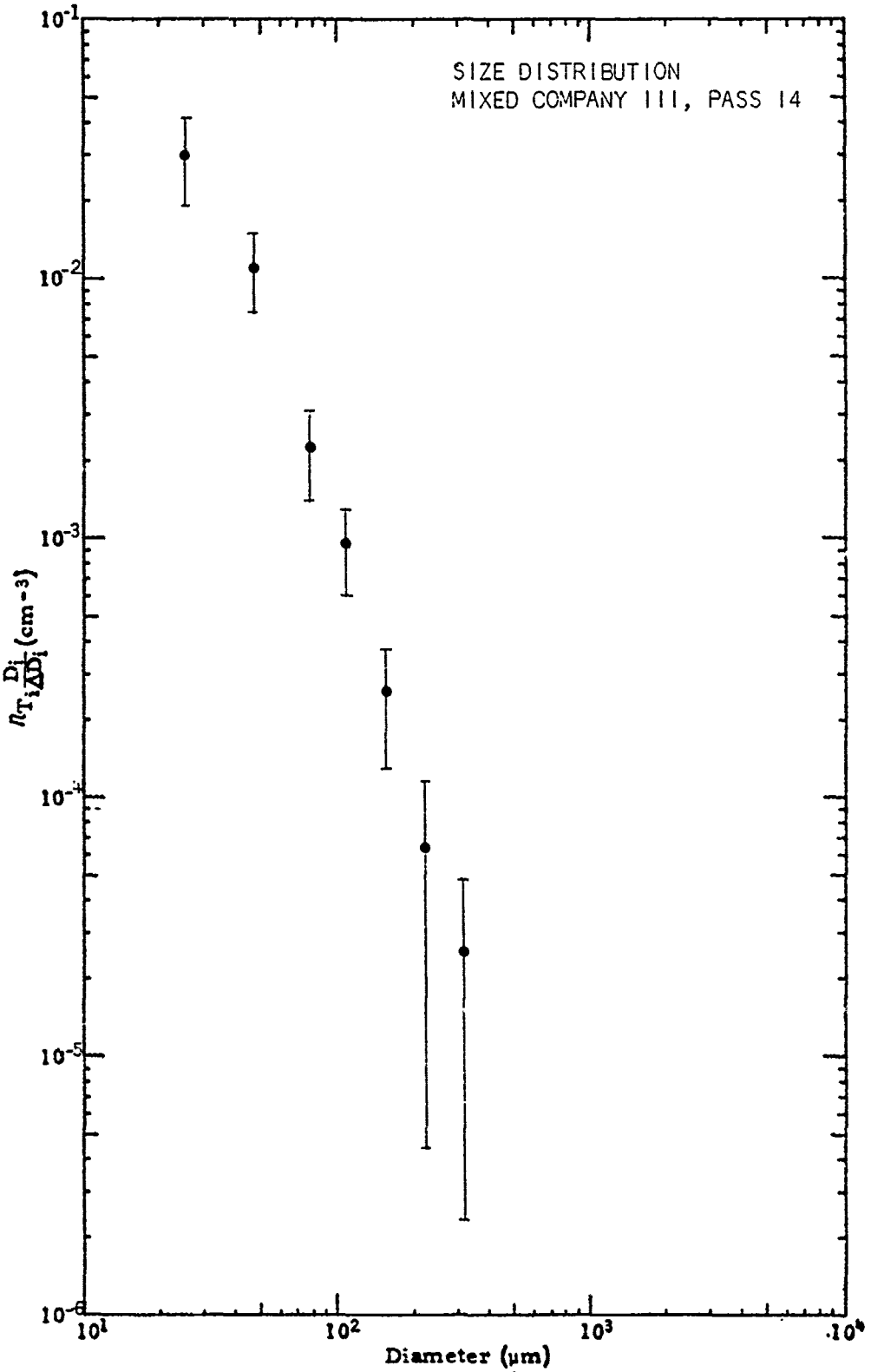
SIZE DISTRIBUTION
MIXED COMPANY III, PASS 14
10^{-1}
10^{-2}
10^{-3}
10^{-4}
10^{-5}
10^{-6}
$n_{T_i} \frac{D_i}{\Delta D_i}$ (cm^{-3})
10^1
10^2
10^3
10^4
Diameter (μm)

APPENDIX VI

SIZE DISTRIBUTION DATA-FALLOUT DUST SAMPLES

SIZE DISTRIBUTION

Middle Gust III Fallout 1000' 60°

Size (Microns)	dN/dLOG D (per cc)	Error +	Error -
26	5.22E+9	7.19E+9	3.24E+9
48	2.19E+9	3.03E+9	1.36E+9
80	1.08E+9	1.49E+9	6.69E+8
112	6.24E+8	8.60E+8	3.88E+8
160	2.41E+8	3.34E+8	1.49E+8
224	1.26E+8	1.78E+8	7.41E+7
320	2.63E+7	3.97E+7	1.29E+7
448	1.98E+7	3.01E+7	9.39E+6
640	1.35E+7	1.81E+7	8.85E+6
896	3.94E+5	6.01E+5	1.86E+5
1280	0.0	0.0	0.0

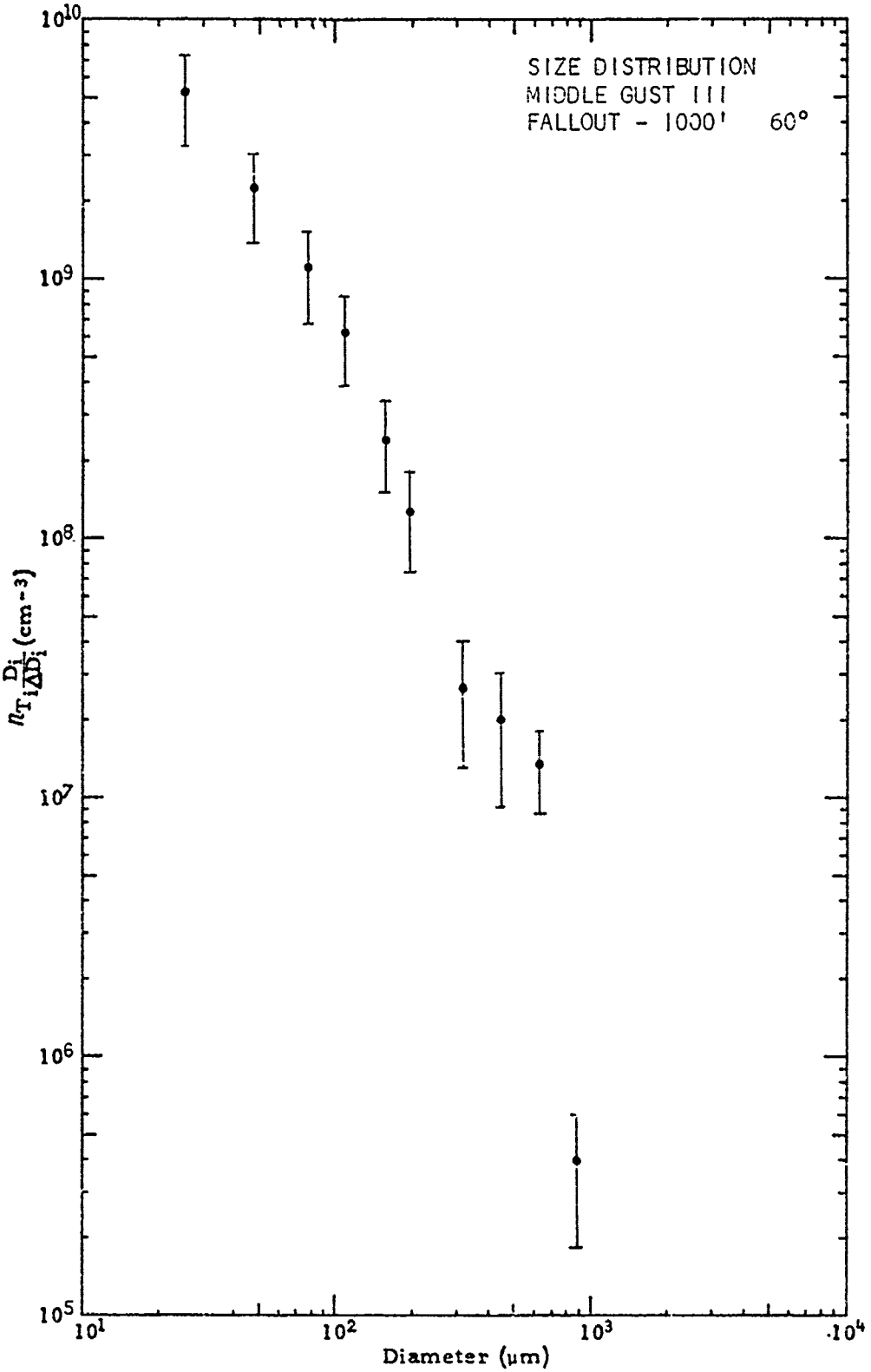
SIZE DISTRIBUTION
MIDDLE GUST III
FALLOUT - 1000' 60°
10^{10}
10^{9}
10^{8}
10^{7}
10^{6}
10^{5}
$n_{T_i} \frac{D_i}{\Delta D_i}$ (cm^{-3})
10^{1}
10^{2}
10^{3}
10^{4}
Diameter (μm)

SIZE DISTRIBUTION

Middle Gust III Fallout 2000' 60°

Size (Microns)	dN/dLOG D (per cc)	Error +	Error -
26	5.26E+5	6.82E+5	3.71E+5
48	1.63E+5	2.12E+5	1.15E+5
80	1.31E+5	1.71E+5	9.15E+4
112	1.45E+5	1.89E+5	1.01E+5
160	1.07E+5	1.38E+5	7.60E+4
224	7.98E+4	1.03E+5	5.68E+4
320	2.17E+4	2.83E+4	1.52E+4
448	9.45E+3	1.31E+4	5.79E+3
640	9.00E+2	1.68E+3	1.21E+2
896	0.0	0.0	0.0
1280	0.0	0.0	0.0

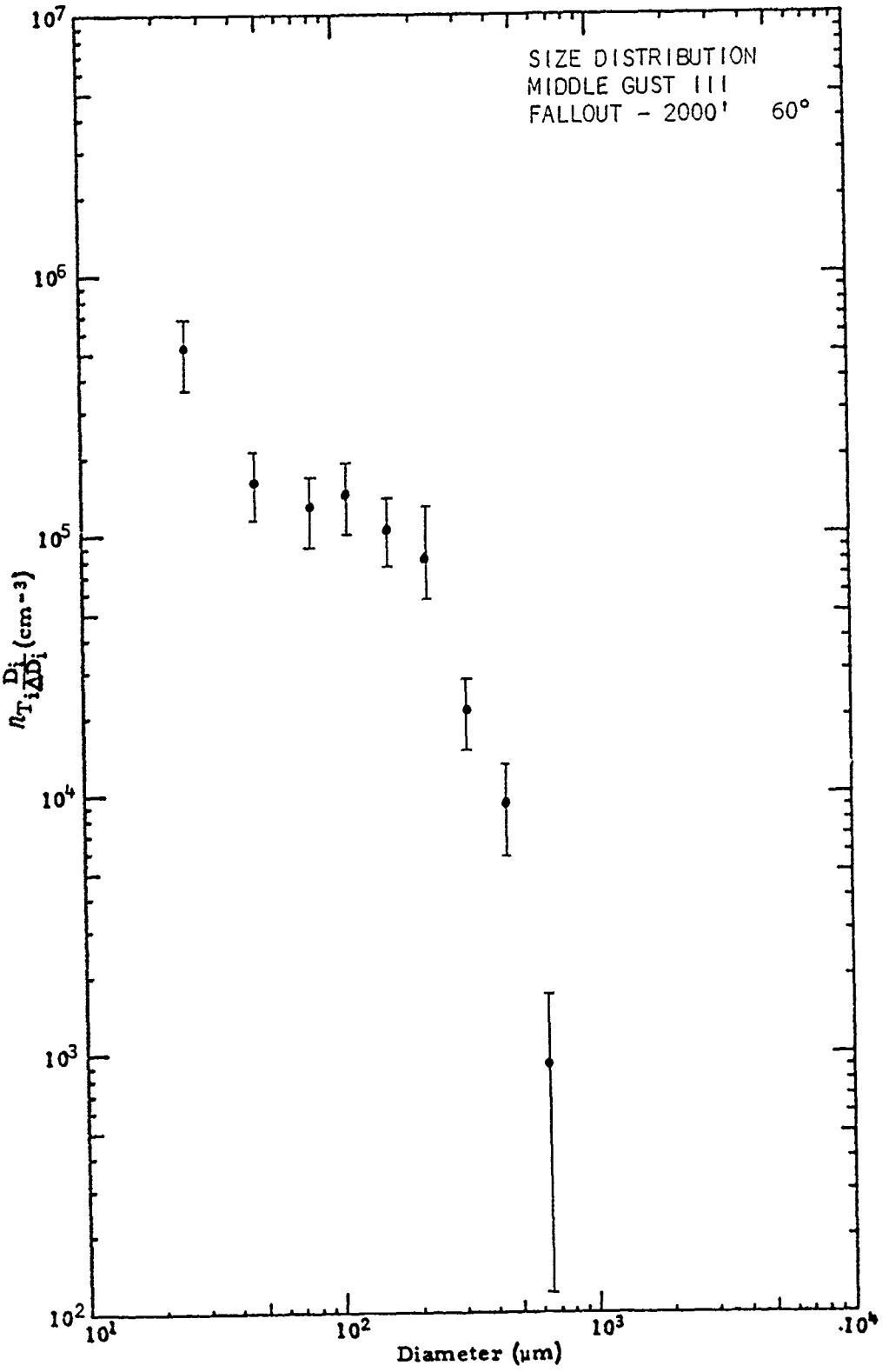
SIZE DISTRIBUTION
MIDDLE GUST III
FALLOUT - 2000' 60°
10^7
10^6
10^5
10^4
10^3
10^2
$n_{T_i} \frac{D_i}{\Delta D_i}$ (cm^{-3})
10^1
10^2
10^3
10^4
Diameter (μm)

SIZE DISTRIBUTION

Middle Gust III Fallout 8000' 60°

Size (Microns)	dN/dLOG D (per cc)	Error +	Error -
26	1.44E+5	1.78E+5	1.10E+5
48	4.92E+4	6.11E+4	3.73E+4
80	1.52E+4	1.93E+4	1.12E+4
112	4.01E+3	5.51E+3	2.52E+3
160	3.62E+3	4.74E+3	2.51E+3
224	6.76E+3	8.70E+3	4.82E+3
320	2.41E+3	3.21E+3	1.62E+3
448	2.32E+3	3.12E+3	1.52E+3
640	3.17E+3	3.87E+3	2.46E+3
896	3.38E+3	3.94E+3	2.82E+3
1280	0.0	0.0	0.0

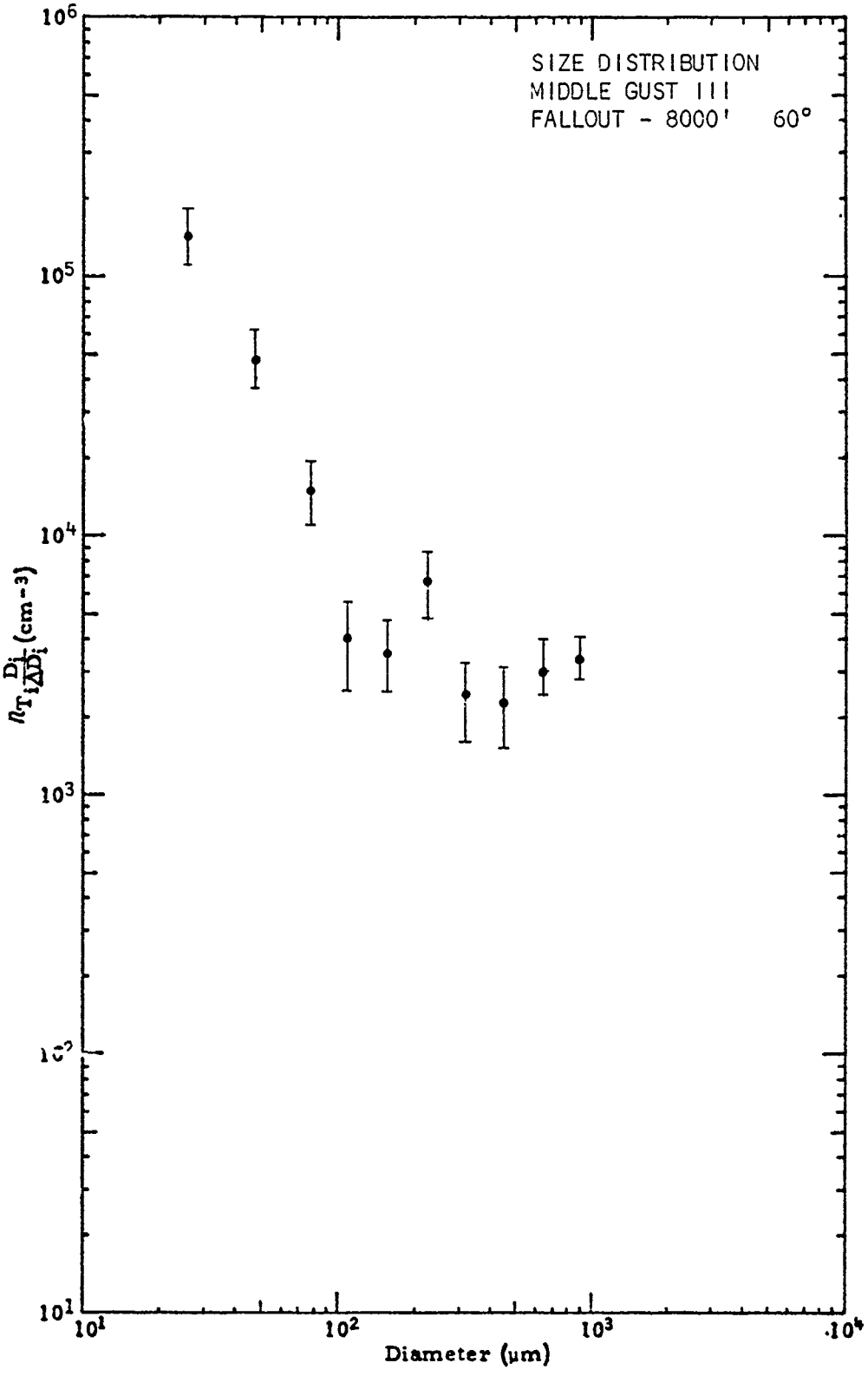
SIZE DISTRIBUTION
MIDDLE GUST III
FALLOUT - 8000' 60°
10^6
10^5
10^4
10^3
10^2
10^1
$n_{T_i} \frac{D_i}{\Delta D_i}$ (cm^{-3})
10^1
10^2
10^3
10^4
Diameter (μm)

SIZE DISTRIBUTION

Middle Gust IV Fallout 1000' 280°

Size (Microns)	dN/dLOG D (per cc)	Error +	Error -
26	1.17E+8	2.04E+8	2.98E+7
48	4.45E+7	7.75E+7	1.15E+7
80	1.56E+7	2.72E+7	3.94E+6
112	5.03E+6	8.90E+6	1.15E+6
160	3.59E+6	6.55E+6	6.28E+5
224	3.46E+6	6.36E+6	5.56E+5
320	2.94E+6	5.09E+6	7.94E+5
448	1.40E+6	2.59E+6	2.05E+5
640	3.49E+5	7.43E+5	-------
896	1.05E+5	2.23E+5	-------
1280	4.99E+4	8.37E+4	1.60E+4

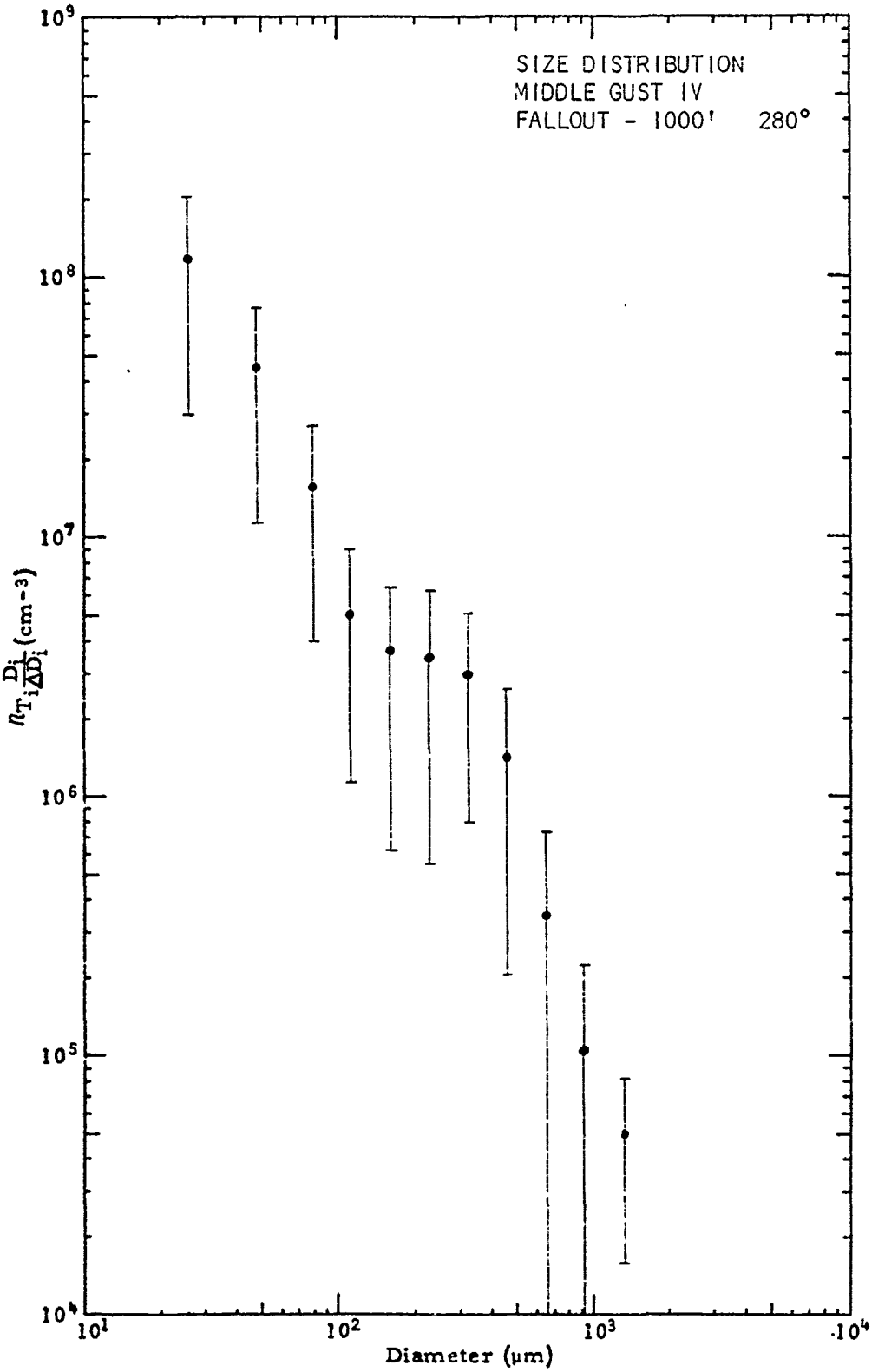
SIZE DISTRIBUTION
MIDDLE GUST IV
FALLOUT - 1000' 280°
10^9
10^8
10^7
10^6
10^5
10^4
$n_{T_i} \frac{D_i}{\Delta D_i}$ (cm^{-3})
10^1
10^2
10^3
10^4
Diameter (μm)

SIZE DISTRIBUTION

Middle Gust IV Fallout 1000' 320°

Size (Microns)	dN/dLOG D (per cc)	Error +	Error -
26	1.07E+7	1.67E+7	4.64E+6
48	2.64E+6	4.12E+6	1.16E+6
80	1.03E+6	1.61E+6	4.47E+5
112	7.98E+5	1.25E+6	3.46E+5
160	4.03E+5	6.33E+5	1.73E+5
224	2.18E+5	3.51E+5	6.48E+4
320	1.02E+5	1.62E+5	4.19E+4
448	1.91E+4	3.85E+4	-------
640	3.31E+4	4.78E+4	1.83E+4
896	0.0	0.0	0.0
1280	0.0	0.0	0.0

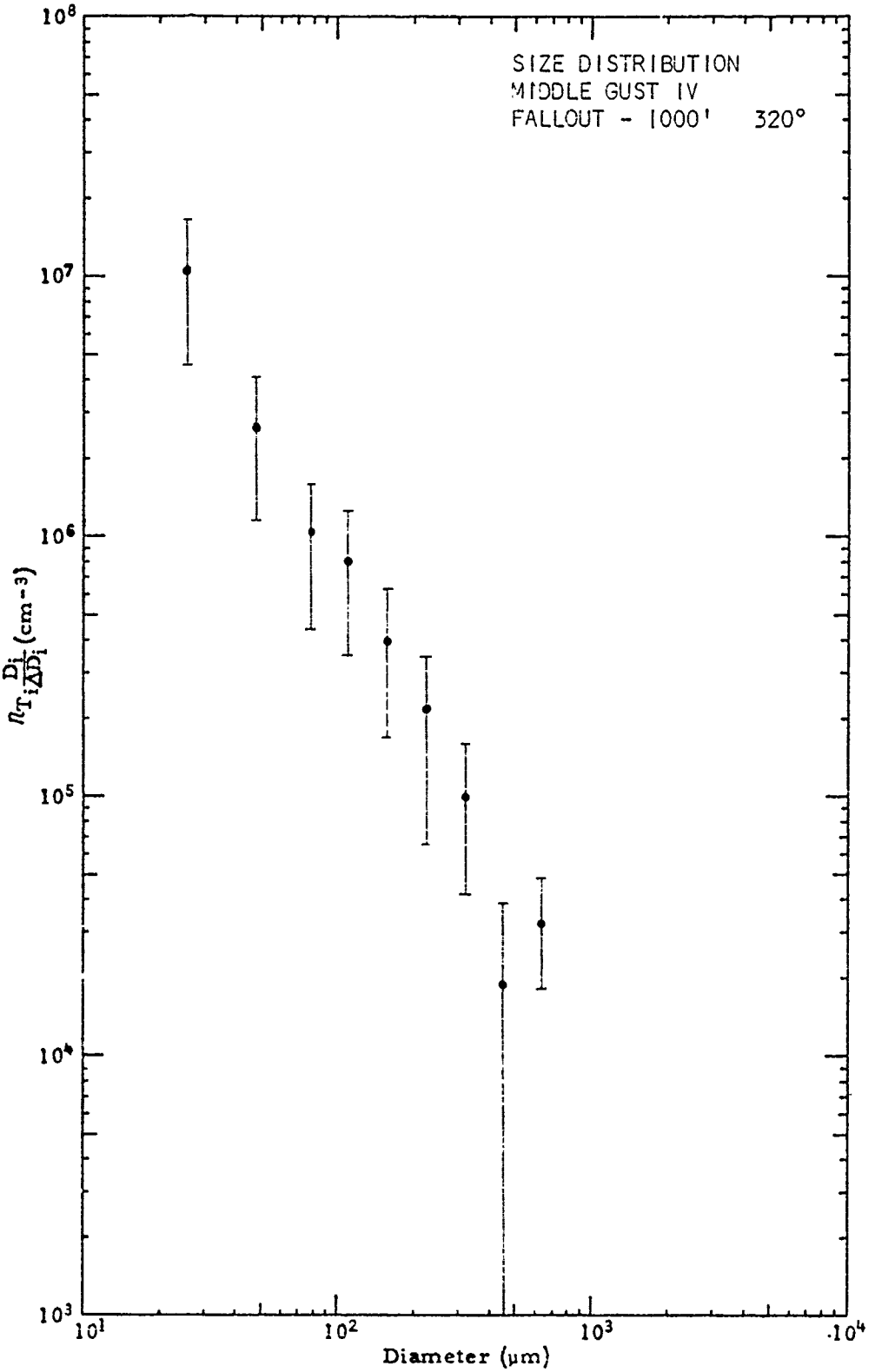
SIZE DISTRIBUTION
MIDDLE GUST IV
FALLOUT - 1000' 320°
10^8
10^7
10^6
10^5
10^4
10^3
$n_{T_i} \frac{D_i}{\Delta D_i}$ (cm^{-3})
10^1
10^2
10^3
10^4
Diameter (μm)

SIZE DISTRIBUTION

Mixed Company III Fallout 1000' 60°

Size (Microns)	dN/dLOG D (per cc)	Error +	Error -
26	6.72E+6	1.15E+7	1.97E+6
48	3.42E+6	5.80E+6	1.03E+6
80	1.67E+6	2.67E+6	6.62E+5
112	6.21E+5	9.61E+5	2.82E+5
160	4.45E+5	6.85E+5	2.05E+5
224	2.60E+5	4.02E+5	1.18E+5
320	1.09E+5	1.68E+5	4.94E+4
448	7.66E+4	1.22E+5	3.10E+4
640	2.26E+4	3.75E+4	7.68E+3
896	4.55E+3	8.78E+3	3.26E+2
1280	4.40E+3	6.87E+3	1.93E+3

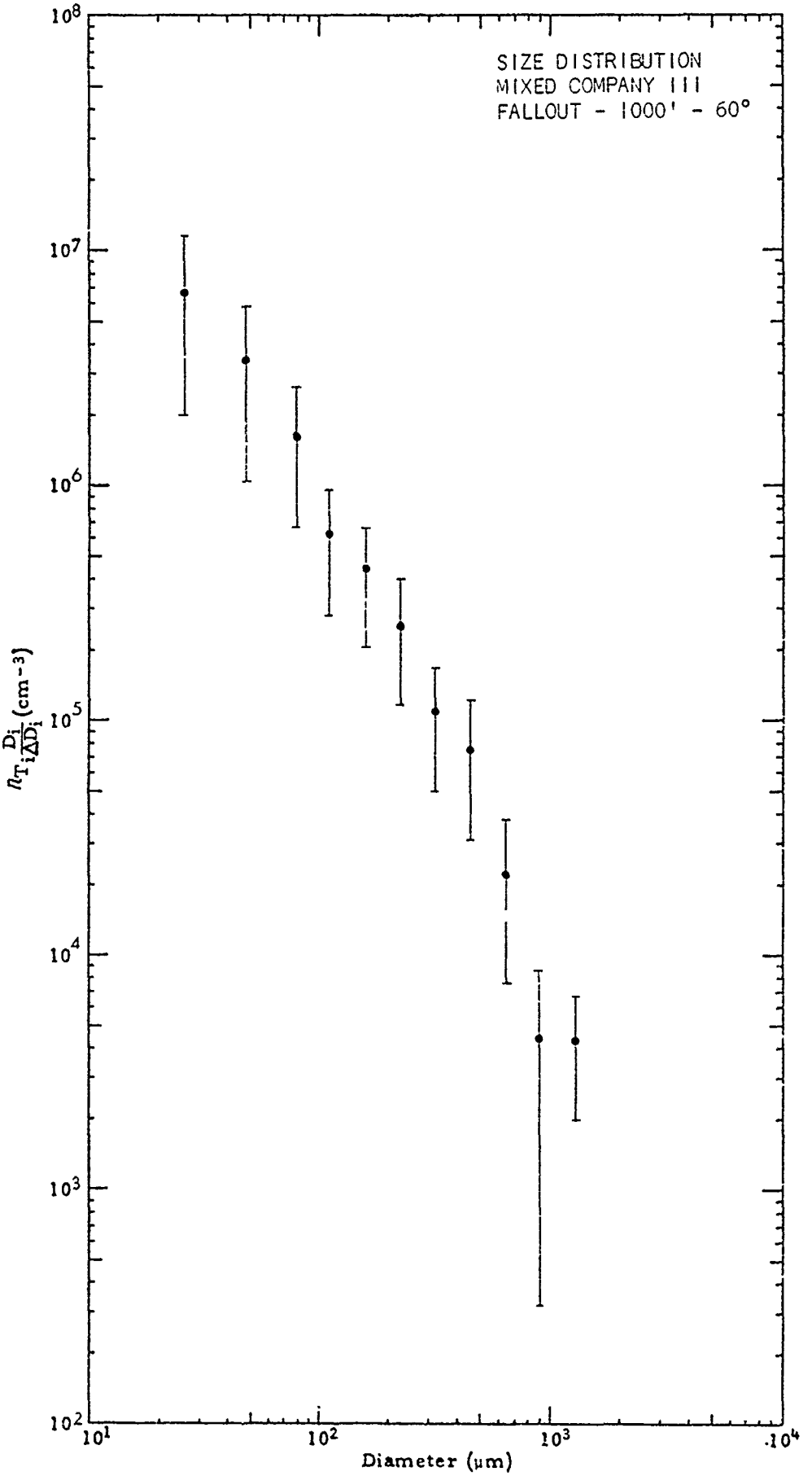
SIZE DISTRIBUTION
MIXED COMPANY III
FALLOUT - 1000' - 60°
10^8
10^7
10^6
10^5
10^4
10^3
10^2
$n_{T_i} \frac{D_i}{\Delta D_i}$ (cm^{-3})
10^1
10^2
10^3
10^4
Diameter (μm)

SIZE DISTRIBUTION

Mixed Company III Fallout 3000' 60°

Size (Microns)	dN/dLOG D (per cc)	Error +	Error -
26	1.38E+7	2.84E+7	-------
48	7.74E+6	1.50E+7	4.48E+5
80	2.49E+6	4.22E+6	7.69E+5
112	8.50E+5	1.28E+6	4.17E+5
160	6.40E+5	1.03E+6	2.53E+5
224	4.32E+5	7.23E+5	1.40E+5
320	2.37E+5	3.45E+5	1.29E+5
448	1.17E+5	1.71E+5	6.18E+4
640	2.26E+4	3.38E+4	1.13E+4
896	8.50E+3	1.44E+4	2.57E+3
1280	8.68E+2	1.85E+3	-------

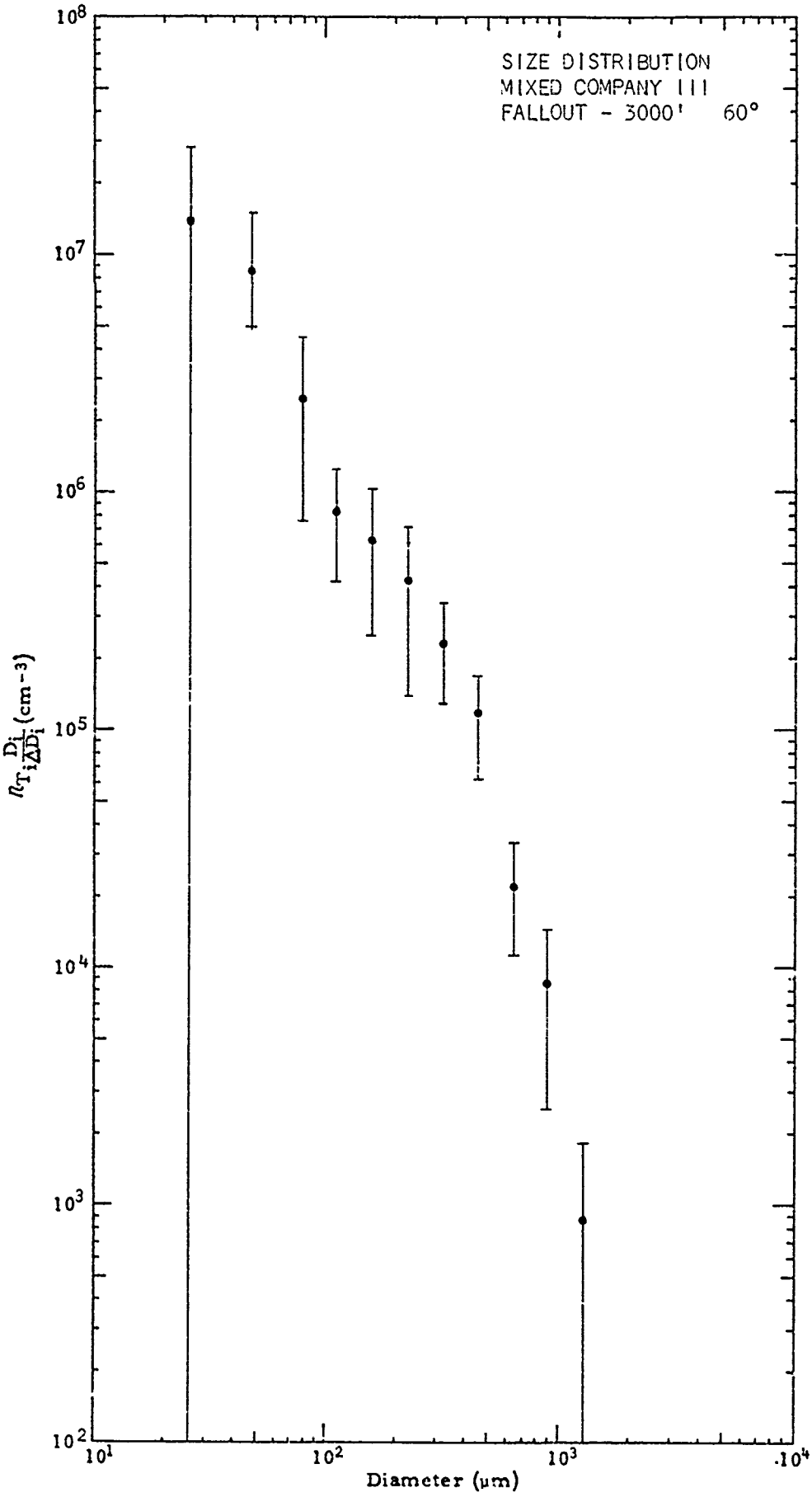
SIZE DISTRIBUTION
MIXED COMPANY III
FALLOUT - 3000' 60°
10^8
10^7
10^6
10^5
10^4
10^3
10^2
$n_{T_i} \frac{D_i}{\Delta D_i}$ (cm^{-3})
10^1
10^2
10^3
10^4
Diameter (μm)

SIZE DISTRIBUTION

Mixed Company III Fallout 6000' 60°

Size (Microns)	dN/dLOG D (per cc)	Error +	Error -
26	4.18E+6	5.46E+6	2.90E+6
48	1.62E+6	2.10E+6	1.15E+6
80	5.06E+5	6.63E+5	3.50E+5
112	3.31E+5	4.33E+5	2.28E+5
160	2.63E+5	3.42E+5	1.85E+5
224	2.44E+5	3.16E+5	1.72E+5
320	1.81E+5	2.32E+5	1.31E+5
448	1.07E+5	1.40E+5	7.45E+4
640	5.82E+4	7.36E+4	4.28E+4
896	1.66E+4	2.30E+4	1.03E+4
1280	2.51E+3	4.20E+3	8.27E+2

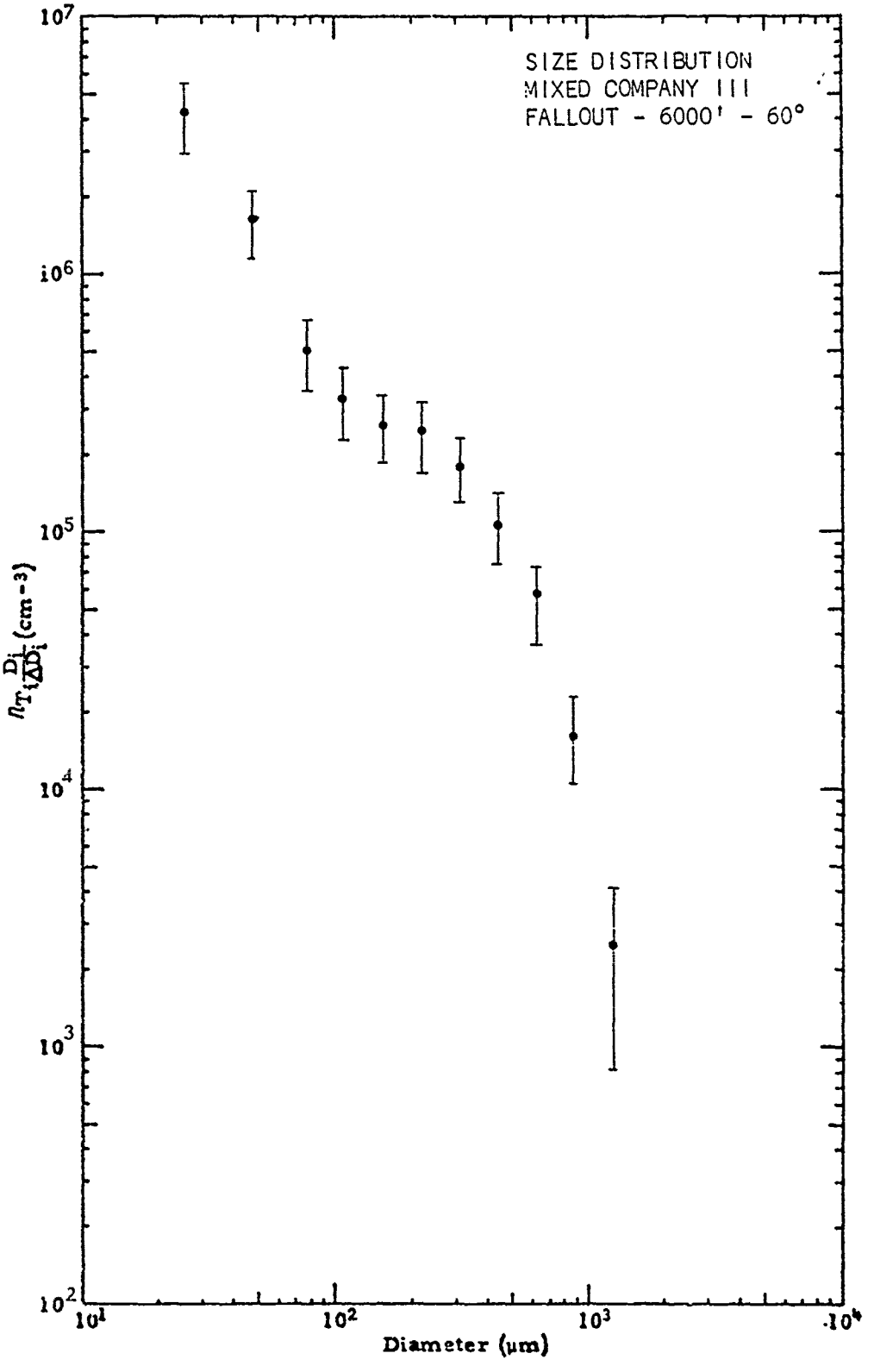
SIZE DISTRIBUTION
MIXED COMPANY III
FALLOUT - 6000' - 60°
10^7
10^6
10^5
10^4
10^3
10^2
$n_{T_i} \frac{D_i}{\Delta D_i}$ (cm^{-3})
10^1
10^2
10^3
10^4
Diameter (μm)

APPENDIX VII

PARTICLE DENSITY DATA-AIRBORNE AND FALLOUT SAMPLES

PARTICLE DENSITY

Middle Gust I Pass 1

Size (Microns)	RHO (gm/cc)	RHO +	RHO -
26	2.61	3.48	1.74
48	2.62	3.53	1.71
80	2.58	3.44	1.72
112	2.62	3.56	1.68
160	2.63	3.61	1.65
224	2.65	3.77	1.53
320	2.61	4.11	1.11
448	2.64	4.28	1.00
640	2.64	3.94	1.34
896	2.10	5.01	-0.81
1280	2.10	3.71	0.49

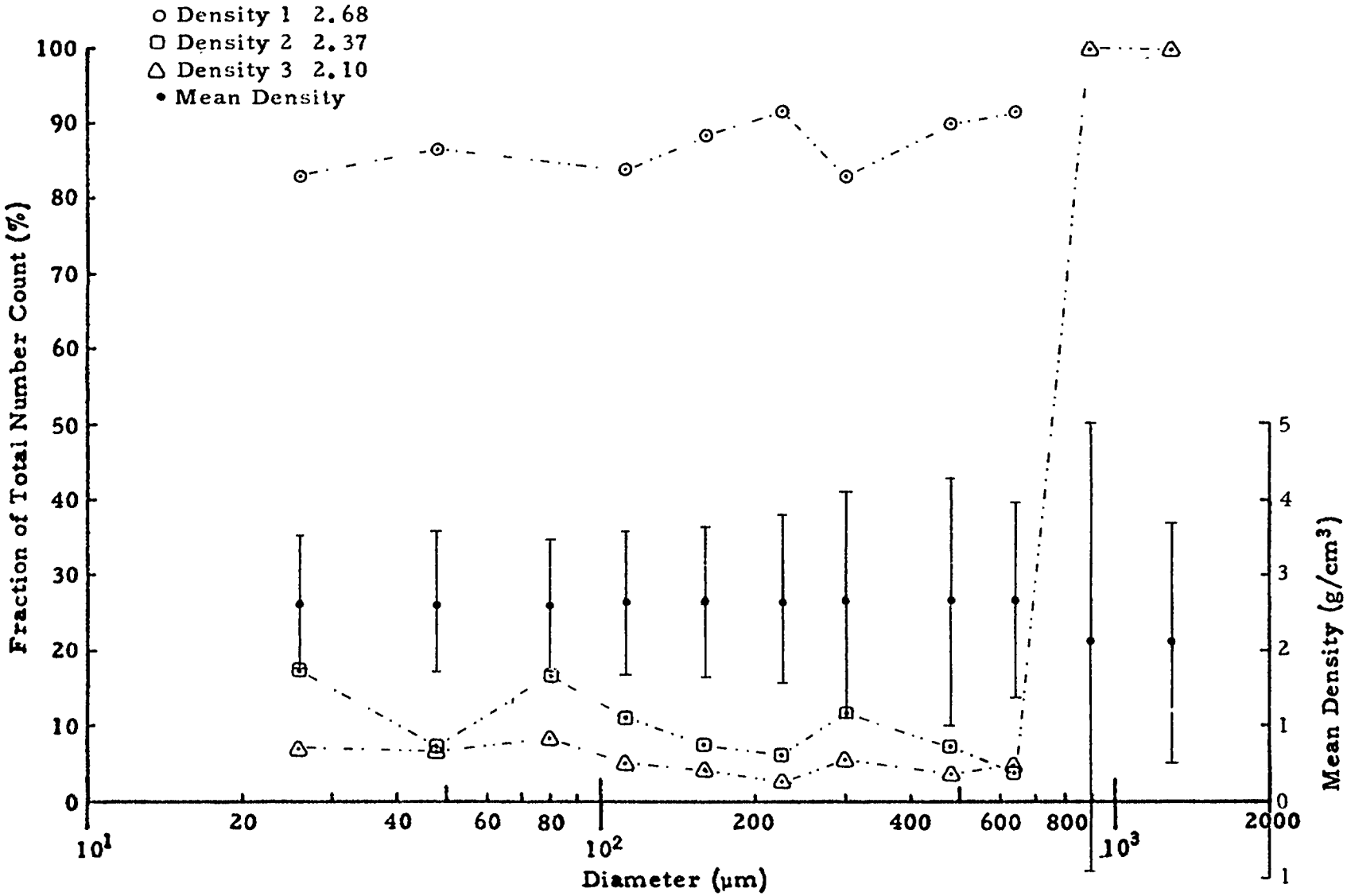

PARTICLE DENSITY
MIDDLE GUST I, PASS I

PARTICLE DENSITY

Mine Throw I Pass 4

Size (Microns)	RHO (gm/cc)	RHO +	RHO -
26	2.40	2.85	1.95
48	2.39	2.84	1.94
80	2.40	2.87	1.93
112	2.40	2.89	1.91
160	2.41	2.97	1 85
224	2.33	3.25	1.41
320	2.32	3.83	0.81
448	2.19	3.82	0.56
640	2.04	3.49	0.59
896	0.0	0.0	0.0
1280	0.0	0.0	0.0

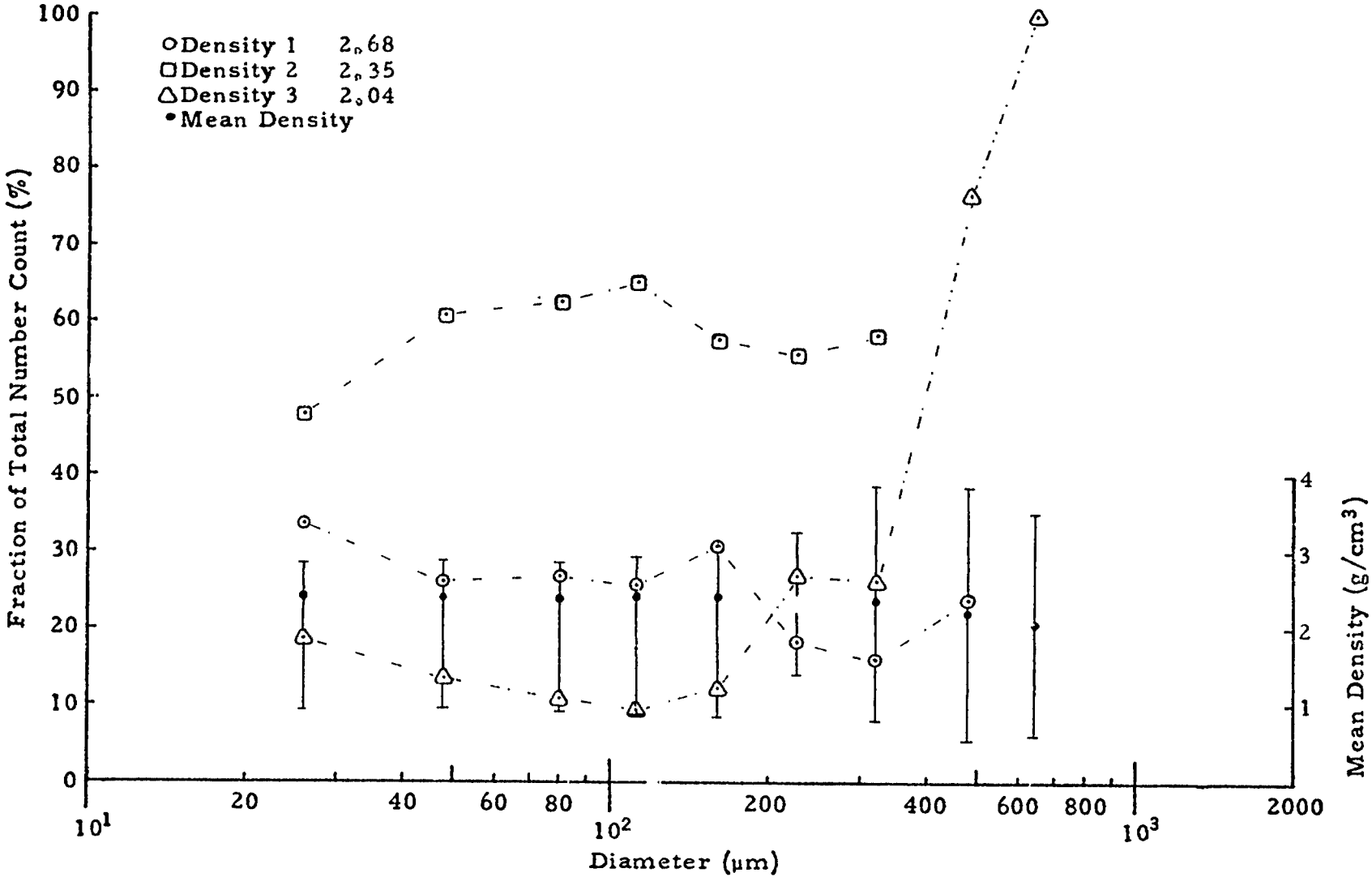

PARTICLE DENSITY
MINE THROW 1, PASS 4

PARTICLE DENSITY

Middle Gust III Pass 1

Size (Microns)	RHO (gm/cc)	RHO +	RHO -
26	2.19	2.69	1.69
48	2.28	2.73	1.83
80	2.28	2.75	1.81
112	2.32	2.80	1.84
160	2.34	2.87	1.81
224	2.34	2.99	1.69
320	2.30	3.00	1.60
448	2.32	3.26	1.38
640	2.31	3.17	1.45
896	1.81	2.97	0.65
1280	0.0	0.0	0.0

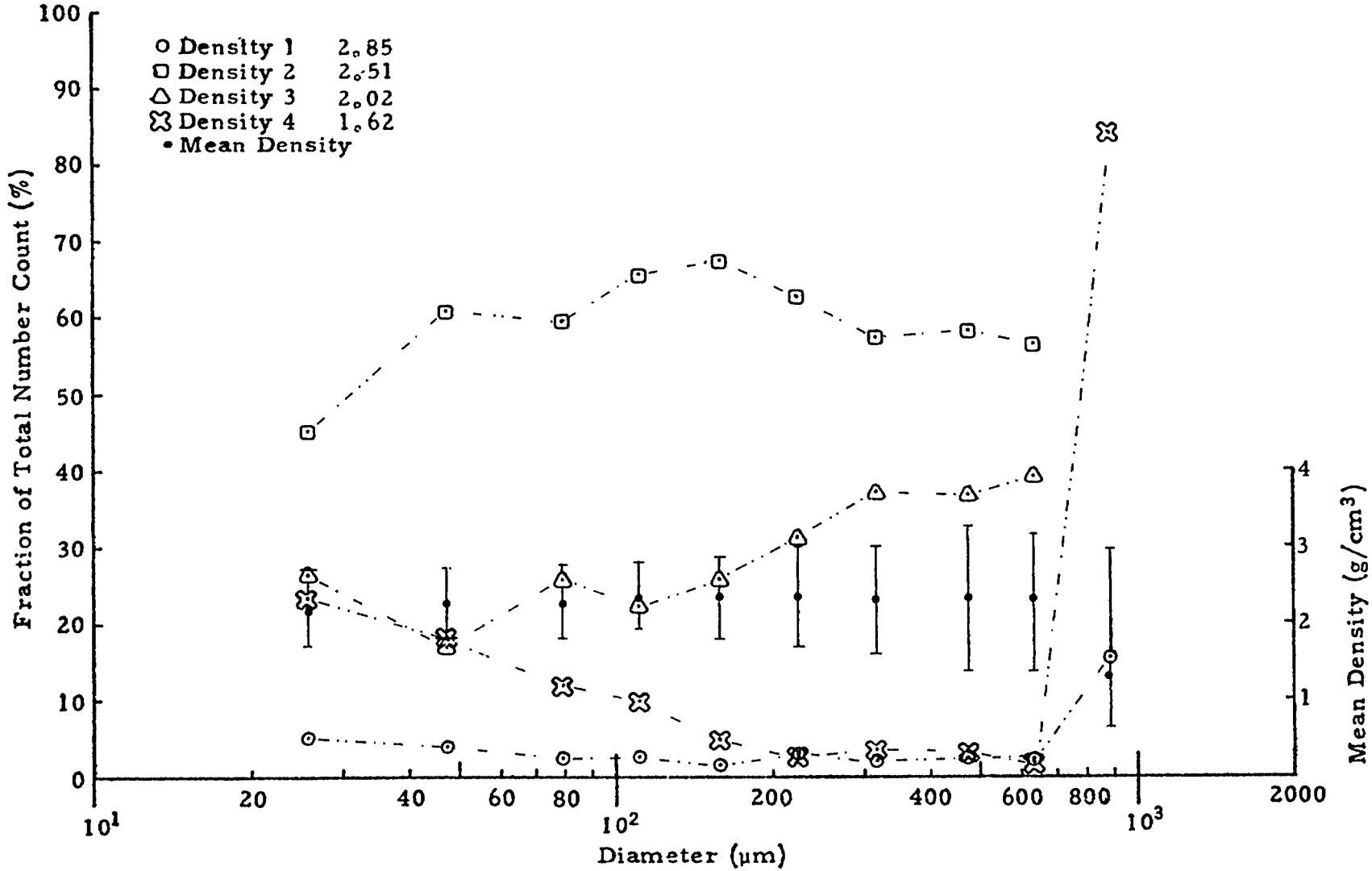

PARTICLE DENSITY
MIDDLE GUST III, PASS I

PARTICLE DENSITY

Middle Gust III Pass 2

Size (Microns)	RHO (gm/cc)	RHO +	RHO -
26	2.41	3.03	1.79
48	2.39	3.03	1.75
80	2.38	3.05	1.71
112	2.40	3.07	1.73
160	2.47	3.18	1.76
224	2.47	3.33	1.61
320	2.56	3.50	1.62
448	2.54	3.74	1.34
640	2.51	3.85	1.17
896	2.53	6.62	****
1280	2.45	4.63	0.27

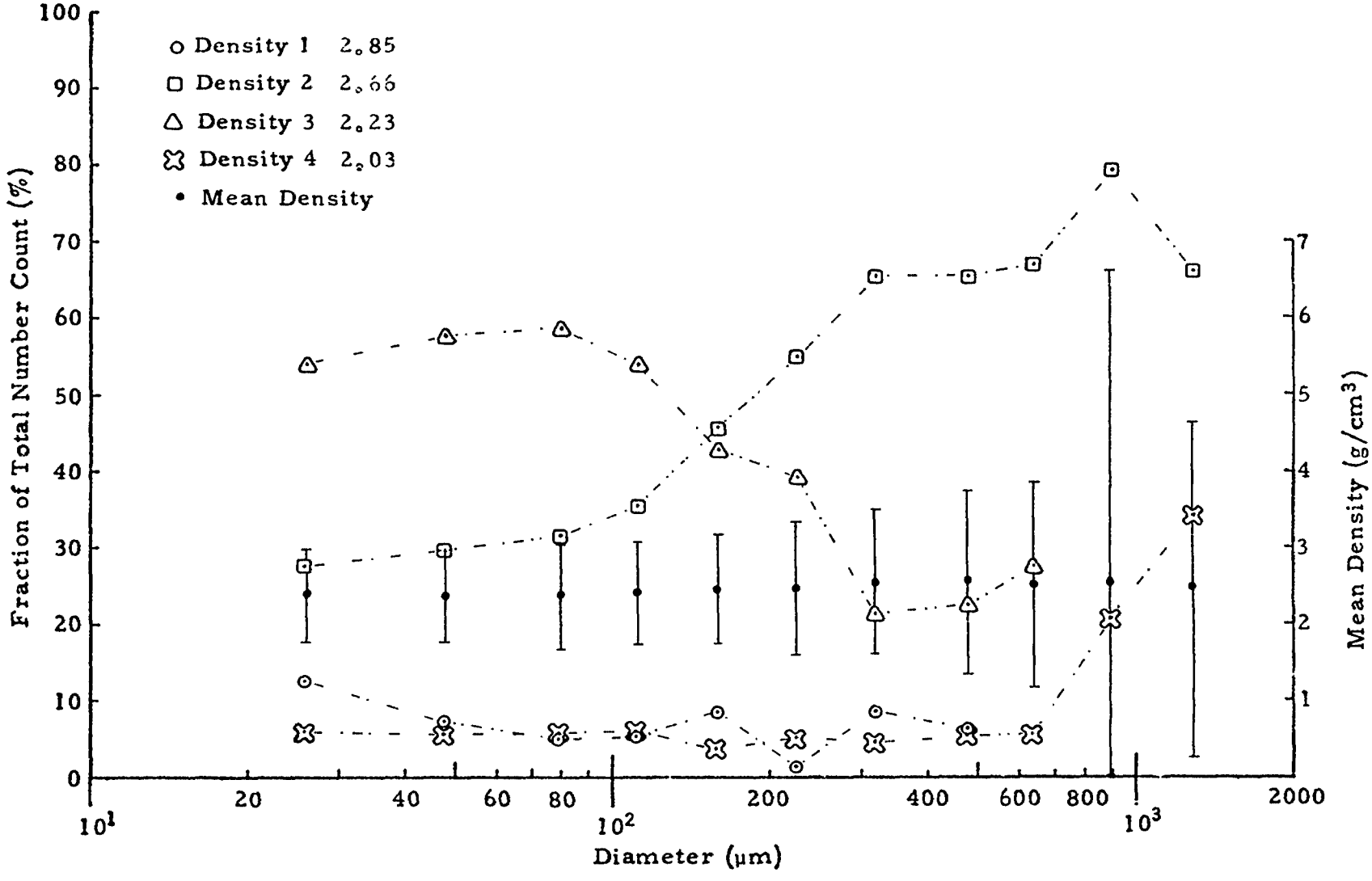

PARTICLE DENSITY
MIDDLE GUST III, PASS 2

PARTICLE DENSITY

Middle Gust III Pass 3

Size (Microns)	RHO (gm/cc)	RHO +	RHO -
26	2.56	3.19	1.93
48	2.37	2.99	1.75
80	2.46	3.06	1.86
112	2.44	3.07	1.81
160	2.43	3.11	1.75
224	2.52	3.24	1.80
320	2.38	3.11	1.65
448	2.41	3.39	1.43
640	2.38	4.07	0.69
896	2.65	5.89	-0.59
1280	2.03	2.99	1.07

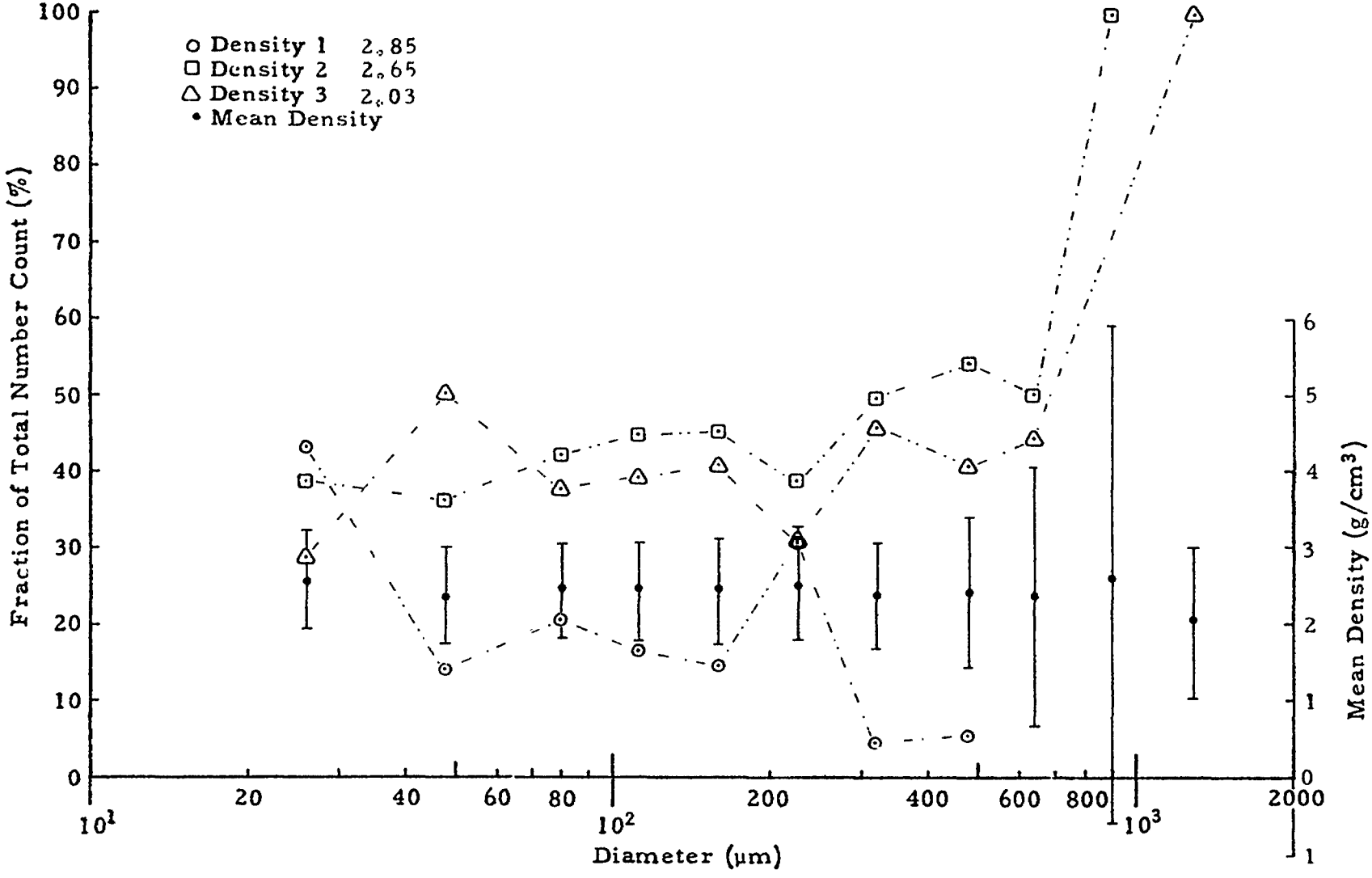

PARTICLE DENSITY
MIDDLE GUST III, PASS 3

PARTICLE DENSITY

Middle Gust III Pass 5

Size (Microns)	RHO (gm/cc)	RHO +	RHO -
26	2.37	3.25	1.49
48	2.26	3.29	1.23
80	2.33	3.26	1.40
112	2.37	3.29	1.45
160	2.32	3.36	1.28
224	2.43	3.52	1.34
320	2.46	3.49	1.43
448	2.38	4.01	0.75
640	2.48	4.76	0.20
896	2.64	3.89	1.39
1280	0.0	0.0	0.0

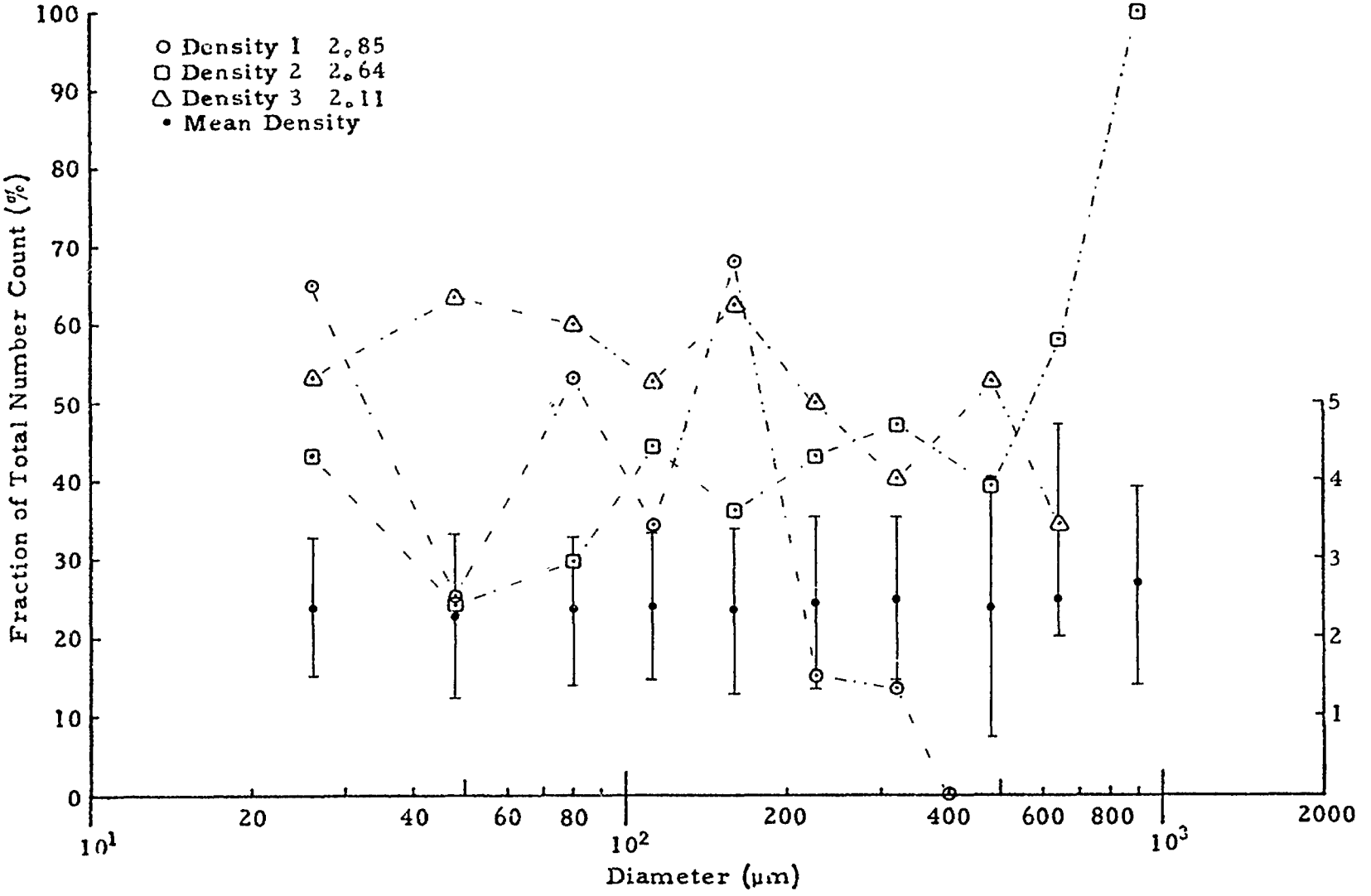

PARTICLE DENSITY
MIDDLE GUST III, PASS 5

PARTICLE DENSITY

Middle Gust III Fallout 1000' 60°

Size (Microns)	RHO (gm/cc)	RHO +	RHO -
26	2.51	3.39	1.63
48	2.48	3.37	1.59
80	2.47	3.38	1.56
112	2.51	3.44	1.58
160	2.55	3.57	1.53
224	2.57	3.78	1.36
320	2.55	4.22	0.88
448	2.62	4.52	0.72
640	2.57	3.90	1.24
896	2.24	3.69	0.79
1280	0.0	0.0	0.0

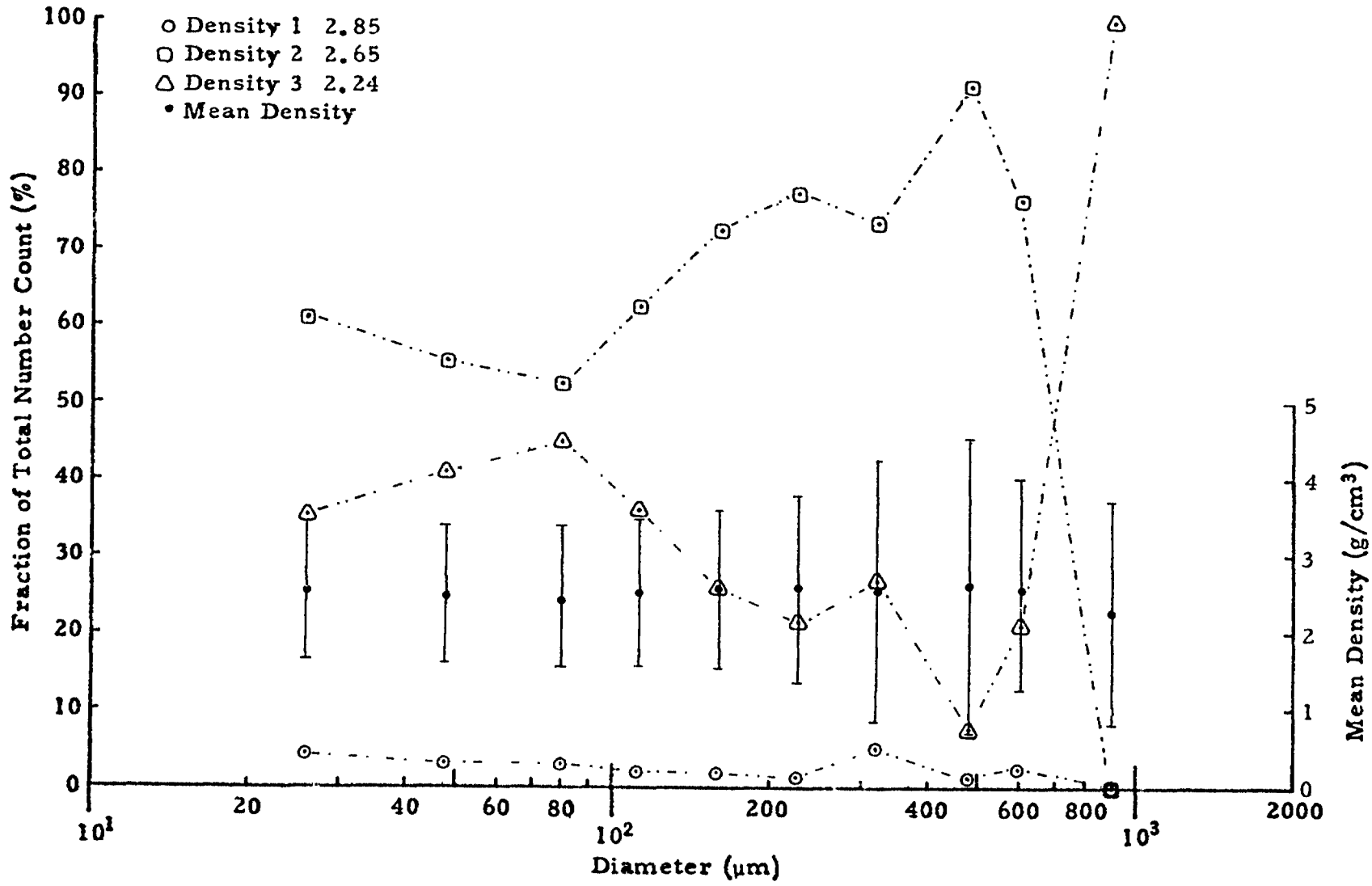

PARTICLE DENSITY
MIDDLE GUST III, FALLOUT - 1000' 60°

PARTICLE DENSITY

Mixed Company I Pass 1

Size (Microns)	RHO (gm/cc)	RHO +	RHO -
26	2.54	3.26	1.82
48	2.54	3.25	1.83
80	2.57	3.27	1.87
112	2.58	3.30	1.86
160	2.58	3.36	1.80
224	2.58	3.46	1.70
320	2.58	3.46	1.70
448	2.57	4.84	0.30
640	2.62	5.52	-0.28
896	0.0	0.0	0.0
1280	2.85	4.76	0.94

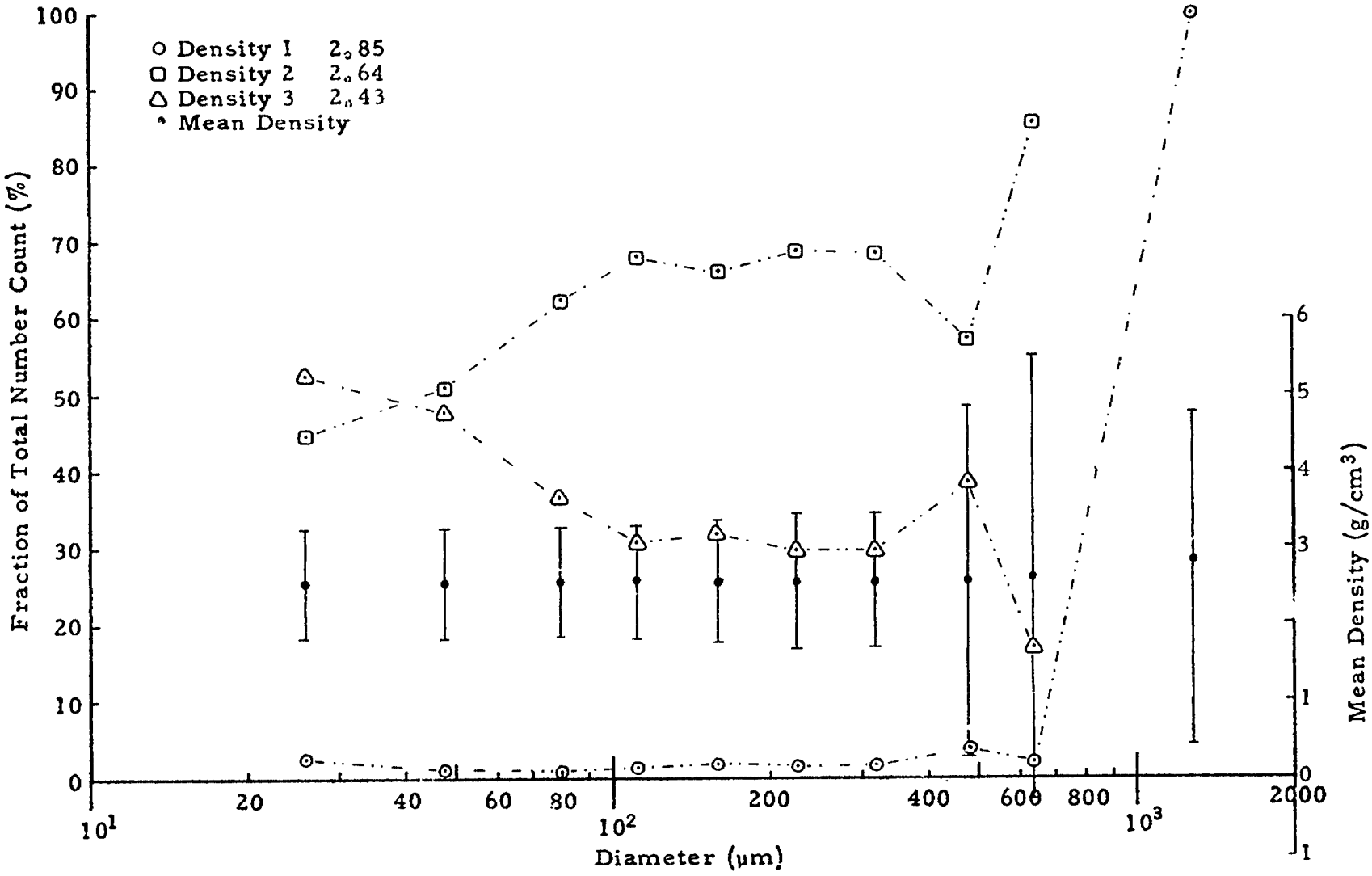

PARTICLE DENSITY
MIXED COMPANY 1, PASS 1

PARTICLE DENSITY

Mixed Company I Pass 2

Size (Microns)	RHO (gm/cc)	RHO +	RHO -
26	2.62	3.26	1.98
48	2.59	3.16	2.02
80	2.58	3.11	2.05
112	2.58	3.10	2.06
160	2.58	3.12	2.04
224	2.59	3.23	1.95
320	2.59	3.34	1.84
448	2.62	3.97	1.27
640	2.59	3.99	1.19
896	0.0	0.0	0.0
1280	0.0	0.0	0.0

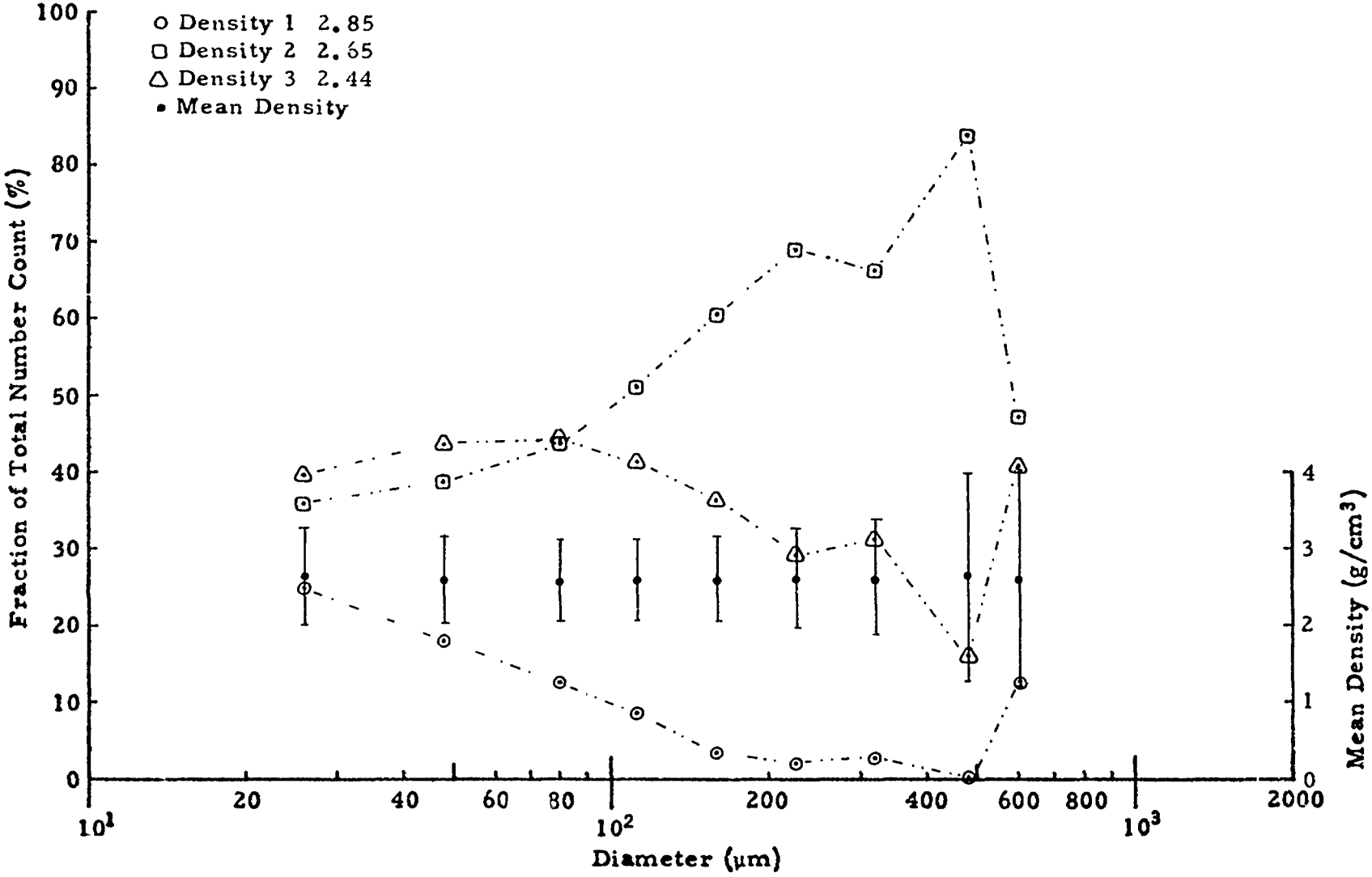

PARTICLE DENSITY
MIXED COMPANY 1, PASS 2

PARTICLE DENSITY

Middle Gust IV Pass 2

Size (Microns)	RHO (gm/cc)	RHO +	RHO -
26	2.10	3.24	0.96
48	2.10	3.23	0.97
80	2.11	3.24	0.98
112	2.12	3.26	0.98
160	2.12	3.39	0.85
224	2.11	3.66	0.56
320	2.08	3.50	0.66
448	2.13	4.69	-0.43
640	2.15	5.00	-0.70
896	2.65	7.01	****
1280	2.06	3.25	0.87

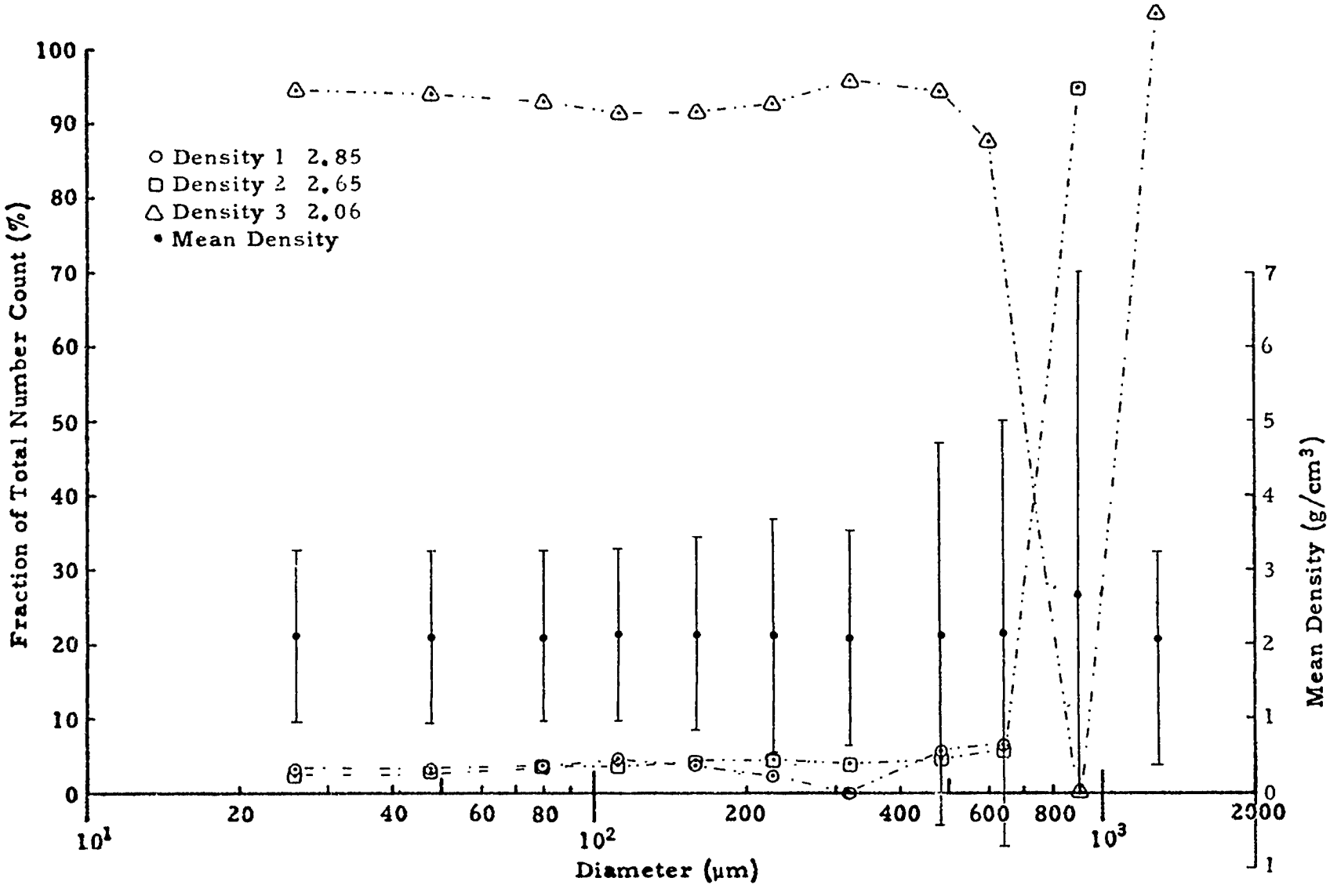

PARTICLE DENSITY
MIDDLE GUST IV, PASS 2

PARTICLE DENSITY

Middle Gust IV Pass 4

Size (Microns)	RHO (gm/cc)	RHO +	RHO -
26	2.35	3.34	1.36
48	2.32	3.24	1.40
80	2.31	3.27	1.35
112	2.21	3.23	1.19
160	2.24	3.34	1.14
224	2.23	3.52	0.94
320	2.23	3.74	0.72
448	2.32	4.50	0.14
640	2.66	5.01	0.31
896	2.32	4.03	0.61
1280	0.0	0.0	0.0

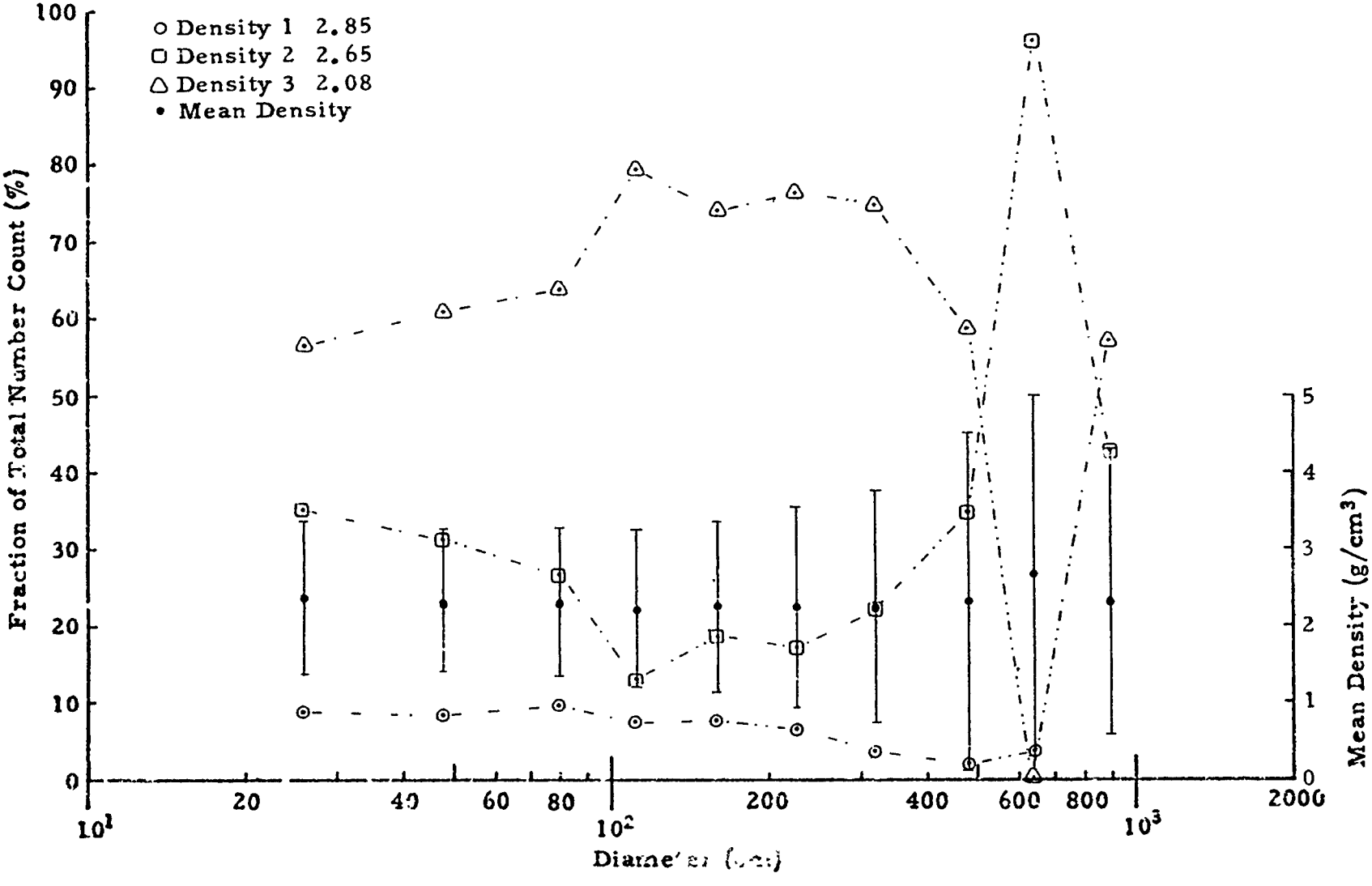

PARTICLE DENSITY
MIDDLE GUST IV, PASS 4

PARTICLE DENSITY

Mixed Company III Pass 2

Size (Microns)	RHO (gm/cc)	RHO +	RHO -
26	2.63	3.58	1.68
48	2.59	3.48	1.70
80	2.52	3.44	1.60
112	2.50	3.47	1.53
160	2.51	3.47	1.55
224	2.57	3.61	1.53
320	2.59	3.66	1.52
448	2.50	3.93	1.07
640	2.57	4.09	1.05
896	0.0	0.0	0.0
1280	2.33	4.34	0.32

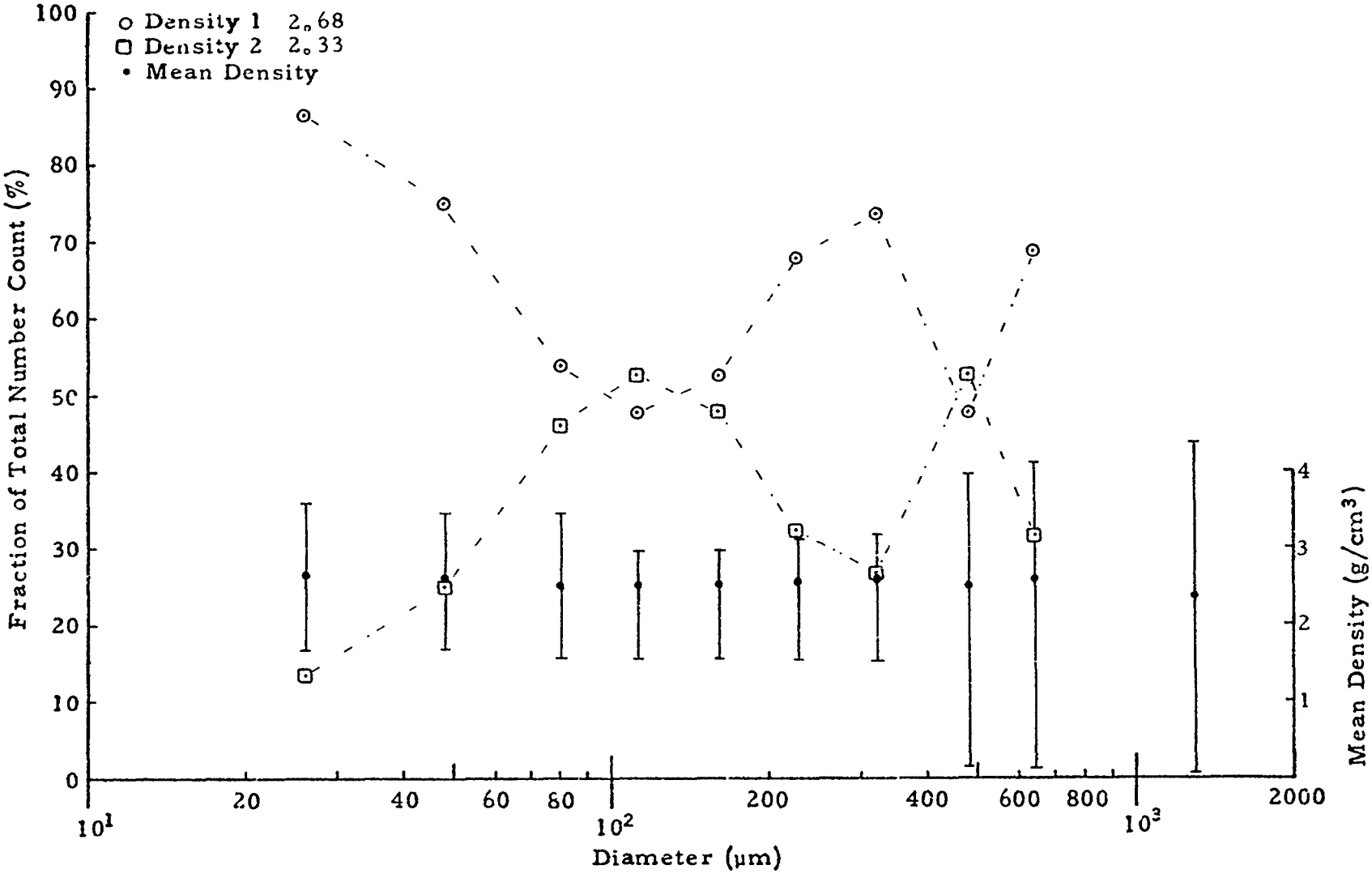

PARTICLE DENSITY
MIXED COMPANY III, PASS 2

PARTICLE DENSITY

Mixed Company III Pass 3

Size (Microns)	RHO (gm/cc)	RHO +	RHO -
26	2.29	2.77	1.81
48	2.27	2.81	1.73
80	2.29	2.79	1.79
112	2.37	2.83	1.91
160	2.42	2.91	1.93
224	2.46	3.10	1.82
320	2.42	3.09	1.75
448	2.39	4.32	0.46
640	2.01	2.94	1.08
896	0.0	0.0	0.0
1280	0.0	0.0	0.0

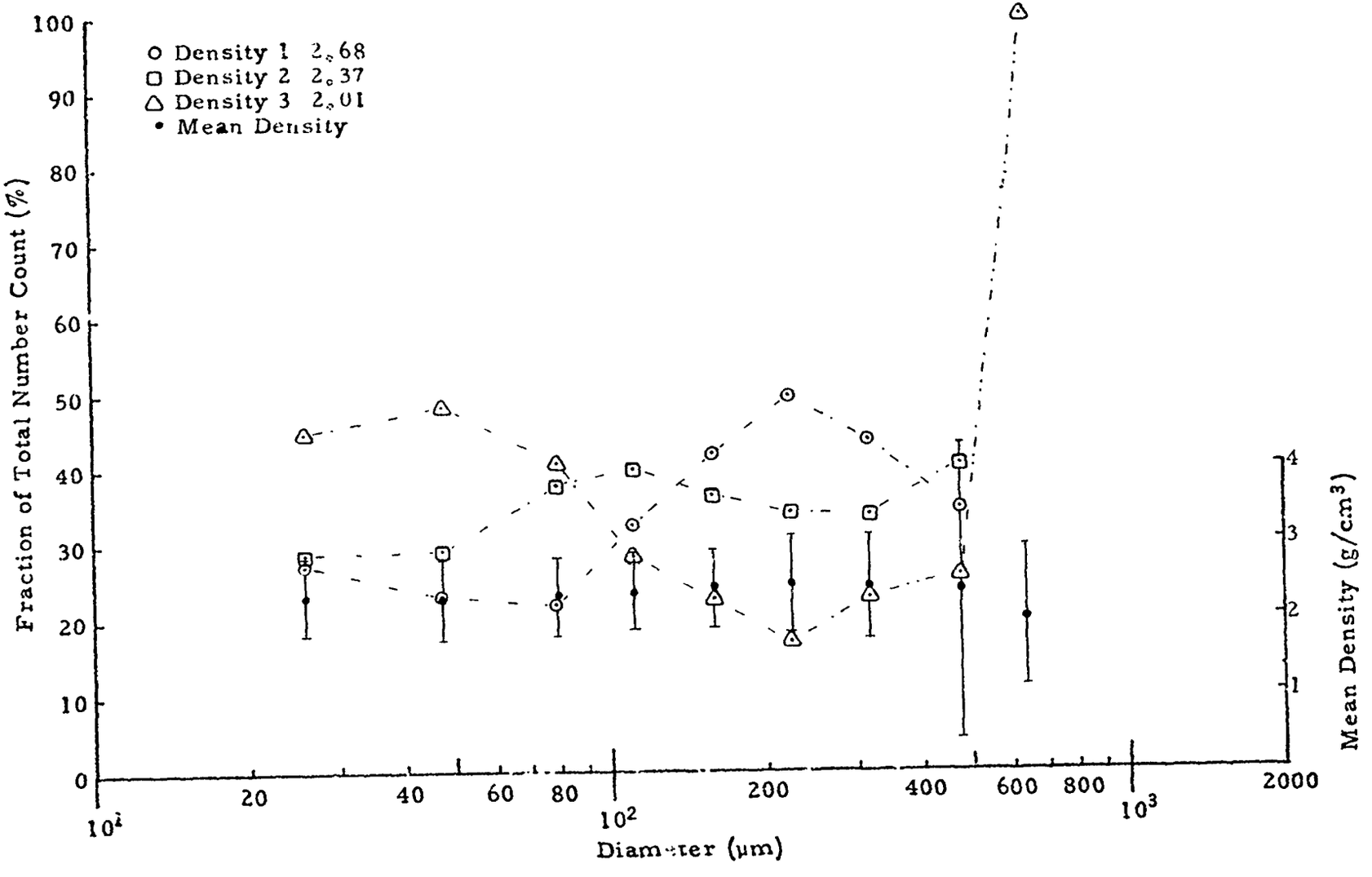

PARTICLE DENSITY
MIXED COMPANY III, PASS 5

PARTICLE DENSITY

Mixed Company III Pass 5

Size (Microns)	RHO (gm/cc)	RHO +	RHO -
26	2.26	2.83	1.69
48	2.29	2.85	1.73
80	2.32	2.84	1.80
112	2.38	2.92	1.84
160	2.37	3.01	1.73
224	2.42	3.27	1.57
320	2.42	3.30	1.54
448	2.39	4.38	0.40
640	2.25	5.09	-0.59
896	0.0	0.0	0.0
1280	0.0	0.0	0.0

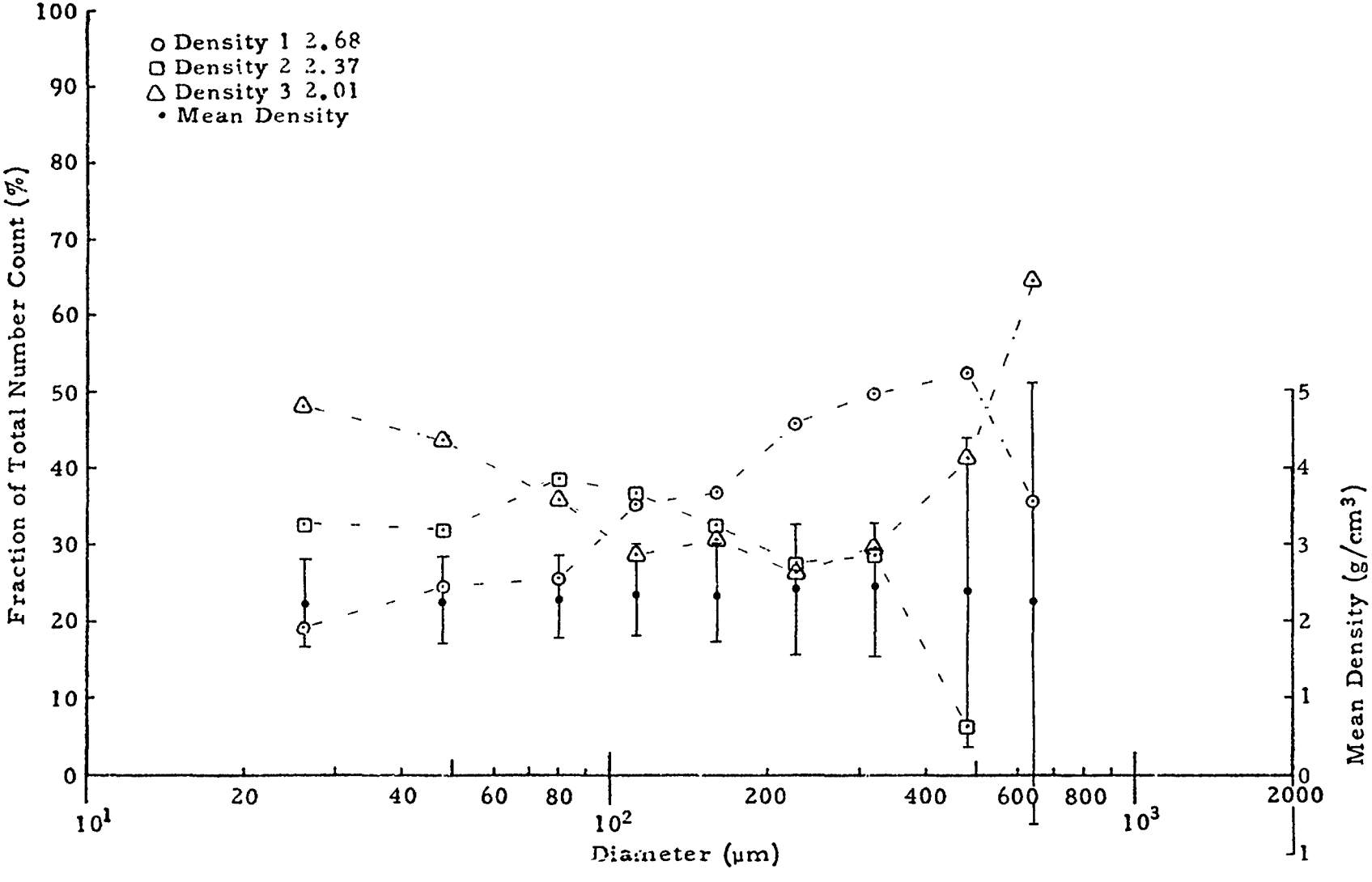

PARTICLE DENSITY
MIXED COMPANY III, PASS 5

PARTICLE DENSITY

Mixed Company III Fallout 1000' 60°

Size (Microns)	RHO (gm/cc)	RHO +	RHO -
26	2.51	4.59	0.43
48	2.51	4.59	0.43
80	2.46	4.06	0.86
112	2.41	3.67	1.15
160	2.38	3.63	1.13
224	2.34	3.62	1.06
320	2.33	3.67	0.99
448	2.37	4.12	0.62
640	2.46	4.76	0.16
896	2.39	5.36	-0.58
1280	2.54	4.68	0.40

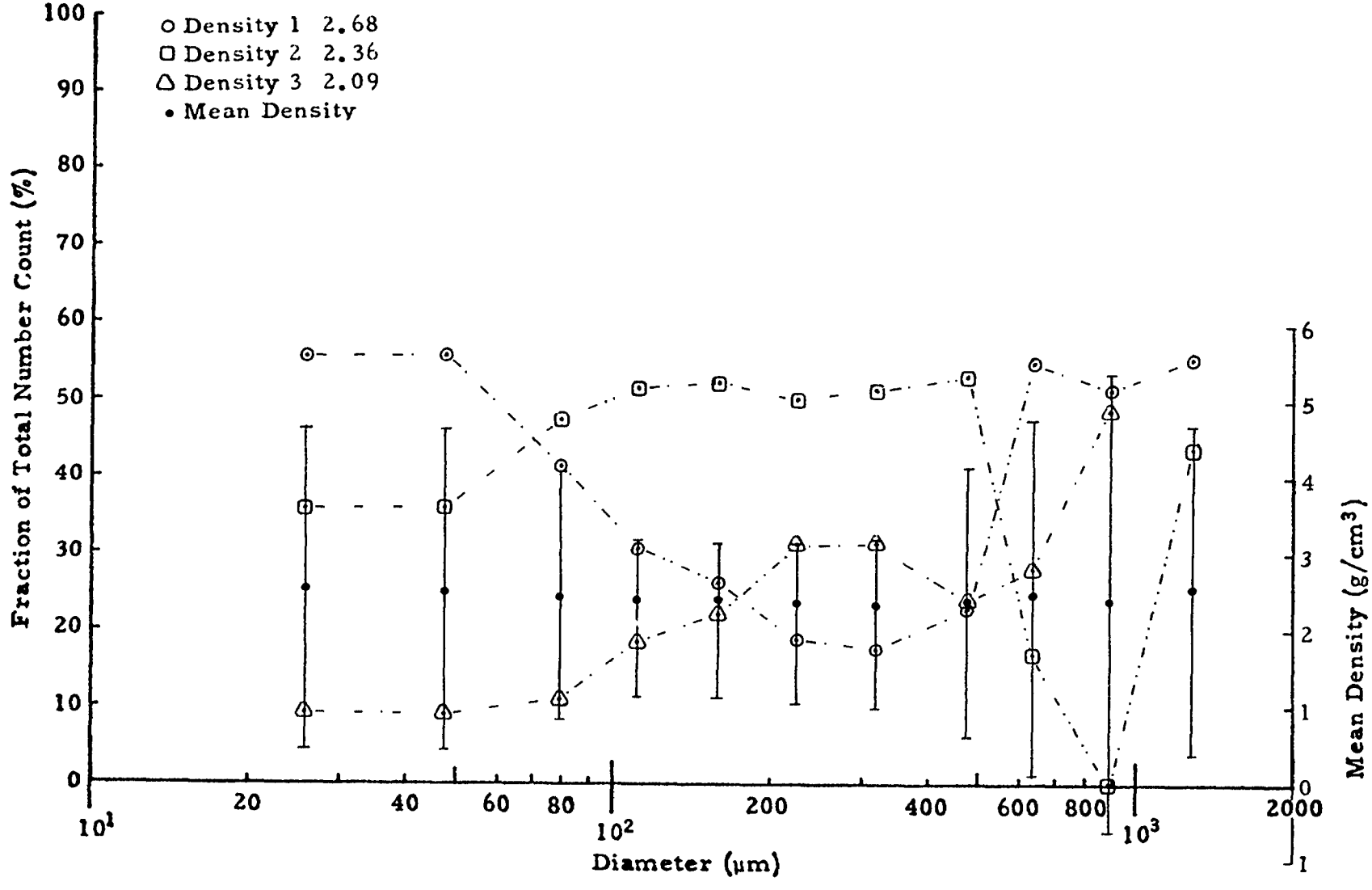

PARTICLE DENSITY
MIXED COMPANY III, FALLOUT - 1000' 60°

PARTICLE DENSITY

Mixed Company III Fallout 3000' 60°

Size (Microns)	RHO (gm/cc)	RHO +	RHO -
26	2.06	4.96	-0.84
48	2.12	4.76	-0.52
80	2.26	4.12	0.40
112	2.40	3.59	1.21
160	2.41	4.09	0.73
224	2.41	4.43	0.39
320	2.48	3.73	1.23
448	2.46	3.78	1.14
640	2.41	3.88	0.94
896	2.41	4.80	0.02
1280	2.01	5.21	****

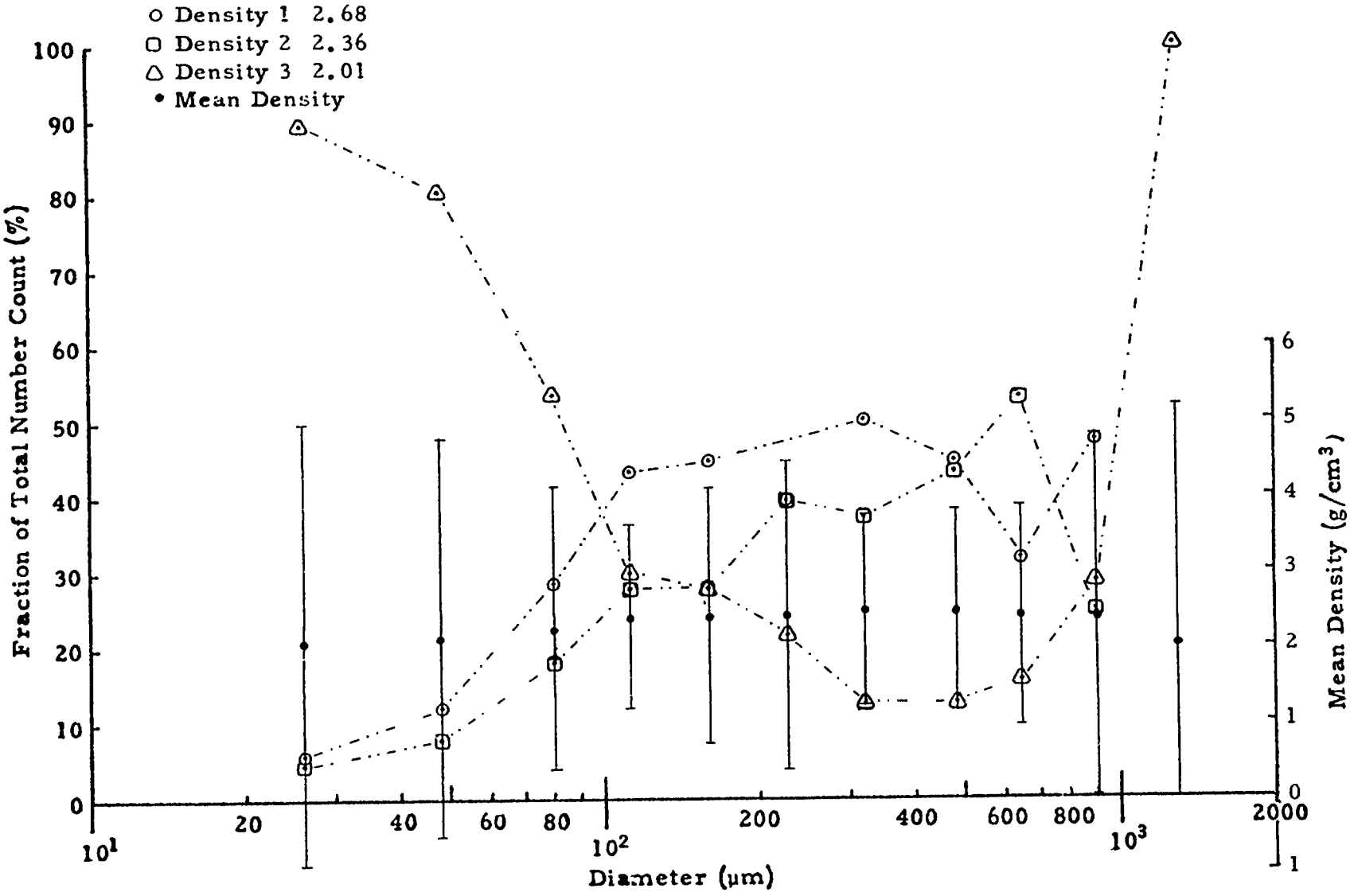

PARTICLE DENSITY
MIXED COMPANY III, FALLOUT - 3000' 60°

PARTICLE DENSITY

Mixed Company III Fallout 6000' 60°

Size (Microns)	RHO (gm/cc)	RHO +	RHO -
26	2.35	2.96	1.74
48	2.40	2.96	1.84
80	2.36	2.99	1.73
112	2.37	3.01	1.73
160	2.43	3.04	1.82
224	2.48	3.10	1.86
320	2.52	3.10	1.94
448	2.46	3.22	1.70
640	2.46	3.11	1.81
896	2.29	3.49	1.09
1280	2.19	4.33	0.05

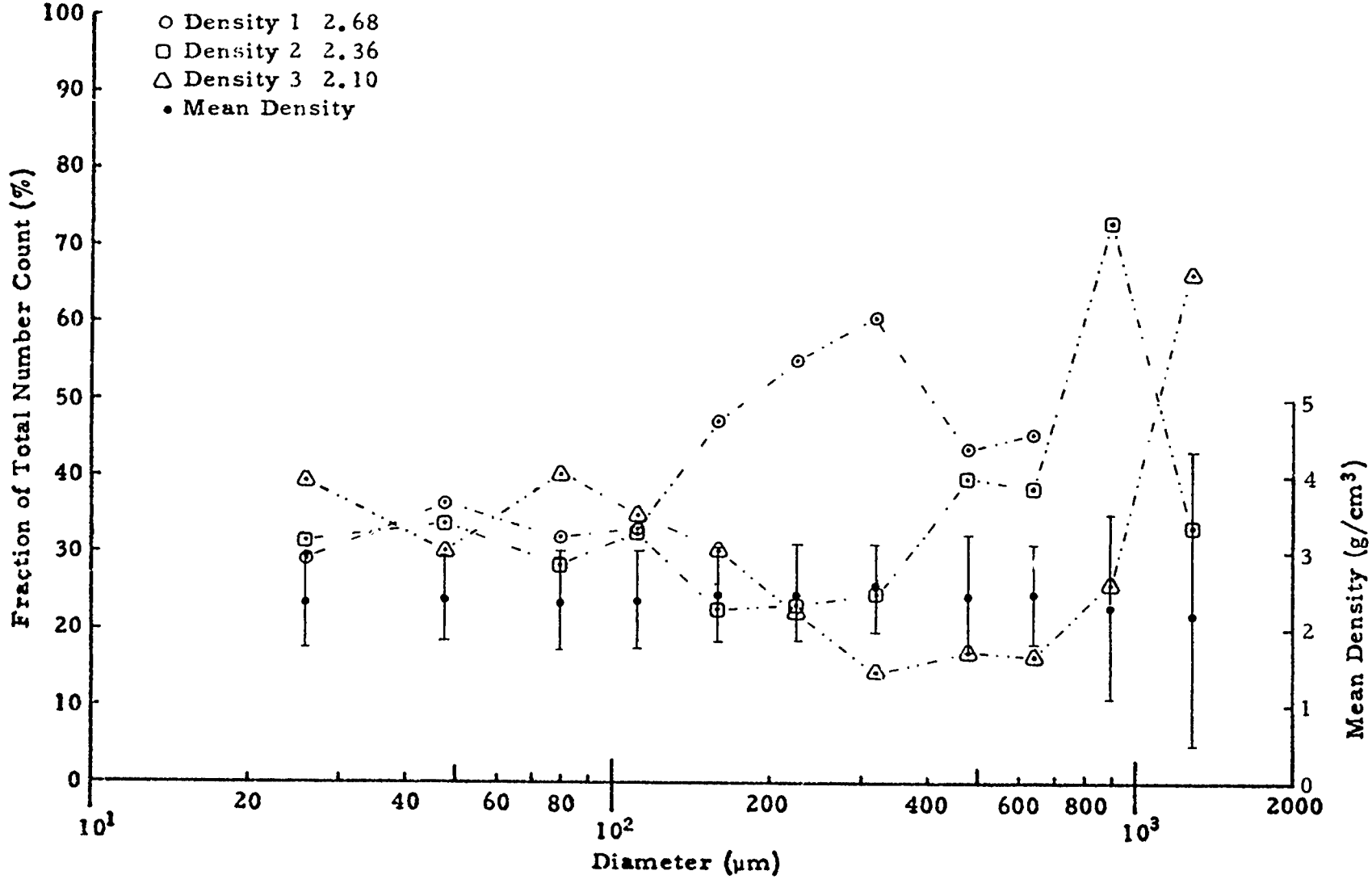

PARTICLE DENSITY
MIXED COMPANY III, FALLOUT 6000' 60°

APPENDIX VIII

MIXED COMPANY III - ENVIRONMENTAL IMPACT DATA

Special Report

13 November 1972

To
Headquarters
Defense Nuclear Agency
Washington, D. C. 20305

From
Meteorology Research, Inc.
464 West Woodbury Road
Altadena, California 91001

19 January 1973

TABLE OF CONTENTS

I. INTRODUCTION

This report covers air quality data obtained from the Mixed Company III event, a 500-ton tangent sphere TNT detonation near Grand Junction, Colorado, on November 13, 1972. Data from the resulting dust cloud was collected by two aircraft and includes real time measurements of nitric oxide, ozone, carbon monoxide, particulates, and condensation nuclei as well as analysis of integrated gas samples collected within the cloud. Particle size distributions for one airborne dust sample and one fallout sample are also included.

This work was done to assist in the prediction of the environmental impact of the PACE program. It represents the first collection of gas data from a large yield cloud and provides comparison with theoretical predictions and the results from small scale detonations.

II. SAMPLING PROCEDURES

Two aircraft were used for data and sample collection. The principal aircraft was a C-205 equipped for real time measurement of nitric oxide, ozone, carbon monoxide, particulates, and condensation nuclei as well as collection of integrated gas samples using an inflation-bag technique. The second aircraft, a C-45, was instrumented to collect real time and integrated dust samples from the torus and stem of the cloud.

A. C-205

The C-205 has been used extensively for pollution monitoring in the Los Angeles basin and other areas of California. It is equipped with a REM NO-NO_x Monitor (Model 642), a REM Ozone Monitor (Model 612), an Andros Model 7000 Carbon Monoxide Analyzer, an Environment One Condensation Nuclei Monitor (Model Rich 100), a Model 2050 MRI Integrating Nephelometer, and an MRI Portable Instrument Package which records altitude, turbulence, temperature, relative humidity and air speed. A Metrodata (Model 620) data logging system records all data on magnetic tape with each parameter being recorded approximately two-and-a-half times per second. A special manifold to permit the collection of gas samples in inflatable bags was installed for the Mixed Company III event.

Air samples are collected outside the aircraft by three forward-facing sampling inlets approximately one and one-half inches in diameter which are mounted at the side of the aircraft. The gas samples are conducted directly to the continuous monitoring instruments by a network of air lines inside the cabin. An outlet from one of the main lines is connected to the manifold which is used to fill the gas sampling bags.

Gas samples were collected in two-liter aluminized mylar bags during the first six penetrations of the cloud. Inflation of the bags began on entry into the cloud with approximately ten to fifteen seconds required to completely fill the bags. Background air samples were also collected; one background sample was collected before detonation, and one was obtained after detonation in clear air in an area remote from the dust cloud.

The C-205 circled over Glade Park at an altitude of 16,000 feet until T-0. Entry into the cloud was delayed until the cloud had stabilized, with the first pass penetrating the top of the cloud six minutes and thirty seconds after detonation. The second and third passes were through the center of the cloud, the fourth and fifth through the base of the cloud, and the sixth, seventh, and eighth passes penetrated the stem. The time, altitude, heading, air speed, and calculated cloud width for each pass are shown in Table I entitled TIMES AND LOCATIONS OF CLOUD PENETRATIONS.

TABLE I

Times and Locations of Cloud Penetrations

Pass	Time		Elapsed Time	Altitude		Heading	Air Speed	Cloud Width	Cloud Region
	Entry (Min. : Sec.)	Exit (Min. : Sec.)	(Sec.)	Entry (Ft. above GZ)	Exit (Ft. above GZ)	(degrees)	(mph)	(meters)	Sampled
1	6:30	7:23	53	7700	7300	320°	122	2890	Top
2	9:12	10:02	50	6700	6770	50°	131	2930	Center
3	11:12	12:32	80	6700	6500	255°	114	4080	Center
4	14:06	15:16	70	6300	6500	50°	103	3230	Base
5	15:58	17:01	63	6500	6500	225°	117	3300	Base
6	22:18	23:37	79	2400	2400	55°	103	3640	Stem
7	25:12	26:03	51	2600	2700	240°	105	2390	Stem
8	27:52	28:29	37	2700	2700	75°	120	1980	Stem

B. C-45

The C-45 was equipped with various particulate and atmospheric parameter sensing instruments, including two cyclone dust separators. It sampled the Mixed Company III dust cloud for approximately one hour, making 20 passes through the stem and the main cloud. The seventeenth pass penetrated the main part of the cloud fifty minutes after detonation. Data related to the total mass loading and size distribution of dust particles in the cloud at that time will be presented later in this report.

Similarly, a fallout sample was collected from the roof of a truck at the Technical Observation Point approximately fifteen to thirty minutes after detonation. It is not a quantitative sample; however, it does provide an index of the type of material being deposited by the cloud at a point about 9000' from ground zero. More extensive data from a system of fallout-collecting trays will be available at a later date.

III. ANALYTICAL PROCEDURES

A. Continuous Monitoring Instruments

The NO-NO_x monitor detects nitric oxide (NO) by measuring the intensity of light generated by the chemiluminescent reaction between nitric oxide and ozone. The ozone is generated internally and mixed with the air sample in a reaction chamber. A photomultiplier tube detects light resulting from the reaction. The instrument can also be operated in the NO_x mode in which both nitric oxide and nitrogen dioxide (NO_2) are measured. The nitrogen dioxide is first converted to nitric oxide, then the total concentration of nitric oxide is measured.

The ozone monitor measures ozone concentration by mixing the air sample with ethylene and using a photomultiplier tube to measure the intensity of the light emitted by the chemiluminescent reaction between ozone and ethylene.

The carbon monoxide analyzer uses a dual-isotope-fluorescence technique where a beam of infrared radiation, which is alternately specific for CO^{16} and CO^{18}, is passed through the sample chamber. Carbon monoxide in the sample absorbs the CO^{16} radiation but not the CO^{18} radiation. A solid state infrared detector system measures the alternating CO^{16} and CO^{18} radiation levels and computes the carbon monoxide concentration from the ratio of the two signals. This method eliminates interference by particulates. water vapor or other gases.

The condensation nuclei monitor humidifies the air sample and then rapidly expands it in a cloud chamber, causing high water vapor supersaturation and associated condensation on the particles. The resulting droplets attenuate a light beam which is focused on a light-sensitive detector.

The nephelometer measures the scattering coefficient of light resulting from suspended particulate matter in the air. A high intensity flashlamp illuminates the air sample, causing the particles to scatter light which is detected by a photomultiplier tube at the end of the instrument. With the proper calibrations and a knowledge of the size distribution of the suspended material, the measurement of the scattering coefficient can be related directly to mass concentration according to the equation

$$C\,\mu g/m^3 = Ka\,b_{scat}$$

where Ka is a size dependent coefficient and b_{scat} is the measured scattering coefficient. Operating in real time, the instrument can provide dust concentration profiles across the cloud.

B. Analysis of Gas Samples

The gas samples collected in the inflation bags were analyzed primarily by gas chromatography and mass spectroscopy. Half of the gas volume in each sample was used for this analysis. Sample components were identified principally by gas chromatography, with mass spectroscopy providing supporting analysis and detection of a few additional species. A portion of the first half of the sample was analyzed for carbon monoxide and methane by separating the gases on a molecular sieve column where carbon monoxide is retained momentarily while the methane is eluted. Both gases in the stream are then passed over a nickel catalyst which leaves the methane unchanged but converts the carbon monoxide to methane. The gases enter a flame ionization detector which detects two separate methane peaks, the first peak resulting from the methane originally in the air sample and the second one from the carbon monoxide which was converted to methane.

The remaining half of each gas sample was bubbled through water, and the walls of the gas-sampling bags were washed down with water to absorb nitrogen dioxide and ammonia, which can become adsorbed on the walls. Nitrogen dioxide in the resulting solution was determined by the Saltzman method and ammonia by the Nessler method.

Analysis of the gas samples was delayed until about 72 hours after the samples were collected. It is possible that components of the sample may have reacted with each other or with the walls of the gas-collecting bags during this time, but there is no direct evidence that this occurred.

C. Particle Size Distributions

The particle size distributions which are presented in this report are only preliminary. The samples were examined under a microscope, and particles in representative portions of the sample were categorized by size to determine the size distribution.

IV. RESULTS

Table II, SUMMARY OF DATA FROM CONTINUOUS MONITORING INSTRUMENTS, shows the average and maximum (minimum for ozone, which decreases in the cloud) concentrations of gases and particulates within the cloud as measured by the aircraft monitoring instruments. Data has been corrected for altitude variations.

Measurements of carbon monoxide were inconclusive due to an unusually high noise level (6 to 8 ppm or considerably higher than the carbon monoxide concentrations detected in the collected gas samples) and zero drift on the carbon monoxide monitor. The instrument had been removed from the aircraft for servicing, which was not completed when it was reinstalled for the Mixed Company III event.

The results of the chemical analysis of the collected gas samples are shown in Table III, GAS SAMPLE ANALYSIS RESULTS. Samples were collected inside the cloud for the first six passes only and background samples were obtained both before and after detonation. In addition to the compounds listed in Table III, a number of compounds obviously originating from the chemical composition of the gas-collecting bags were detected but are not reported here.

Concentrations reported for the first background sample seem unusually high, and there are wide variations between the two background samples. It is suspected that the first background sample was contaminated. Due to a short supply of bags, both of the background sample bags were used to check out the gas-collecting system. This may have resulted in contamination of the first sample bag (the bags which were used to collect samples within the dust cloud had not been used previously). Alternately, residual gases and particulates in the inlet manifold may have entered the first sample during inflation.

Some variations among the samples may be due to segregation of gases in different parts of the cloud, but no trend was identifiable. As no significant pattern was discerned, the analyses were treated on a collective basis and are presented in Tables IV and V, COLLECTIVE GAS ANALYSIS RESULTS. In Table IV, the maximum concentration for each sample component is the highest reported cloud sample concentration (from Table III), corrected by subtracting the lower of the two background sample concentrations. The minimum reported is the lowest cloud sample concentration, corrected by subtracting the higher of the two background values. The average is determined by subtracting the average background concentration from the average concentration of the six cloud samples in Table III.

TABLE II

Summary of Data From Continuous Monitoring Instruments

Pass	NO Concentration		O_3 Concentration		Condensation Nuclei		Scattering Coefficient	
	Average (ppm)	Maximum	Average (pphm)	Minimum	Average ($\times 10^3$ nuclei/cm^3)	Maximum	Average (^{b}scat $\times 10^{-4}$ m^{-1})	Maximum
1	.08	.164	2.58	1.29	9.0	23.2	≥ 77.3	≥ 117
2	.14	.366	2.00	1.03	10.3	20.4	≥ 77.6	≥ 118
3	.10	.202	2.12	0.73	9.8	23.2	≥ 71.3	≥ 118
4	.03	.142	2.78	1.03	5.7	16.6	≥ 53.1	≥ 117
5	.06	.130	2.60	0.91	8.8	23.1	≥ 45.3	≥ 119
6	0.0	0.0	3.81	3.70	1.0	1.94	4.0	12.1
7	0.0	0.0	4.15	3.70	0.47	0.60	2.2	6.2
8	0.0	0.0	3.92	3.58	0.34	0.52	3.8	8.7

Background Concentrations:

Ozone: 4.1 to 4.4 pphm

Condensation Nuclei: .1 to .2 $\times 10^3$ nuclei/cm^3

NO: not detected

Nephelometer: clean air = 0.23 ^{b}scat $\times 10^{-4}$ m^{-1}

TABLE IV

Collective Gas Analysis Results

Maximum, Average, and Minimum Concentrations with Respect to Two Background Samples

Compound	Concentration (ppm) Maximum	Average	Minimum
Ethane	0.40	< 0	< 0
Propane	0.030	< 0	< 0
Butane	0.0043	< 0	< 0
Isopentane	0.0072	0.0013	0
Hexane	0.0075	0.0012	0
Ethylene	0.015	< 0	< 0
1 - Butene	0.025	0.0084	< 0
Benzene	0.32	0.045	< 0
Toluene	0.024	0.0045	< 0
Methanol	0.21	< 0	< 0
Ethanol	0.09	< 0	< 0
n - Propanol	0.032	< 0	< 0
iso - Propanol	0.026	< 0	< 0
Methane	17	< 0	< 0
Carbon Monoxide	2.3	1.1	0
Nitrogen Dioxide	0	< 0	< 0
Ammonia	9	< 0	< 0

Data has been corrected with respect to two background air samples, collected before and after detonation.

TABLE V

Collective Gas Analysis Results

Maximum, Average, and Minimum Concentrations with Respect to Second Background Sample

Compound	Concentration (ppm) Maximum	Average	Minimum
Ethane	.40	.12	.011
Propane	.030	.014	.00004
Butane	.0043	.001[illegible]	0
Isopentane	.0072	.0013	0
Hexane	.0075	.0012	0
Ethylene	0	< 0	< 0
1 - Butene	.025	.0086	0
Benzene	.32	.093	< 0
Toluene	.017	.001	< 0
Methanol	.21	.086	< 0
Ethanol	.05	< 0	< 0
n - Propanol	.032	0	< 0
iso - Propanol	.026	< 0	< 0
Methane	17	7.6	0.9
Carbon Monoxide	2.3	1.1	0
Nitrogen Dioxide	0	< 0	< 0
Ammonia	9	4	< 0

Data has been corrected with respect to a background air sample collected after detonation.

The results presented in Table V have been determined in a similar manner using only the second background sample for each correction. If it is assumed that the second background was not contaminated, these results (Table V) have the highest confidence level of the two treatments of the data.

Table VI, GASES DETECTED IN VARIOUS CLOUD REGIONS, reports for each pass and for each cloud region sampled those compounds present in concentrations significantly above the concentrations in the second background sample.

Preliminary particle size distributions for one dust cloud and one fallout sample are shown in Table VII, DUST CLOUD SAMPLE, T+50 MINUTES, and Table VIII, FALLOUT SAMPLE, 9000' FROM GZ. Additional particle size data will be available later when data from all the airborne samples and from a system of fallout trays is completely analyzed. For comparison, particle-size distributions for airborne dust samples collected during the Middle Gust III test, a 100-ton tangent spherical detonation conducted on April 13, 1972, near Crowley, Colorado are reported in the Appendix. These samples were collected by the same instrument as the Mixed Company III samples, and size distributions were determined by the same method.

TABLE VI

Gases Detected in Various Cloud Regions*

Top	Center		Base		Stem
Pass 1	Pass 2	Pass 3	Pass 4	Pass 5	Pass 6
Ethane	Ethane	Ethane	Ethane		Ethane
Propane	Propane	Propane	Propane	Propane	Propane
Butane	Butane		Butane	Butane	Butane
Isopentane	Isopentane				
Hexane					
1 - Butene	1 - Butene		1 - Butene	1 - Butene	1 - Butene
Benzene	Benzene	Benzene		Benzene	Benzene
		Toluene		Toluene	
Methanol	Methanol			Methanol	Methanol
		Ethanol			
n - Propanol		n - Propanol			
				iso - Propanol	iso - Propanol
Methane	Methane	Methane	Methane	Methane	Methane
Carbon Monoxide	Carbon Monoxide		Carbon Monoxide	Carbon Monoxide	Carbon Monoxide
Ammonia	Ammonia	Ammonia	Ammonia		Ammonia

*Gases listed are those which were significantly above the levels of the second background sample.

Table VII
Dust Cloud Sample

Size Range (diameter, μm)	Percent by Number	Cumulative Percent by Number	Percent by Volume	Cumulative Percent by Volume
0-30	98.659	98.659	67.55	67.55
30-60	1.290	99.949	23.84	91.39
60-90	.03725	99.986	3.19	94.58
90-120	.00823	99.995	1.93	96.51
120-150	.00414	99.999	2.06	98.57
150-201	.00093	100.00	0.74	99.31
201-259	.00023	100.00	0.56	99.87
259-317	.00003	100.00	0.12	99.99

Pass:	17	Heading:	90°
Time:	50:05 to 51:54 (min. sec.)	Cloud Width:	8500 meters
Altitude:	6, 400 Feet above ground level	Sample Mass:	26. 1 mg
Sample:	Cyclone	Dust Concentration:	0. 107 x 10^{-8} gm/cm^3

Table VIII

Fallout Sample, 9000' from GZ

Size Range (diameter, μm)	Percent by Number	Cumulative Percent by Number	Percent by Volume	Cumulative Percent by Volume
30-60	38.34	38.34	0.93	0.93
60-90	17.97	56.31	2.02	2.96
90-120	10.47	66.78	3.23	6.19
120-150	7.13	73.91	4.68	10.87
150-180	8.35	82.25	10.00	20.87
180-210	7.25	89.50	13.23	34.10
210-240	5.44	94.94	16.54	50.64
240-270	1.25	96.19	5.51	56.15
270-300	0.837	97.03	5.17	61.32
300-330	1.68	98.70	13.99	75.27
330-360	0.835	99.54	9.15	84.42
360-432	0.220	99.76	4.64	89.06
432-489	0.130	99.89	3.33	92.39
489-547	0.041	99.93	1.49	93.88
547-604	0.041	99.97	2.04	95.92
604-662	0.008	99.98	0.55	96.47
662-719	-	-	-	-
719-777	0.008	99.98	0.89	97.36
777-834	0.008	99.99	1.12	98.48
834-892	0.008	100.00	1.38	99.86

V. DISCUSSION

A. Real Time Measurements

The data obtained from the continuous monitoring instruments (Table II) shows that concentrations of nitric oxide, condensation nuclei, and particulates within the cloud are clearly above background levels. Concentrations in the torus were consistently higher than in the stem (see Table I for locations in the cloud). This may be an indication that the detonation and combustion products are concentrated in the cloud; however, the stem was sampled at a later time and the trend may reflect simple dilution of the gas. The nitric oxide concentration in the torus is comparable to the results predicted by small scale detonations, as will be discussed later.

The decrease in ozone below the natural background level (Footnote: Table II) is due to reaction with the nitric oxide, unsaturated hydrocarbons (e.g., ethylene) and other materials produced in the detonation. The decrease is most evident in the main part of the dust cloud.

B. Integrated Gas Samples

Of the compounds listed in Tables III through VI, benzene, toluene, and the alcohols can occur as contaminants from the bags, but the amounts detected are higher than would result from contamination alone. Isopentane and hexane may also be contaminants from the bags. The remaining compounds are detonation products or by-products. Examination of Table VI shows ethane, propane, butane, 1-butene, benzene, methanol, methane, carbon monoxide, and ammonia to be the most significant products. These compounds occur above background levels in four or more samples.

The results presented for nitrogen dioxide and ammonia may be high (up to two times) if a significant amount of these compounds had been adsorbed on the walls of the sample bags prior to analysis. Half of each sample was first removed for analysis by gas chromatography and mass spectroscopy while nitrogen dioxide and ammonia from the remaining half and from the walls of the sample bag were dissolved in water for wet chemical analysis. The concentration reported in Table III considers the analyzed amount to have originated from half of the gaseous sample.

The Mixed Company III results can be compared with theoretical values and the results of small-scale chamber detonation by extrapolating these values and charge sizes upward to a 500-ton equivalent yield and then determining the concentration of the products in a volume equal to the volume of the Mixed Company III cloud at the time of sampling. The volume of the dust cloud used in the comparison was computed by averaging the cloud width

for the five penetrations of the main cloud (Passes 1 through 5). The cloud was assumed to have a spherical shape, resulting in a total volume of $1.8 \times 10^{10}\ m^3$.

C. Comparison with Small-Scale Detonations

The results of a 1.5 lb. TNT detonation in a chamber having a volume of 800 ft^3 (Ref. 1) are extrapolated by the procedure described in the preceding paragraph and compared in Table IX to the averaged results from Mixed Company III (Table V).

The Mixed Company III results are lower in nitrogen dioxide, comparable in nitric oxide, and higher in ammonia, methane, and carbon monoxide. The high concentrations of ammonia, methane, and carbon monoxide may indicate that the oxidation of detonation products is less complete during a large scale test such as MC-III, where considerable slow burning is observed after the initial detonation. Alternately, some of these reduced gases may represent degradation products of more complex compounds formed at high temperatures. In any case, the differences between the small-scale detonation and the real situation are significant.

A number of compounds which were not detected in the small-scale tests were found in the Mixed Company III samples. This suggests differences in detonation, combustion, or degradation processes. Hydrogen cyanide, which was a product of the small-scale detonation, was not found in the samples, but it would not have been detected at concentrations less than 1 ppm by the analytical method used for the Mixed Company III samples. This does not exclude its possible presence in very low concentrations.

D. Comparisons with Theoretical Values

The measured concentrations of ammonia, methane and methanol are high when compared with the theoretical detonation products predicted by Loving (Ref. 2), as shown in Table X (COMPARISON WITH THEOPETICAL DETONATION PRODUCTS). Loving's data is a prediction of detonation products and thus, ignores possible incomplete or subsequent combustion of products after detonation. The low concentration of carbon monoxide in Table X and the presence of carbonaceous material in the dust samples and on the ground near ground zero implies a strong case for incomplete combustion and the associated formation of reduced or partially oxidized species.

Another prediction of detonation products by Cook (Ref. 3) gives lower values for ammonia (0.3 ppm) and no methane. Mixed Company III averages (from Table V) were 4 ppm ammonia and 8 ppm methane.

TABLE IX

Comparison with Small Scale Detonation Results

	A Detonation Products From 1.5 lb of TNT in 800 ft.^{3} chamber (ppm)	B Extrapolation of A to 500 tons in 1.8×10^{10} m^3 (ppm)[a]	MC III Results[c] (ppm)
CO_2	12,000	1.1[b]	
CO	1,500	0.13	1.1
NO_2	1,200	0.11	0
NO	750	0.067	0.09[d]
N_2O	300	0.027	
HCN	300	0.027	
H_2O	> 1,500	> 0.13	
C_3O_2	trace		
HNO_3	trace		
CH_4	trace		8
NH_3	trace		4

[a] volume of cloud determined from average cloud widths, Passes 1 to 5.

[b] less than natural level

[c] average results from Table V, unless otherwise indicated

[d] average of instrument readings, passes 1 to 4

TABLE X

Comparison with Theoretical Detonation Products

	A Theorectical Detonation Products (moles/kg.)	B Extrapolation of A to 500 tons in 1.8×10^{10} m^3 (ppm)[a]	MC III Results (ppm)[b]
Carbon Monoxide	11.7	10.5	1.1
Methane	1.73	1.6	8
Ammonia	0.082	0.07	4
Methanol	0.0004	0.0005	0.1

[a] average volume of cloud, Passes 1 through 5

[b] average results from Table V

E. Summary - Theoretical and Small-Scale Test Comparisons

These results suggest that theory and small-scale experiments are not adequate substitutes for in situ measurements. The differences between the MC-III measurements and the predictions from theory and small detonations have several possible origins. An increase in the charge size may affect the speed of detonation and the subsequent oxidation of primary reaction products. Physical or chemical effects caused by the presence of soil, grass, and test structures in the area are not determined by laboratory experiments or predicted by theory.

Some delay occurred between the time the integrated gas samples were collected and the time of analysis. As a result, some changes may have occurred in the gas mixture but these changes would have favored the presence of more oxidized species. The analysis indicates the opposite, with an unexpectedly high concentration of reduced gases and unoxidized hydrocarbons.

Variations in gas concentrations as a function of cloud region and time may occur. MRI personnel operating the C-45 reported strong odors in the stem of the cloud at about T + 5 minutes, but no odors were noticed by the personnel in the C-205 a few minutes later as the aircraft penetrated the top of the cloud.

F. Dust Samples

Data on the specific dust environment generated by the Mixed Company III detonation is limited at the present time to the fallout sample at TOP and the airborne sample collected on pass #17 of the C-45. After all the fallout and dust cloud samples have been analyzed, a comprehensive report will be delivered.

Based on the single sample from pass #17 collected 50 minutes after detonation, the dust concentration was 0.107×10^{-8} grams/cm^3. The total weight of suspended dust in the cloud, assuming the sample was representative and the cloud was still spherical (probably a false assumption due to shearing of the cloud by winds aloft) was 3.4×10^8 grams with more than 50% of the mass in particles 30 microns or less in diameter.

VI CONCLUSIONS

The presence of nitric oxide in the dust cloud resulting from a large TNT detonation has been confirmed. Carbon monoxide, ammonia, and methane exist in concentrations higher than predicted by smaller detonationes and, for ammonia and methane, higher than predicted by theory. Ethane, propane, butane, 1-butane, benzene, and methanol are also present. Hydrogen cyanide, if present, occurs in concentrations less than 1 ppm. The ozone concentration decreases below its natural atmospheric level due to reaction with gases and other materials in the cloud. Condensation nuclei and high concentrations of particulates were also found.

VII RECOMMENDATIONS

Gas sample containers made of glass, stainless steel, or other non-reactive substance would eliminate possible reactions between the sample and the container. Such containers would also eliminate the introduction of contaminants into the sample, as occurs with mylar sampling bags. A pressurized sample-collecting system, however, is not recommended because changes in pressure and temperature can cause changes in reaction rates and decomposition rates among sample components.

Increased use of continuous monitoring instruments provides a more complete cloud profile and reduces the possibility of subsequent reactions between sample components. If a large number of components must be measured, the investment and availability of separate monitors favors the integrated gas sample approach with analysis to be performed shortly after the samples are returned to the ground. More rapid analysis of collected gas samples could be accomplished by locating portable analyzers at or near the landing field.

The present gas-sampling program was assembled on extremely short notice, using available equipment. In view of the somewhat limited data recovered and some of the implications generated by the deviations from theoretical and small chamber tests, it would be advisable to collect additional data if the opportunity is presented. The occurrence of incompletely oxidized gases and relatively high loadings of carbonaceous materials implies a significant variance from the results expected from relatively unconfined, instantaneous detonations.

REFERENCES

1. Air Force Weapons Laboratory, Pace Environmental Statement. December 1, 1972, Draft. Table 4-8, p. 4-17.

2. Air Force Weapons Laboratory, Pace Environmental Statement. December 1, 1972, Draft. Table 4-5, p. 4-14.

3. Defense Nuclear Agency, Mixed Company Environmental Statement. October 6, 1972. Table 1, p. 14.

Appendix

MIDDLE GUST III PARTICLE SIZE DISTRIBUTIONS

The particle counts in the following particle size distributions
are normalized to a total of 20, 000 particles
to facilitate comparison

MIDDLE GUST III

13 April 1972

Cyclone Samples

Pass 1

Time: 1:32 - 1:39

Altitude: 3500 ft. (above ground level)

Heading: 10 degrees

Cloud Width: 370 meters

Dust Concentration: 45.1×10^{-8} gms/cc

Diameter (microns)	Number	Percent by Number	Volume $X10^6$ $(\mu m)^3$	Percent by Volume
0-30	19,300	96.501	34.1	14.05
30-60	457	2:283	21.8	8.98
60-90	164	0.818	36.1	14.87
90-120	37	0.185	22.4	9.23
120-150	21	0.103	26.5	10.92
150-180	7	0.034	16.0	6.59
180-210	8	0.038	29.5	12.15
210-240	3	0.017	20.3	8.36
240-270	1	0.004	6.9	2.84
270-300	2	0.012	29.1	11.99

Largest Particle: 1300μm

Average Number Diameter: 15μm

Average Volume Diameter: 125 μm

MIDDLE GUST III

13 April 1972
Cyclone Samples

Pass 2

Time: 2:38 - 2:48

Altitude: 3100 ft (above ground level)

Heading: 350°

Cloud Width: 617 meters

Dust Concentration: 11.6×10^{-8} gms/cc

Diameter (microns)	Number	Percent by Number	Volume $X10^6$ $(\mu m)^3$	Percent by Volume
0-30	19,313	96.566	34.1	9.62
30-60	423	2.115	20.2	5.70
60-90	126	0.628	27.7	7.81
90-120	60	0.298	36.1	10.18
120-150	34	0.168	43.3	12.21
150-180	1	0.084	39.5	11.14
180-210	12	0.061	47.4	13.37
210-240	11	0.053	63.2	17.83
240-270	3	0.015	26.0	7.33
270-300	1	0.007	17.0	4.80

Largest Particle: 1300μm

Average Number Diameter: 15 μm

Average Volume Diameter: 155 μm

MIDDLE GUST III

13 April 1972

Cyclone Samples

Pass 3

Time: 4:13 - 4:34

Altitude: 2300 ft (above ground level)

Heading: 130°

Cloud Width: 1170 meters

Dust Concentration: 6.55×10^{-8}

Diameter (microns)	Number	Percent by Number	Volume $X10^6$ $(\mu m)^3$	Percent by Volume
0-30	19,457	97.283	34.4	19.23
30-60	459	2:293	21.9	12.24
60-90	40	0.202	8.9	4.97
90-120	17	0.086	10.4	5.81
120-150	7	0.037	9.5	5.31
150-180	6	0.029	13.6	7.60
180-210	6	0.029	22.5	12.58
210-240	5	0.026	31.0	17.33
240-270	-	-	-	-
270-300	2	0.011	26.7	14.92

Largest Particle: 1450 μm

Average Number Diameter: 16 μm

Average Volume Diameter: 165 μm

MIDDLE GUST III

13 April 1972
Cyclone Samples

Pass 5

Time: 6:24 - 6:35

Altitude: 2300 ft (above ground level)

Heading: 40°

Cloud Width: 679 meters

Dust Concentration: 6.16×10^{-8} gm/cc

Diameter (microns)	Number	Percent by Number	Volume $X10^6$ $(\mu m)^3$	Percent by Volume
0-30	19,286	96.429	34.1	26.94
30-60	606	3.032	28.9	22 83
60-90	75	0.374	16.5	13.03
90-120	17	0.083	10.1	7.98
120-150	9	0.043	11.1	8.77
150-180	5	0.023	10.1	7.98
180-210	2	0.011	8.5	6.71
210-240	-	-	-	-
240-270	-	-	-	-
270-300	1	0.003	7.3	5.77

Largest Particle: 1800 μm

Average Number Diameter: 16 μm

Average Volume Diameter: 65 μm

MIDDLE GUST III

13 April 1972

Cyclone Samples

Pass 6

Time: 7:39 - 8:00

Altitude: 3200 ft (above ground level)

Heading: 150°

Cloud Width: 1300 meters

Dust Concentration: 1.95×10^{-8} gms/cc

Diameter (microns)	Number	Percent by Number	Volume $X10^6$ $(\mu m)^3$	Percent by Volume
0-30	19,478	97.392	34.4	30.31
30-60	442	2.208	21.1	18.59
60-90	47	0.236	10.4	9.16
90-120	19	0.094	11.4	10.04
120-150	6	0.030	7.7	6.78
150-180	3	0.013	6.1	5.37
180-210	3	0.013	10.1	8.90
210-240	1	0.006	7.1	6.26
240-270	1	0.003	5.2	4.58
270-300	–	–	–	–

Largest Particle: 950 μm

Average Number Diameter: 16 μm

Average Volume Diameter: 65 μm

Middle Gust III

13 April 1972

Cyclone Samples

Pass 7

Time: 9:05 - 9:35

Altitude: 4300 ft (above ground level)

Heading: 270°

Cloud Width: 1700 meters

Dust Concentration: 1.98×10^{-8} gms/cc

Diameter (microns)	Number	Percent by Number	Volume $X10^6$ $(\mu m)^3$	Percent by Volume
0-30	19,656	98.278	34.7	20.47
30-60	227	1.135	10.8	6.37
60-90	64	0.318	14.0	8.26
90-120	27	0.134	16.2	9.56
120-150	9	0.045	11.6	6.84
150-180	6	0.028	13.2	7.79
180-210	5	0.025	19.4	11.45
210-240	4	0.020	23.9	14.10
240-270	1	0.005	8.7	5.13
270-300	1	0.007	17.0	10.03

Largest Particle: 700 μm

Average Number Diameter: 15 μm

Average Volume Diameter: 145 μm

Cyclone Samples

Pass 8

Time: 10:48 to 11:17

Altitude: 5100 ft (above ground level)

Heading: 350°

Cloud Width: 1870 meters

Dust Concentration: 0.91×10^{-8} gms/cc

Diameter (microns)	Number	Percent by Number	Volume $X10^6$ $(\mu m)^3$	Percent by Volume
0-30	19,624	98.118	34.7	21.41
30-60	297	1.483	14.2	8.76
60-90	46	0.229	10.1	6.23
90-120	10	0.052	6.3	3.89
120-150	9	0 044	11.3	6.97
150-180	3	0.016	7.5	4.63
180-210	5	0.024	18.6	11.47
210-240	2	0.008	9.5	5.86
240-270	2	0.012	20.8	12.83
270-300	2	0.012	29.1	17.94

Largest Particle: 870 μm

Average Number Diameter: 16 μm

Average Volume Diameter: 175 μm

MIDDLE GUST III

13 April 1972

Cyclone Samples

Pass 9

Time: 13:34 to 14:16

Altitude: 6800 ft (above ground level)

Heading: 150°

Cloud Width: 2270 meters

Dust Concentration: 1.18×10^{-8} gms/cc

Diameter (microns)	Number	Percent by Number	Volume $X10^6$ $(\mu m)^3$	Percent by Volume
0-30	19,634	98.170	34.7	28.82
30-60	322	1.610	15.4	12.79
60-90	21	0.106	4.7	3.90
90-120	11	0.053	6.4	5.32
120-150	6	0.029	7.5	6.23
150-180	3	0.016	7.5	6.23
180-210	2	0.011	8.5	7.06
210-240	3	0.016	19.1	15.86
240-270	1	0.004	6.9	5.73
270-300	1	0.004	9.7	8.06

Largest Particle: 700 μm

Average Number Diameter: 16 μm

Average Volume Diameter: 115 μm

MIDDLE GUST III

13 April 1972

Cyclone Samples

Pass 10

Time: 14:43 to 15:31

Altitude: 7500 ft (above ground level)

Heading: 320°

Cloud Width: 2720 meters

Dust Concentration: 1.11×10^{-8} gms/cc

Diameter (microns)	Number	Percent by Number	Volume $X10^6$ $(\mu m)^3$	Percent by Volume
0-30	19,512	97,561	34.5	30.42
30-60	339	1:695	16.2	14.29
60-90	107	0.535	23.6	20.81
90-120	28	0.139	16.9	14.90
120-150	11	0.054	13.9	12.26
150-180	3	0.013	5.9	5.20
180-210	1	0.003	2.4	2.12
210-240	-	-	-	-
240-270	-	-	-	-
270-300	-	-	-	-

Largest Particle: 475 μm

Average Number Diameter: 16μm

Average Volume Diameter: 75 μm

MIDDLE GUST III

13 April 1972

Cyclone Samples

Pass 11

Time: 17:04 to 18:52

Altitude: 8300 ft (above ground level)

Heading: 50°

Cloud Width: 6660 meters

Dust Concentration: 0.41×10^{-8} gms/cc

Diameter (microns)	Number	Percent by Number	Volume $X10^6$ $(\mu m)^3$	Percent by Volume
0-30	19,390	96.949	34.3	39.88
30-60	523	2.613	24.9	28.95
60-90	72	0.359	15.8	18.37
90-120	14	0.070	8.4	9.77
120-150	2	0.010	2.6	3.02
150-180	-	-	-	-
180-210	-	-	-	-
210-240	-	-	-	-
240-270	-	-	-	-
270-300	-	-	-	-

Largest Particle: 580 μm

Average Number Diameter: 16 μm

Average Volume Diameter: 35 μm

Middle Gust III

13 April 1972

Cyclone Samples

Pass 12

Time: 20:27 to 20:44

Altitude: 8200 ft (above ground level)

Heading: 190°

Cloud Width: 1050 meters

Dust Concentration: 0.34×10^{-8} gms/cc

Diameter (microns)	Number	Percent by Number	Volume $X10^6$ $(\mu m)^3$	Percent by Volume
0-30	19,660	98.302	34.7	66.73
30-60	334	1.669	15.9	30.58
60-90	5	.025	1.1	2.12
90-120	1	.003	0.3	0.58
120-150	–	–	–	–
150-180	–	–	–	–
180-210	–	–	–	–
210-240	–	–	–	–
240-270	–	–	–	–
270-300	–	–	–	–

Largest Particle: 1100 μm

Average Number Diameter: 16μm

Average Volume Diameter: 22 μm

Middle Gust III

13 April 1972

Cyclone Samples

Pass 13

Time: 23:53 to 26:43

Altitude: 7900 (above ground level)

Heading: 50°

Cloud Width: 12,200 meters

Dust Concentration: 0.13×10^{-8} gms/cc

Diameter (microns)	Number	Percent by Number	Volume $X 10^6 (\mu m)^3$	Percent by Volume
0-30	19,652	98.258	34.7	59.93
30-60	326	1.628	15.5	26.77
60-90	17	0.084	3.7	6.39
90-120	6	0.028	3.4	5.87
120-150	0.5	0.002	0.6	1.04
150-180	–	–	–	–
180-210	–	–	–	–
210-240	–	–	–	–
240-270	–	–	–	–
270-300	–	–	–	–

Largest Particle: 350 μm

Average Number Diameter: 15 μm

Average Volume Diameter: 25 μm

MIDDLE GUST III

13 April 1972

Cyclone Samples

Pass 14

Time: 28:57 to 30.09

Altitude: 8000 ft (above ground level)

Heading: 210°

Cloud Width: 4820 meters

Dust Concentration: 0.07×10^{-8} gms/cc

Diameter (microns)	Number	Percent by Number	Volume $X10^6$ $(\mu m)^3$	Percent by Volume
0-30	19,572	97.859	34.6	58.05
30-60	405	2.027	19.3	32.38
60-90	21	0.105	4.6	7.72
90-120	2	0.009	1.1	1.85
120-150	-	-	-	-
150-180	-	-	-	-
180-210	-	-	-	-
210-240	-	-	-	-
240-270	-	-	-	-
270-300	-	-	-	-

Largest Particle: 300 μm

Average Number Diameter: 16 μm

Average Volume Diameter: 26 μm

APPENDIX IX

MIXED COMPANY III
GROUND OPERATIONS SUMMARY

LN-123

13 November 1972

To
Defense Nuclear Agency
Washington, D. C. 20305

From
Meteorology Research Inc.
464 W. Woodbury Road
Altadena, California 91001

TABLE OF CONTENTS

LN 123 GROUND OPERATIONS SUMMARY

MIXED COMPANY III

I. FALLOUT COLLECTION EXPERIMENT

A. Purpose

The collection of fallout and ejecta was necessary to establish complete documentation of material transport as a result of the Mixed Company III HE explosion. Data from the ground can be correlated with the data taken by the aircraft to improve the description of the dust cloud mass loading in terms of particle density and size as a function of time or distance.

The fallout network for the Mixed Company test was designed to provide:

a) Area deposition of dry fallout in terms of grams per square meter of surface.

b) Total sample recovery for subsequent determination of single particle densities and fallout size distributions.

c) Trajectory data and decelerated collection of fragile aggregates.

d) Sequential arrival time data with respect to area deposition and particle size.

Consideration had to be given to the probable direction and speed of the dust cloud in order to get the greatest efficiency out of the equipment available and the restricted accessibility of the test area. A survey of 700 mb (approx. 10,000 msl) winds at Grand Junction was provided by Mr. Jack Reed of Sandia Corporation which indicated a most probable wind from the NNW at about 12 knots. Estimates were made of fallout plume size based on cloud size as derived from Dial Pack data and various possible wind speeds. With these inputs, a distribution of fallout stations was planned.

B. Equipment

1. Fallout Trays

The trays selected for fallout collection were developed and provided by Mr. W. B. Lane of Stanford Research Institute. They have been used over the years to document a wide variety of sizes and types of explosions. The tray is square, two feet by two feet, and two inches deep. Each tray has a gasketed lid which can be clamped in place for shipping with the fallout material still inside. Inside the tray, there is a frame holding about 25 thin metal strips, two feet by three inches, at an angle of 45° to 60° from vertical. These louvers keep material which falls into the tray from bouncing out. The fallout trays are designed primarily to collect samples for subsequent determinations of area mass deposition and small particle size distributions. It is recognized that large particles or aggregates may break up on impact with the trays, thus biasing the size distribution. The solution to the large particle-aggregate problem is presented in the next section.

2. Impact Trays

In the direction of measuring the size, density and direction of impact of larger particles or aggregates which could break up upon impact with the metal surfaces of the trays, a new fallout collection technique was used. A rectangular aluminum tray, eleven inches wide, seventeen inches long and two inches deep was selected as the bed for shock absorbing materials. Several materials were tested by dropping rocks and loose soil fragments from a height of 30 feet into the trays filled with various test materials. Water with a thickening agent and a gelatin mixture were both tried without the desired performance. The thickened water was not stable enough to preserve the trajectory path and the gelatin had a viscosity which varied with temperature. A heavy duty grease was tried, but it also was too viscous at cold temperatures. The best material found was Sta-Lube grease which had a uniform viscosity over a wide temperature range as well as having an easily prepared surface. The workability of the grease allowed a nearly smooth surface to be prepared, a feature which facilitated the identification of fallout particles and impaction craters.

In the testing of the trays, it was found that loosely

aggregated pieces of dirt, 3 centimeters in diameter, just reached the bottom of a one and one-half inch deep layer of grease without breaking up. On this basis, it appeared that all fallout aggregates except the largest ejecta particles would be preserved.

In the field, the trays were filled and the surfaces prepared at the MRI trailer in the Northwest park. Each was covered by aluminum foil to keep the surface clean until they were uncovered on the morning of the test.

3. Sequential Samplers

The sequential sampler was a box 54 inches long, 26 inches wide, and five inches high supported in a level plane about a foot above the ground by four adjustable legs. An open sampling slit 0.5 inches wide and 24 inches long with 0.5 inch high edges was located across the center of the box. A 25 inch by 27 inch metal sheet supported on four runners was allowed to move slowly under the slit. The metal sheet was covered with a piece of adhesive-coated Mylar with the adhesive facing up. The sheet movement was powered by a Negator spring motor and was controlled non-linearly by turning a cone at constant speed. Non-linear motion, decreasing with time, was designed into the sampler to accommodate a heavier fallout rate. Line was released at a progressively slower rate as the cone spiralled from the largest to the smallest diameter. A 27V (120 ma) goverened DC motor drove the cone and was powered by three 9V transistor batteries in series. The motor was controlled by a simple SCR circuit using one of the 9V batteries. When a dry switch closure was made, the SCR turned the motor on and then isolated the sampler from any further dependence on outside circuitry. When the collecting sheet reached the end of its travel, a micro switch was activated and shut the motor off. The nominal travel time for the sheet was 15 minutes.

C. Deployment

A study of the probable wind direction, wind speed and cloud size growth led to the fallout station layout shown in Figures 1 and 2. The station array is biased to the SSE since the most probable wind would be from the NNW. Two grids were designed.

1. Close Grid

The close grid (Fig. 1) was designed geometrically with stations located at distances of 1,000 feet, 3,000 feet and 6,000 feet along 12 lines 30° apart, radiating from GZ.

The stations at 1,000 feet were all surveyed in and staked. The stations at 3,000 feet were surveyed except for the ones at 240° and 270° which were located by USGS map features and the station at 030° which was near a road and was therefore moved for best exposure. The stations at 6,000 feet were all located by USGS map features, alignment of 3,000 foot stakes to GZ, and by pacing from 3,000 feet. It was necessary to survey the stations from the close grid to accurately fix the fallout data. The farther out the station, the greater the tolerance for error.

The stations were identified by a three digit code. The first two digits defined the radial angle to the nearest ten degrees and the third digit defined the distance to GZ in thousands of feet. Because of the probable southward cloud movement, there were no stations located at 3,000 feet and 6,000 feet along the 300° and 000° radials.

The following table lists the close grid stations:

1,000'	3,000'	6,000'
001	---	---
031	033	036
061	063	066
091	093	096
121	123	126
151	153	156
181	183	186
211	213	216
241	243	246
271	273	276
301	---	---
331	333	336

At each station, there were two fallout trays oriented with the louvers perpendicularly to the radial line with the maximum louver openings exposed to particles falling in from ground zero. In addition, two grease impact trays were located at each station out to 6,000 feet. Sequential samplers

were installed at stations 153, 156, 186, and 213 with the collection slit perpendicular to the radial and with the collection sheet moving away from GZ. The four stations were connected in parallel to the T and F remote relay at the southern LN 110 experiment.

2. Extended Grid

The extended grid (Fig. 2) expanded the coverage to the south of GZ as far as the county road network would allow. One station located to the northwest was intended for background zero measurement. The extended grid stations started a little over two miles from GZ and extended to as far as ten miles away.

All of the stations on the extended grid were located from features on USGS maps. The stations were identified by a code consisting of two numbers and a letter. The numbers define the closest 30° radial just as in the close grid code. The letter ranks the distance with "a" being the closest and "e" being the farthest.

The following table lists the extended grid stations:

03a
06a
09a, 09b, 09c, 09d
12a, 12b, 12c, 12d, 12e
15a, 15b
18a, 18b, 18c, 18d
21a, 21b, 21c, 21d
24a, 24b, 24c
27a, 27b
33a

All the stations except 06a had at least one fallout grease tray oriented in the same manner as the close grid trays. Stations 12a, 12c, 15a, 18a, 18b, and 21a had two fallout trays to provide a larger sampling area in the more probable wind directions. Stations 15a and 18a had manually operated sequential samplers.

D. Operating Procedure

D. Operating Procedures

1. Fallout Trays

On the morning of November 13, 1972, the lids were removed from the trays and carefully set aside so they would not contribute material to the fallout sample when they were replaced after the test.

The close grid stations were uncovered between 0530 and 0800 and the extended grid stations were uncovered by 1030.

About two hours after the detonation, the crews began retrieving the trays on the county roads in the extended grid. Each tray was identified with its station code by placing a label inside the tray just before the lid was put on and sealed.

The same procedure was followed for the stations in the close grid. The trays were labelled, covered, clamped and removed as soon as possible after access to the area was granted.

2. Impact Trays

In the morning, the aluminum foil was removed from the impact trays at the same time as the lids were removed from the fallout trays. Some of the foil covers had come into contact with the grease surface, requiring some additional smoothing of the trays at each station. Data from the impact trays were obtained by direct observation and measurement in the field after the detonation. The trays were discarded after the data had been collected.

3. Sequential Samplers

The starter mechanisms for the sequential samplers were primed between 0630 and 0830 of the morning of the 13th. The two cover plates forming the top and sampling slit were removed. The metal sheet was slid to the loaded position with the control line wrapped around the spiral cone and the spring extended to provide the moving energy. The circuit switch was turned on so that the T-10 seconds switch closure from the T & F bunker would start the sampler. The cover plates were reinstalled and finally the protective tape was removed from the sampling slit.

About two hours after detonation, the data from the samplers were removed. The cover plates were removed again and the original cover paper was placed back on the adhesive surface. The metal sheets were removed and the cover paper was taped to the sheets. The station code was written on the cover sheet along with an arrow indicating the direction of ground zero.

E. Performance

All fallout equipment beyond 1,000 feet from GZ operated successfully with the single exception of the sequential sampler at station 15a. During the preparation of the sampler prior to the detonation, the thin Mylar film came loose from the metal sheet and was blown against the operator, adhesive side first. After disengaging himself from this large piece of "fly paper", he decided it would be inadvisable to use the film.

All 1,000 foot trays, both fallout and impact, were staked to the ground with eight inch aluminum tent stakes. Ground and air motions associated with the blast pulled most of these stakes from the ground and dislodged some of the trays. All of the louver inserts were blown out of the fallout trays and many of the fallout trays and impact trays were overturned, particularly at the stations south of GZ.

II TRACER EXPERIMENTS

A. Purpose

Two types of particle tracing experiments were conducted during the Mixed Company III event. One experiment involved the release of five different colors of two to seven micron diameter fluorescent particles at varying distances from ground zero This experiment was designed to measure the sweep up of particles from the blast apron and transport of these particles into the cloud. The second experiment involved the emplacement of 100 pounds of 300 to 750 micron lanthanum tagged sand at a point of 20 feet from ground zero on the 180° radial. This material should have been included in the crater ejecta and subsequently picked up by the fallout samplers or possibly by the sampling aircraft. Neutron activation techniques capable of detecting trace amounts of lanthanum could be used to study the samples.

B. Equipment and Deployment

No equipment was required in the dissemination of the tagged sand. The sand was simply spread over a five foot diameter circle at a point five feet from the edge of the TNT charge (20 feet from the center of the charge).

Each of the five fluorescent particle disseminators consisted of a small (300 cc) gas cylinder, a solenoid valve and a tube containing the fluorescent particle (F. P.) charge (Fig. 3). Prior to firing, the cylinder was filled with 600 psi of dry nitrogen, and the complete assembly was placed inside a styrofoam-cushioned aluminum tube which was buried in the ground. After installation, the top of the F. P. charge tube was flush with the ground surface.

The five solenoids were connected, in parallel, to an open relay which was connected in turn to a 30 volt battery through the open relay in the T and F bunker. When the T and F switch was closed at one second before detonation, the battery relay closed, energizing all five disseminator solenoids. At each station, a cylindrical cloud of powder was produced about 20 feet high and three feet wide.

Each station contained a powder which produces a distintive color when excited by ultraviolet light. The following table defines the colors and distances from ground zero (Fig. 4).

Distance (feet)	Color	Code Number
520	Blue	2205
630	Red-Orange	2220
740	Yellow	2267
850	Green	3206
960	White	2200

C. Performance

All the solenoids fired at T-1 second as designated and the clouds of F. P. were observed as they were drawn into the stem of the cloud. At two of the stations (630' and 740'), the tubes ruptured asymmetrically; however, examination of the units after the test indicated that nearly all the F. P. was released. The major malfunction occurred at the outermost station (960') where the side of the tube blew out, causing about 40% of the powder to remain in the hole.

III CLOUD PHOTOGRAPHY

A. Purpose

Four camera sites were selected to provide photographic documentation of cloud development and motion. Two cameras, operating at speeds of 64 frames per second, were used to record the release of the fluorescent particles and the early time growth of the cloud. Three of the stations were equipped with time lapse cameras to record the complete evolution of the cloud as a function of time and to permit reconstruction of the cloud dimensions during the aircraft penetrations. In addition, infrared photographs were taken of the early cloud to document the location of the fireball with respect to the dust envelope.

B. Equipment and Deployment

1. Station 06a (Technical Observation Point)

A Beauleau 16mm motor driven camera with an automatic exposure zoom lens was used to record the early growth of the cloud and the motions of the fluorescent particle cloudlets. The camera was loaded with 200 feet of Kodachrome II and was operated during the first minute at 64 frames per second with a full telephoto lens setting. The balance of the film in this camera was used to document special characteristics of the cloud and to show the aircraft penetrations from the ground.

A 35mm camera loaded with a 20-exposure cartridge of IE 135 infrared color film was used in an experiment to try and enhance the differentiation between the fireball and the dust envelope.

2. Station 24a

A Kodak K100 was used for high speed telephoto photography of the early development of the cloud. The camera was loaded with 100 feet of Kodachrome II film. A 75mm

lens set at 5-100 was used and the camera was operated at 64 frames per second for about 20 seconds after T-0. The balance of the 100 feet was exposed at 16 frames per second with a 15mm wide angle lens set at f-20.

The second camera at this site was a 16mm Bolex, modified for continuous operation at a slow speed in order to provide a time lapse effect. An external DC motor powered by a 6 volt battery was coupled directly to the eight frame per revolution shaft on the camera. The motor shaft turned at 0.25 revolutions per second, resulting in a framing rate of 2 frames per second. The lens had a focal length of 10mm (very wide angle) and was set at f-20 with a .60ND (25% transmission) filter to compensate for the slow moving shutter disc. A 100 foot roll of Kodachrome II was exposed in this camera.

3. Station VOP (Visitors Observation Point)

The equipment at this site was identical to the Bolex at station 24a in (b) above. The camera was tripod mounted with a sweep second clock in the field of view for timing reference. About thirty minutes of cloud growth and movement was recorded at this site.

4. Station 03a

Another Bolex 16mm camera was used at this site to provide a third time lapse record of the cloud development. The camera was a Bolex M-16 with a modified shutter for use with an MRI Model 107E intervalometer. The timer was bypassed and the drive motor operated continuously at a rate of 1.3 frames per second. The 10mm focal length lens was set at f-16 with a 0.40ND filter.

C. Performance

The high speed cameras at 06a and 24a worked properly, providing the data required. The time lapse camera at VOP operated perfectly.

The time lapse camera at 24a operated oroperly in the mechanical sense; however, the lens turret was not in a detent position and therefore, the lens was not optically in line with the film

gate. This resulted in the loss of ground reference and clock time. Despite this problem, cloud growth can be measured from the film and azimuth orientation can be fixed by the stem of the cloud. Time can be correlated with the VOP film (and hence a clock) by matching unambiguous events from both locations such as shock halos, pilius caps and jet contrails.

The camera at 03a malfunctioned mechanically. The film jammed in the camera and no film was exposed.

IV WIND MEASUREMENTS

A. Purpose

Wind data were taken in the vicinity of the detonation to help define the cloud motions which quickly became dominated by the atmospheric flow fields. The surface wind was recorded to show the speed and direction of the surface layer and to give an indication of the turbulence level. Winds aloft were measured by balloon (Pibal) observations to document the changes in the flow pattern with altitude. Since the cloud has vertical structure and vertical motion, it is very important to collect as much three-dimensional flow data as possible to augment the visual analysis of the motion of the cloud. With the cloud position and wind flow data, a fall-out pattern can be predicted based on the wind stress applied to fall-out particles after they have left the cloud.

B. Equipment and Deployment

1. Surface Wind

A conventional three cup anemometer driving a DC generator was used to measure wind speed. The performance of this sensor is equivalent to an MRI Model 1074-6 sensor. The wind direction sensor was a sensitive wind vane driving a low torque potentiometer. A two-channel Esterline Angus recroder was operated at 0.75 inches per hour by spring drive. Each recorder channel was matched to the sensor output to provide the desired scale. The sensor crossarm was mounted on a tripod at the Northwest Trailer Park with the sensing elements at about 10 feet above the ground. An exposure was chosen which minimized interference from any nearby structures.

2. Winds Aloft

Single theodolite Pibal ascents were made from station 032 at 0930, 1000, 1100, and 1150 hours. Also, two uncalibrated balloons were released from station 24a prior to T-0 for a qualitative measurement of the lower level flow. In addition, Pibal data were available from a double theodolite station operated by the Air Weather Service and from Grand Junction airport.

C. Performance

The anemometer and wind vane operated properly. It was planned to operate the recorder at 0.75 inches per minute during the final hours before and after the detonation; however, the servicing of the fallout and impact trays required substantially more time than planned and the visit to the Northwest Trailer Park to change the chart speed was eliminated. The wind trace shows a persistent direction from the ESE between 1000 and 1100 hours, backing to ENE from 1100 to 1230. The wind speed was decreasing from about 10 mph at 1030 to about 5 mph at 1130 and continued at an average of about 5 mph until 1230.

The Pibal observations (Figs. 5, 6, and 7) show a complex vertical profile with two shear zones forming at about 2,500 feet (8,800 feet msl) and 5,500 feet (11,800 feet msl). Further analysis of this data as well as other winds aloft data is required before a satisfactory description of the local flow can be made.

The two balloon releases from station 24a showed a strong flow from the east. Both balloons were lost to the unaided eye without a direction change being observed.

V GENERAL COMMENTS

A. Weather and Ground Conditions

The nature of the fallout station network required extensive travel within the test site, largely without benefit of roads. Outside the test site, many miles had to be driven over country roads which, under some conditions, required four-wheel drive vehicles. 19 of the 32 test site stations were surveyed and staked. The remaining 13 (all 10 of the 6,000 foot stations and 3 of the 3,000 foot stations) had to be located by triangulations, map details and pacing. All 26 of the country road stations had to be located and staked. Each station was visited a minimum of five times to locate, install equipment, dry run, uncover and recover. Some

additional visits were made to acquaint assigned personnel with their stations. For this part of the ground operation, traveling was the largest part of the job. The adverse weather and soil conditions caused a considerable hardship which would have resulted in assignment failures except for the outstanding performance of the field crew.

The temperature and snow/ice cover on the morning of the 13th caused considerable problems in keeping to the prescribed time schedules. Each of the 64 impact trays had a frozen crust of ice over the aluminum foil cover. This had to be carefully removed and the grease smoothed where it touched the foil as a result of the weight of the snow.

Some of the fallout trays in the higher elevations to the south were completely hidden by the snowfall and had to be exhumed and relocated on top of the snow pack. The loading and setting of the sequential sampler was doubly difficult because of the cold. Any future field programs of this type should employ equipment more easily handled in ice and cold conditions.

B. The MRI Field Crew

As mentioned above, the field program was conducted under relatively difficult conditions. Three seasoned local residents were hired along with their four-wheel drive vehicles to form the backbone of the crew. The Foreman was Mr. Ken Weimer and the other two were Mr. Carl Baker and Mr. Leo "Shorty" James. These three were assisted by Mr. Ernie Caldwell and Mr. Bob Massaro. The sixth member was Mr. Bert Lane of SRI, the scientist who provided the fallout trays and advised in the design and layout of the fallout collection network. The last three on the field crew were fr. MRI, including Mr. Jim Munger who took Pibal observations and operated the camera at 03a, Mr. Tom Lockhart who directed the field program and kept all the phases of MRI's responsibilities moving toward a successful conclusion, and Mr. William Green who supervised the overall project, including the aircraft operations. All performed well under trying conditions, but a special commendation was earned by Ken Weimer and Bert Lane.

C. Test Command Support

Special appreciation is extended to LTC A. L. Knapper,

Test Director, who realized the problems we and other experimenters were encountering due to the adverse weather and who modified the test schedule to accomodate these delays.

We wish to acknowledge the cooperation and interest exhibited by LCDR T. L. Freeman, LCDR T. K. McBride and Major R. B. Williams during our conduct of the field program. Without their help, we would not have succeeded in our mission.

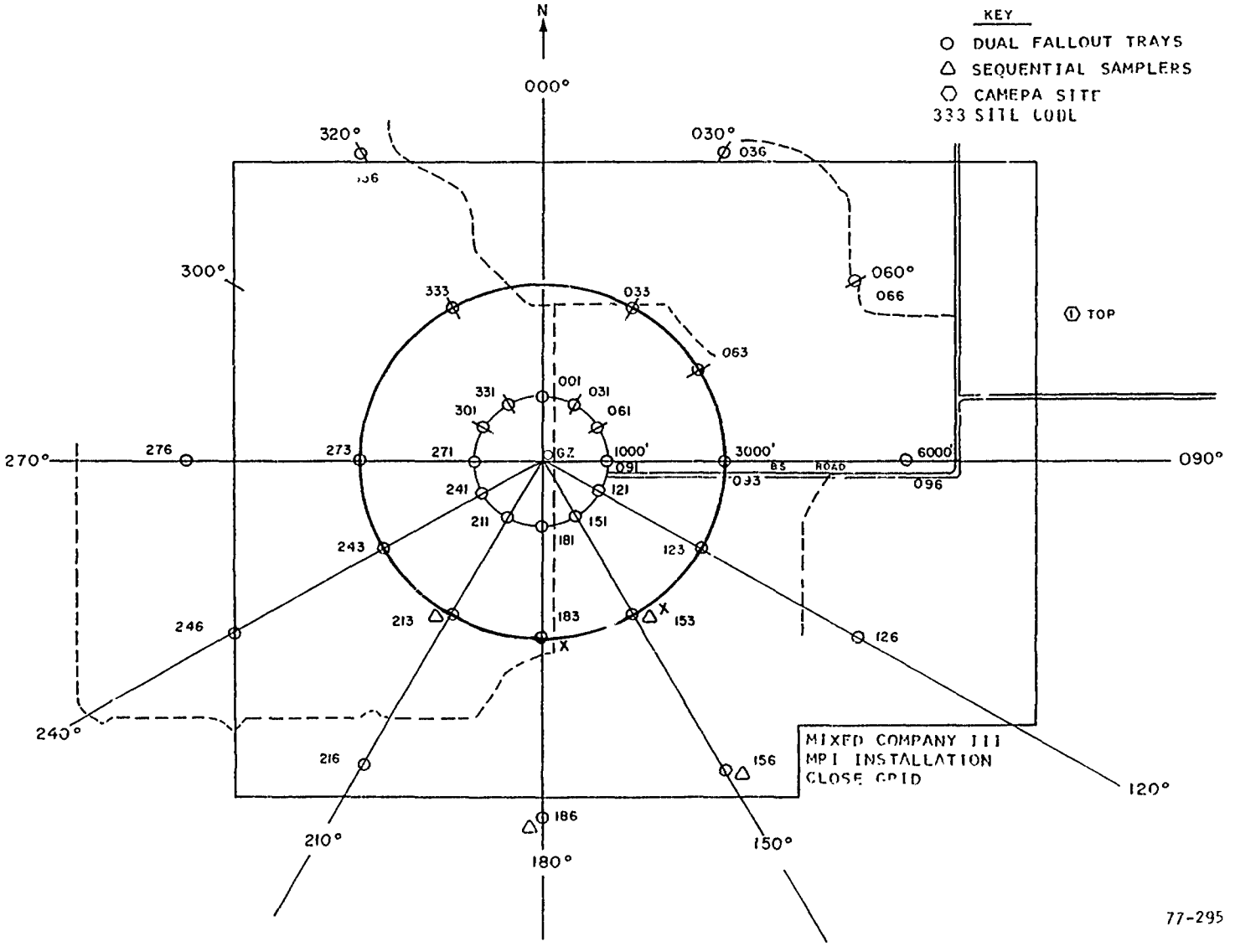

Figure 1. Mixed Company III - Fallout collectors close grid.

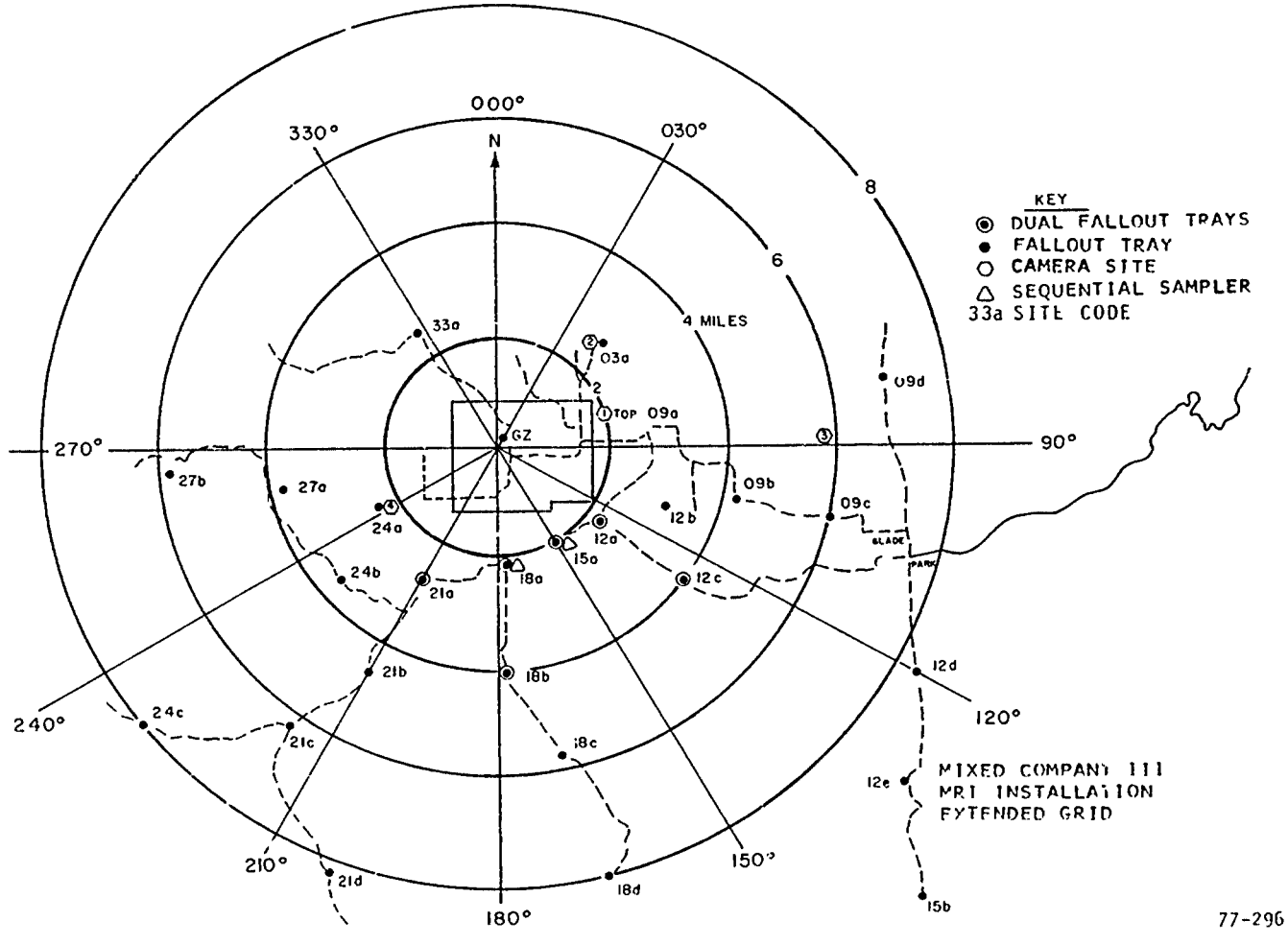

Figure 2. Mixed Company III - Fallout collectors extended grid.

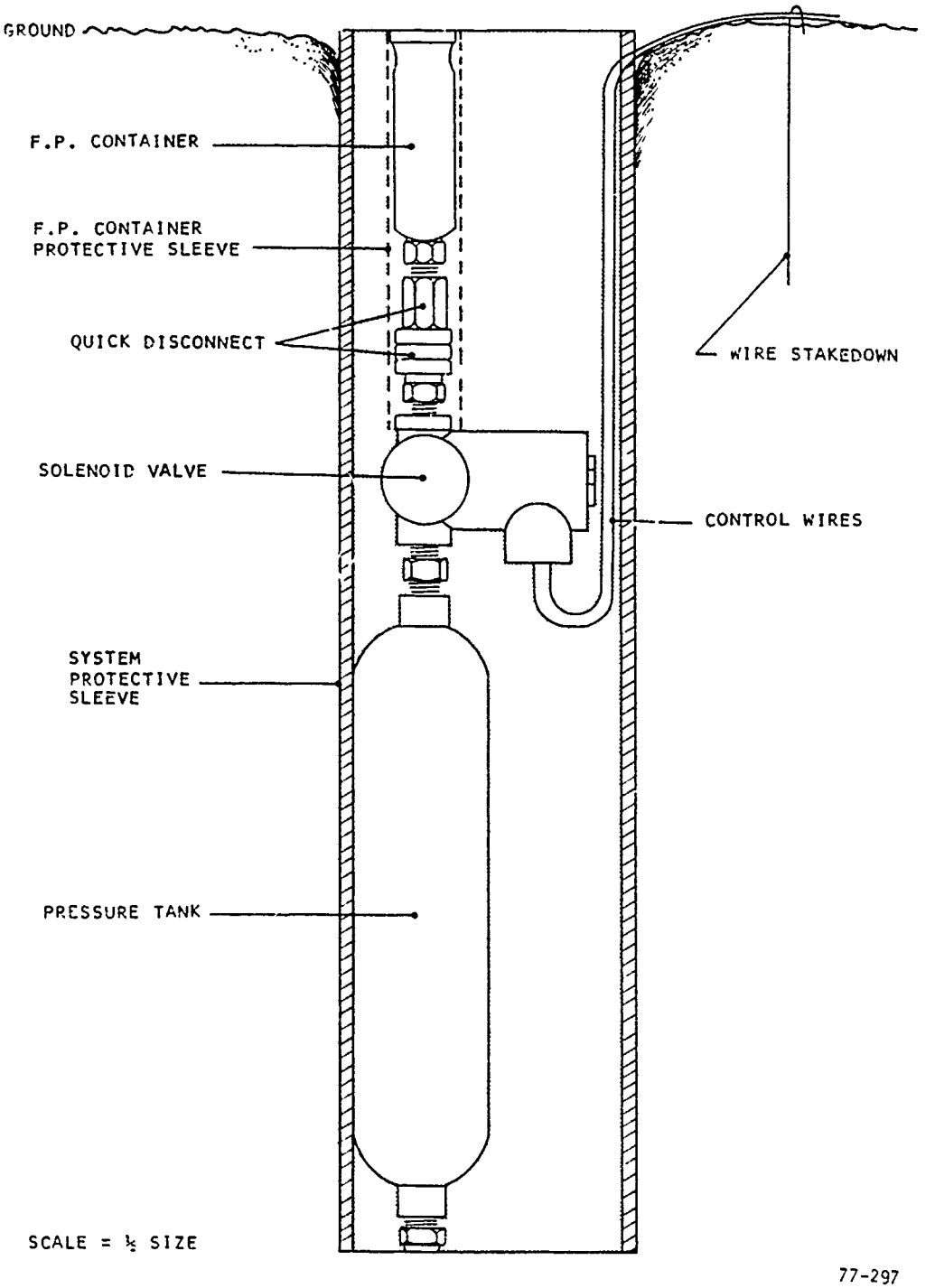

Figure 3. Fluorescent Particle (F.P.) Dispenser.

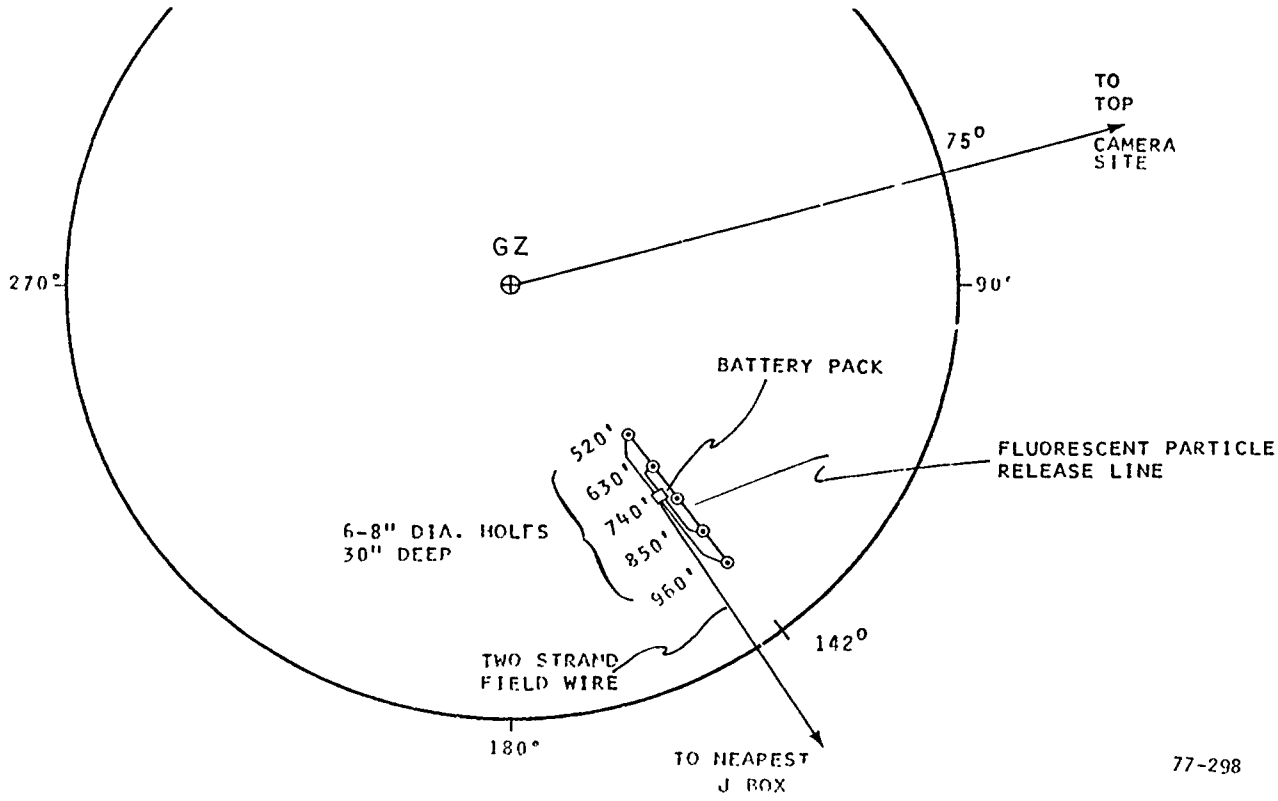

Figure 4. Middle Gust I - Location of glass beands and fluorescent particle (F.P.) releases.

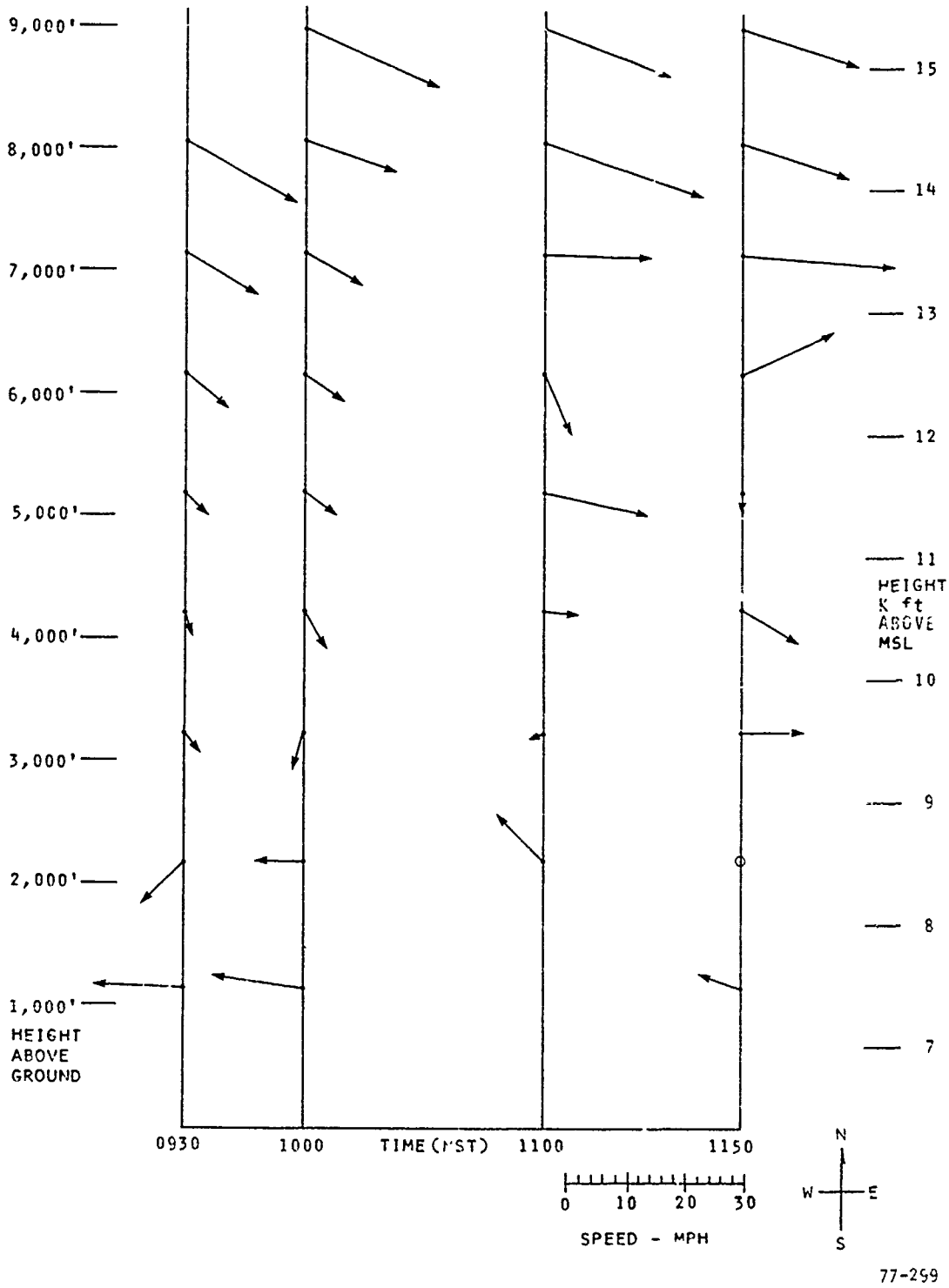

Figure 5. Winds aloft at Station 03a - 13 November 1972.

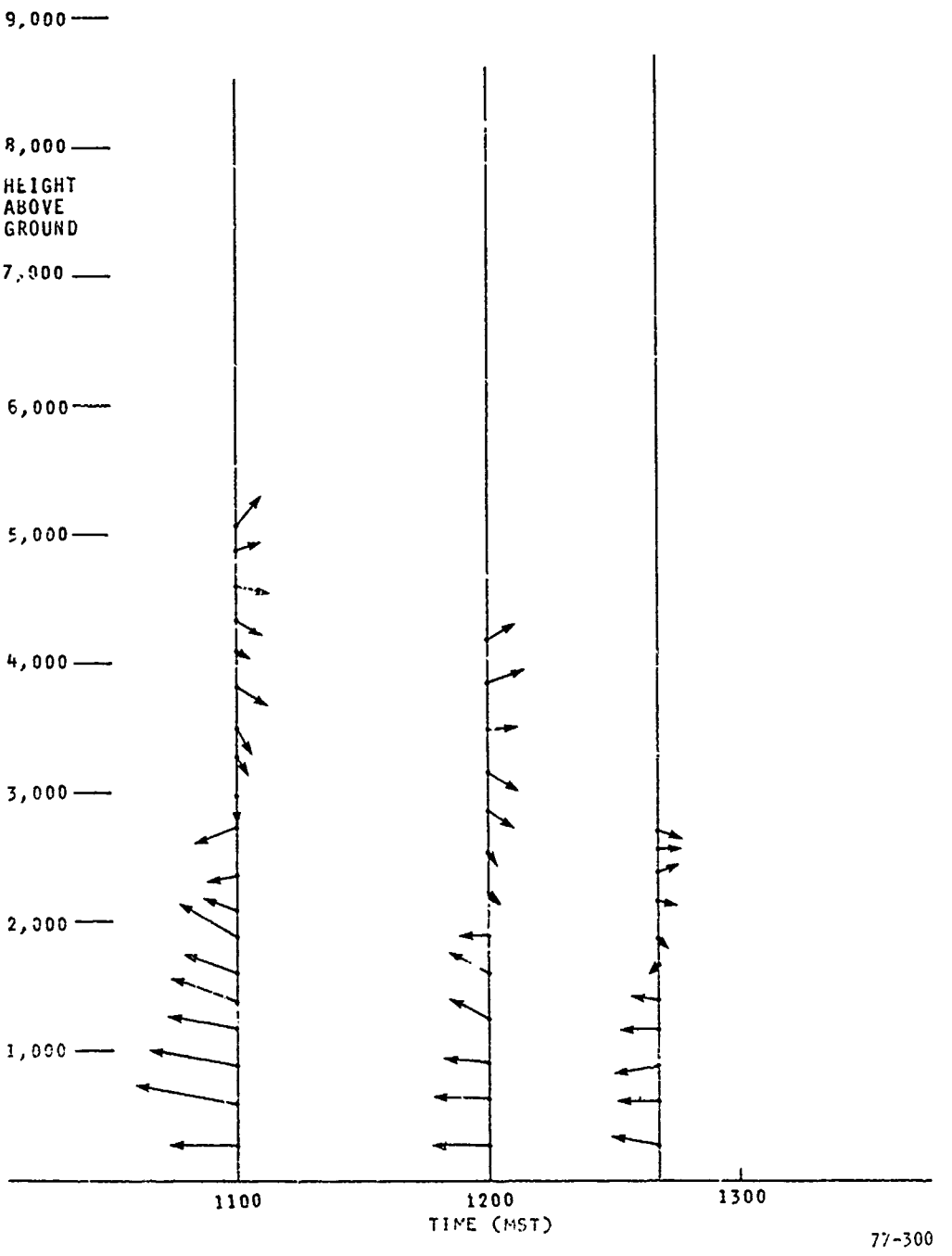

Figure 6. Winds aloft at TOP - 13 November 1972.

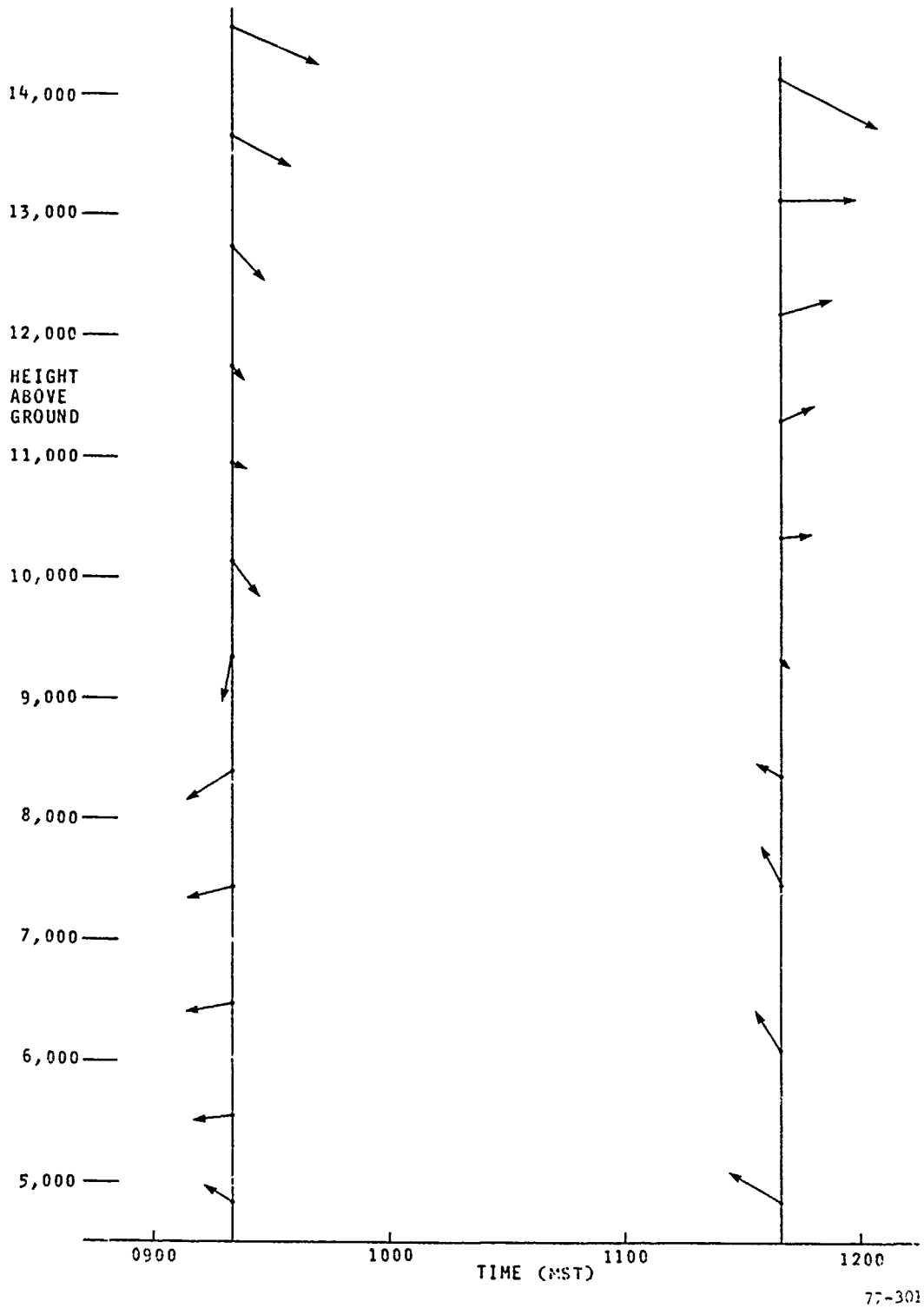

Figure 7. Winds aloft at Grand Junction, Colorado - 13 November 1972.

APPENDIX X

MIXED COMPANY III - SIEVE ANALYSIS OF FALLOUT SAMPLES

(Summary of report submitted by
Stanford Research Institute)

The following tables were prepared at Stanford Research Institute. under subcontract from MRI.

The sample number identifies the compass direction (radial) and the distance from ground zero. The first two digits indicate the radial (i.e., 03 = 30°, 15 = 150°) and the last digit refers to the distance from GZ (i.e., 3 = 3000', 6 = 6000'). Where a letter replaces the last digit, the site location was on the extended grid (see Appendix VI, Figure 2). Total (sieve) weight refers to the total weight of fallout recovered from the tray. In the cases where two numbers are shown, two trays were placed at the indicated location. At 12 of the sites, sufficient material was recovered to permit sieve analysis using standard Taylor screens. In all other cases the sample was simply weighed and reported.

At a later date, selected samples were sized at MRI using the Quantimet 720. These data are reported in Appendix VI.

MIXED COMPANY SIEVE DATA

Sample Number	Total Sieve Wt (gm)	Sieve Fraction Weights (grams) Greater 2794μ	2794μ 991μ	991μ 350μ	350μ 125μ	125μ 44μ	less 44μ	Remarks
033	7.05 0.42	--	0.78	2.02	2.00	2.01	0.58	
036	2.32 2.70	--	0.02	0.62	2.56	1.58	0.14	
061	6.40 5.75	--	2.21	5.84	1.79	1.61	0.40	
063	6.95 1.90	0.08	1.84	1.96	1.76	2.74	0.38	
066	9.56 7.62	--	0.12	4.65	7.92	4.10	0.38	
091	10.88	2.32	1.70	1.78	1.48	2.98	0.55	Light tan color.
093	3.98 3.70	0.08	0.76	3.08	1.92	1.52	0.28	
096	1.68 1.44	--	0.04	0.20	0.80	1.82	0.26	
123	1.35	--	0.20	0.34	0.30	0.42	0.08	
151	20.18	9.40	3.02	1.40	2.06	3.08	1.16	No clips on tray; tan color.
211	51.54	0.15	0.99	3.18	18.33	25.00	3.89	No clips; tan color.
330	1.98 2.42	--	0.15	1.22	1.68	1.10	0.22	

MIXED COMPANY SIEVE DATA

Sample Number	Total Wt (gm) <495μ	Remarks
153	0.0972	
153	0.1199	
156	0.0200	
156	0.0201	
183	0.2663	
183	0.3169	
27a	0.0510	
33a	0.0431	
33d	nil	
126	0.0990	
126	0.0886	
186	0.0175	
216	0.0550	
216	0.0336	
243	0.1203	
243	0.2204	
246	0.0315	
246	0.0439	
213	0.2692	
213	0.4570	
273	0.0640	
273	0.0950	
276	0.0808	
276	0.0652	

MIXED COMPANY SIEVE DATA

Sample Number	Total WT (gm) <495μ	Remarks
33G	0.0270	
33G	0.0562	
09a	0.5764	
09b	0.1870	
09c	0.1269	
09d	0.4000	
12a	0.0278	
12a	0.0312	
12b	0.1140	
12b	0.0750	
12c	0.0482	
12c	0.0531	
12d	0.0352	
12e	0.0253	
15a	0.0618	
15a	0.0805	
15b	0.0408	
18a	0.0342	
18a	0.0169	
18b	0.0336	
18b	0.0247	
18c	0.01625	
18d	0.0397	

MIXED COMPANY SIEVE DATA

Sample Number	Total Wt (gm) $<495\mu$	Remarks
21a	0.0555	
21a	0.0234	
21b	0.0106	
21c	0.0133	
21d	0.0187	
24a	1.5249	No clips; obviously not fallout; no clips.
24a	0.0956	
24b	0.0113	
24b	0.0714	
24c	0.0185	

DISTRIBUTION LIST

DEPARTMENT OF DEFENSE

Defense Documentation Center
Cameron Station
12 cy ATTN: TC

Director
Defense Intelligence Agency
ATTN: DT-1C, Nuc. Eng. Branch
ATTN: DI-7D
ATTN: DT-2, Wpns. & Sys. Div.

Director
Defense Nuclear Agency
ATTN: DDST
ATTN: TISI Archives
ATTN: SPSS
2 cy ATTN: SPAS
3 cy ATTN: TITL Tech. Library

Commander
Field Command Defense Nuclear Agency
ATTN: FCPR

Director
Joint Strat. Tgt. Planning Staff, JCS
ATTN: JLTW-2
ATTN: JPTM
ATTN: JPTP

Chief
Livermore Division, Fld. Command, DNA
ATTN: FCPRL

OJCS/J-5
The Pentagon
ATTN: J-5, Plans & Policy Force Planning & Reprogramming Div.

Studies Analysis and Gaming Agency
Joint Chiefs of Staff
ATTN: SDEB

Under Sec'y of Def. for Rsch. & Engrg.
ATTN: S&SS (OS)
ATTN: AD/ET, J. Persh

DEPARTMENT OF THE ARMY

Director
BMD Advanced Tech. Ctr.
ATTN: ATC-T, Melvin T. Capps

Program Manager
BMD Program Office
ATTN: DACS-BMT, Clifford E. McLain
ATTN: DACS-BMT, John Shea

Commander
BMD System Command
ATTN: BDMSC-TEN, Noah J. Hurst

Dep. Chief of Staff for Rsch. Dev. & Acq.
ATTN: NCB Division

DEPARTMENT OF THE ARMY (Continued)

Commander
Harry Diamond Laboratories
ATTN: DELHD-NP
ATTN: DELHD-RC

Commander
Picitinny Arsenal
ATTN: Al Loeb

Director
TRASANA
ATTN: R. E. Dekinder, Jr.

Director
U.S. Army Ballistic Research Labs.
ATTN: Richard Vitali
ATTN: Robert E. Eichelberger

Commander
U.S. Army Mat'l. & Mechanics Rsch. Ctr.
ATTN: DRXMR-HH, John F. Dignam

Commander
U.S. Army Materiel Dev. & Readiness Cmd.
ATTN: DRCDE-D, Lawrence Flynn

Commander
U.S. Army Missile Command
ATTN: DRSMI-RRR, Bud Gibson

Commander
U.S. Army Nuclear Agency
ATTN: ATCA-NAW

DEPARTMENT OF THE NAVY

Chief of Naval Operations
ATTN: Code 604C3, Robert Piacesi

Director
Naval Research Laboratory
ATTN: Code 5180, Mario A Persechino

Commander
Naval Sea Systems Command
ATTN: ORD-0333A, Marlin A. Kinna

Officer-in-Charge
Naval Surface Weapons Center
ATTN: Code WA501, Navy Nuc. Prgms. Off.

Director
Strategic Systems Project Office
ATTN: NSP-272

DEPARTMENT OF THE AIR FORCE

AF Materials Laboratory, AFSC
ATTN: MBC, Donald L. Schmidt
ATTN: MBE, George F. Schmitt

DEPARTMENT OF THE AIR FORCE (Continued)

AF Weapons Laboratory, AFSC
ATTN: SAB
ATTN: SUL
ATTN: DYM, Maj Gary Ganong

Headquarters
Air Force Systems Command
ATTN: XRTO
ATTN: SOSS

Commander
Foreign Technology Division, AFSC
ATTN: TDFBD, J. D. Pumphrey

Hq. USAF/RD
ATTN: RDQSM
ATTN: RDPM

Hq. USAF/XO
ATTN: XOOSS

SAMSO/MN
ATTN: MNN
ATTN: MNNH

SAMSO/RS
ATTN: RSSE
ATTN: RSTP

Commander in Chief
Strategic Air Command
ATTN: XPFS
ATTN: XPQM
ATTN: XOBM

DEPARTMENT OF ENERGY

Division of Military Application
ATTN: Doc. Con. for CDR Richard E. Peterson

University of California
Lawrence Livermore Laboratory
ATTN: G. Staihle, L-24
ATTN: Joseph B. Knox, L-216

Sandia Laboratories
Livermore Laboratory
ATTN: Doc. Con. for Thomas B. Cook, Org. 8000

Sandia Laboratories
ATTN: Doc. Con. for M. L. Merritt

DEPARTMENT OF DEFENSE CONTRACTORS

Acurex Corporation
ATTN: C. Nardo

Aerospace Corporation
ATTN: R. Mortensen

Avco Research & Systems Group
ATTN: George Weber, J230
ATTN: William G. Reinecke, K 100

Battelle Memorial Institute
ATTN: E. Unger

California Research & Technology, Inc.
ATTN: M. Rosenblatt

DEPARTMENT OF DEFENSE CONTRACTORS (Continued)

University of Dayton
Industrial Security Super, KL-505
ATTN: John Barker

General Electric Company
Space Division
Valley Forge Space Center
ATTN: B. M. Maguire
ATTN: Phillip Cline

General Electric Company
TEMPO-Center for Advanced Studies
ATTN: DASIAC

Institute for Defense Analyses
ATTN: Joel Bengston

Kaman Sciences Corporation
ATTN: Jerry L. Harper

Lockheed Missiles & Space Co., Inc.
ATTN: P. J. Schneider

Martin Marietta Corporation
Orlando Division
ATTN: William A. Gray, MP-61
ATTN: James M. Potts, MP-61

Meteorology Research, Inc.
ATTN: William D. Green
ATTN: M. J. Fegley

R & D Associates
ATTN: F. A. Field
ATTN: Harold L. Brode
ATTN: Cyrus P. Knowles

The Rand Corporation
ATTN: R. Robert Rapp

Raytheon Company
ATTN: Library

Science Applications, Inc.
ATTN: John Warner

Science Applications, Inc.
ATTN: William M. Layson
ATTN: William R. Seebaugh

SRI International
ATTN: Philip J. Dolan

TRW Defense & Space Sys. Group
ATTN: A. Zimmerman
2 cy ATTN: D. H. Baer, R1-2136

TRW Defense & Space Sys. Group
San Bernardino Operations
ATTN: Earl W. Allen, 520/141
ATTN: E. Y. Wong, 527/712
ATTN: W. Polich

LFE Corp., Environmental Anal. Lab. Div.
ATTN: Marcel Nathans